PHYSICAL REVIEW LETTERS

VOLUME 5 SEPTEMBER 15, 1960 NUMBER 6

HYDRODYNAMIC ORIGIN OF COSMIC RAYS*

Stirling A. Colgate
Lawrence Radiation Laboratory, University of California, Livermore, California

and

Montgomery H. Johnson†
Aeronutronic Division of Ford Motor Company, Newport Beach, California

(Received August 29, 1960)

We have proposed that the material spalled from the surface of an exploding supernova is the source of cosmic radiation. Nuclei in the surface of the star may acquire many orders of magnitude more than the average energy per particle released in the explosion because of the large ratio of matter density between the core and the outer mantle. A shock from a sudden pressure increase in the core intensifies as it advances into lower-density material, thereby imparting extreme relativistic energies to the outermost layers. We are presenting a preliminary account of our investigations covering the mechanism of supernova explosions, the hydrodynamic motion following the explosion, the subsequent flow of radiation, and the structure of relativistic shock fronts, all of which are significant influences on cosmic radiation.

Astronomical evidence indicates that a supernova is a highly evolved star with a central temperature of 300-500 kev in which the nuclear fuel has burned to the most stable form, i.e., Fe. If we assume the total mass of such a star to be $10M_\odot$ ($M_\odot$ = mass of the sun), the radial density and temperature distribution as determined from hydrostatic and radiative equilibrium conditions are those shown in Fig. 1. In the explosion mechanism currently under study,[1] the energy source is the gravitational instability occurring when the adiabatic equation of state in the core corresponds

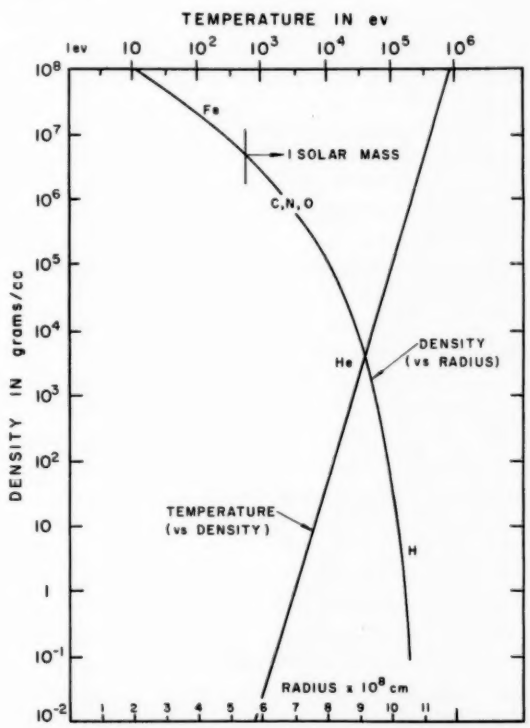

FIG. 1. Pre-supernova density and temperature distributions. The central density for 10 solar masses has been chosen from the estimates of Burbridge et al., [1] with a density distribution corresponding to radiative equilibrium ($\rho \approx T^{3.25}$).

to a ratio of specific heats of less than 4/3. This condition can arise for temperatures in the neighborhood of 500 kev, at which nuclei begin to dissociate and the resulting dissociation energy is a considerable part of the heat capacity. We hope ultimately to start the hydrodynamic calculation with the onset of instability[2] and follow in detail the gravitational collapse to provide the initial conditions for the subsequent explosion.

Current hydrodynamic calculations are made with a one-dimensional hydrodynamic code.[3] The validity of the code in following shock propagation through a medium in which the density changes by many orders of magnitude has been verified by comparison with known analytic solutions[4] for special cases.

Since astronomical evidence indicates that approximately one-tenth of the mass (i.e., $1M_{\odot}$) is ejected in a supernova explosion, the calculation begins with an energy release in the core adjusted so that one solar mass escapes from the gravitational field. The required energy is about 5×10^{17} ergs/g or 10^{52} ergs altogether which gives the necessary 2×10^{18} ergs/g to the outer solar mass. The resulting fluid velocity behind the shock is shown in Fig. 2. The velocity increases by approximately a factor 10 to a value of 1×10^{10} cm/sec at the point where the density has fallen to 30 g/cm^3. The fluid velocity well after the passage of the shock, also shown in Fig. 2, has reached twice the corresponding fluid velocity behind the shock.

At velocities greater than 10^{10} cm/sec, relativistic effects become important. Relativistic equations of motion (including shock continuity conditions), obtained by setting the divergence of the energy-momentum tensor equal to zero, have been considerably studied.[5] In the present application, the internal energy behind the shock is almost entirely in the radiation field; consequently the temperature never exceeds 100 kev and the equation of state is that of a radiation gas. The relativistic equations are being programmed for the IBM 709 computer, so that the numerical calculations shown in Fig. 2 can be extended to the lower densities at which the energies of cosmic-ray magnitude appear.

Meanwhile, we have found analytic solutions of considerable generality. Characteristic space-time curves exist for the one-dimensional relativistic equations. They are the trajectories of sound waves traveling in the same or the opposite direction to the fluid. They differ from nonrelativistic characteristics only in that the fluid and sound velocities are added according to the relativistic composition law for velocities. In case the fluid is isentropic or in case the fluid satisfies the equation of state $p=E/3$, the characteristic equations are integrable. For the latter case, the quantities $[(1+\beta)/(1-\beta)]E^{\sqrt{3}/2}$ and $[(1+\beta)/(1-\beta)]E^{-\sqrt{3}/2}$ are constant on the forward and backward characteristic, respectively, corresponding to the Riemann invariants of classical hydrodynamics. In these relations β is the fluid velocity divided by the velocity of light c, p is the pressure in the fluid at rest, and E is the

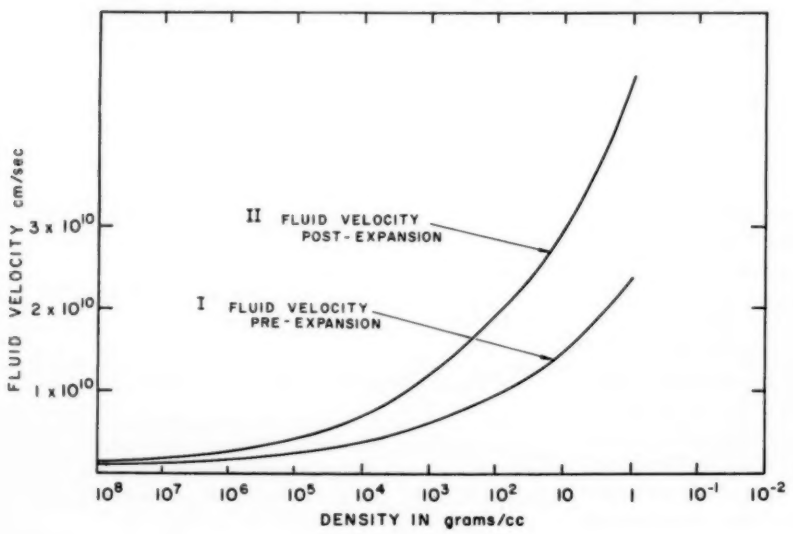
FLUID VELOCITY cm/sec
3 x 10^10
2 x 10^10
1 x 10^10
II FLUID VELOCITY POST-EXPANSION
I FLUID VELOCITY PRE-EXPANSION
10^8 10^7 10^6 10^5 10^4 10^3 10^2 10 1 10^-1 10^-2
DENSITY IN grams/cc

FIG. 2. Fluid velocity. Curve I: the velocity of the fluid immediately behind the shock as a function of initial density at the shock position. Curve II: the final velocity of the fluid after expansion with gravitation as a function of its initial density. These calculations were made for the star shown in Fig. 1 where the initial energy inserted at the center of the star has been adjusted so that the total energy behind the shock corresponds to escape for all points beyond the solar mass cut.

proper energy density. The expansion into a vacuum can be treated analogously to the corresponding well-known problem of classical hydrodynamics. If the initial energy density of the fluid is $\mu\rho_0 c^2$, where ρ_0 is the rest mass density of the constituent fluid particles, the kinetic energy per gram of rest mass after expansion is $\frac{1}{2}\mu^3$ for $\gamma >> 1$. The flow behind a shock can also be integrated because, in the case of interest, the preponderance of internal energy behind the shock is in the radiation field and $p = E/3$ accurately represents the equation of state. Then the final kinetic energy per gram of material having an initial density ρ_0 is $(\frac{1}{2})^{1+\sqrt{3}}(E_0/\rho_0 c^2)^{0.5(3-\sqrt{3})}$, where $E_0^{\sqrt{3}/2}$ is the value of the invariant on the forward characteristic, assumed the same at the shock front and in the subsequent expansion. An approximate value of E_0 is $30c^2$ ergs/cc, corresponding to the density 30 g/cm^3 at which the shock becomes relativistic. A more accurate value of E_0 as well as the actual change in E_0 during the expansion will be obtained from the numerical calculations.

The final kinetic energy of the expanded material gives directly the energy distribution of cosmic radiation. According to the polytrop solution[6] of the hydrostatic and radiative equilibrium conditions, the density ρ at any radius r is proportional to the temperature T at the same radius to the 3.25 power. In the outer layers of the star where the pressure is just the weight of material beyond r, the mass of this material is then proportional to $\rho T \approx \rho^{1.31}$. From the previous paragraph, γ, the final energy of material originally at density ρ, is proportional to $\rho^{-0.64}$, whence $M(<\rho) \propto N(>\gamma) \propto \gamma^{-(1.31/0.64)} = \gamma^{-2}$. It is expected that the numerical calculations for more accurate values of E_0 referred to above will show a somewhat less rapid decrease in intensity at higher energies, in better agreement with the experimental law, $N(>\gamma) \propto \gamma^{-1.6 \cdot 7,8}$

Above 10^4 Bev the initial density estimated from the analytic solution is less than 10^{-5} g/cm^3, and the mass in the remaining mantle of the star, less than 1 g/cm^2, is insufficient to contain the radiation field. However, it appears that plasma oscillations (to be discussed below) provide a mechanism by which the shock can propagate to much lower densities. Such a shock would be dissipated when the Debye length becomes equal to the scale height which occurs at a density of 10^{-12} g/cm^3. The corresponding material energy is about 10^8 Bev per nucleon, which is about the upper limit of the observed cosmic-ray spectrum.

The absolute intensity of cosmic radiation can be estimated from the frequency of supernova explosions, about 1 per 100 years, and the mean life of a cosmic ray within the galaxy, about 5×10^8 years, corresponding to an average density of 0.1 particle/cm^3 in the galaxy.[9] Since the volume of the galaxy is $\approx 5\times10^{66}$ cm^3, the radiation from a single explosion therefore occupies on the average a volume of 10^{62} cm^3. We estimate that the initial density corresponding to a final expansion energy of 10 Bev is about 1 g/cm^3. The mass in the star's mantle beyond this point is about 10^{26} g or 6×10^{49} protons, which distributed over a volume of 10^{62} cm^3 gives a density of 6×10^{-13} per cm^3. The corresponding total cosmic-ray flux is 0.02 per cm^2 sec, which agrees with experiment within the uncertainties in the estimate. As the cosmic-ray population at any instant represents the product of 5×10^6 supernova explosions diffused through the galaxy, density fluctuations should be very small.

The distribution of elements in cosmic radiation agrees well with that expected in the outermost parts of the supernova star as represented by the outer mantle of the sun. However, it is probable that the distribution is altered in the relativistic shock front. Viewed from the shock frame of reference, material is entering the shock front with velocity c and, in equilibrium with the radiation field, is leaving the shock front with a velocity $c/3$. Processes within the shock front must produce the created equilibrium radiation field and must also decelerate the ions to the velocity $c/3$. The radiation field acts directly on the electrons so that the width of the shock front is determined in part by the Compton scattering length and in part by the distance required for bremsstrahlung to effect radiative equilibrium. Within the shock width an electric field due to charge separation by the radiation pressures on the electrons decelerates the ions, predominantly hydrogen. Since the charge-to-mass ratio of the nonhydrogenic nuclei is one half that of hydrogen, these nuclei lose only one half their energy in traversing the electric field. Proton collisions, which are in part responsible for bringing these nuclei to rest, then become sufficiently disruptive to destroy the nuclear species for final energies larger than a few Bev.

The shock structure can be profoundly modified by plasma oscillations. The relative velocity of electrons and ions due to the charge separation described above produces a two-stream instability by which plasma oscillations may grow. Conse-

quently, it is likely that the internal energy in the first part of the shock is entirely carried in large-amplitude oscillations.[10] The majority of heavy ions may then be brought to relative rest by virtue of their phase with respect to these oscillations with very little destruction of the nuclear species. As mentioned above, these oscillations also provide a mechanism for the transmission of the shock to much lower densities. The damping of such oscillations by wave and by particle interactions and behavior of the material after the oscillations break up are subjects currently under study.

A final problem under investigation is the disposition of the blown-off material with energies below a few Bev. The amount of such material is at least one order of magnitude too large to be contained as cosmic radiation by the estimated galactic magnetic fields. We are examining mechanisms whereby such material is confined by local magnetic fields to the neighborhood of the explosion long enough to lose its energy by synchrotron radiation, as appears to be the present situation in the Crab nebula.

It is a pleasure to acknowledge discussions with and suggestions from many of our colleagues. We are particularly indebted in this regard to Dr. Edward Teller.

*Work done under the auspices of the U. S. Atomic Energy Commission.

†Consultant to the Lawrence Radiation Laboratory.

[1]E. M. Burbridge, G. R. Burbridge, W. A. Fowler, and F. Hoyle, Revs. Modern Phys. 29, 547 (1957).

[2]W. H. Grasberger is currently performing these calculations.

[3]R. H. White has performed these calculations using a hydrodynamic code which has been modified to include gravitation.

[4]We are indebted to J. M. Burgers who brought to our attention one such solution in plane parallel geometry; W. P. Robbertse and J. M. Burgers, Proc. Koninkl. Ned. Akad. Wetenschap. Amsterdam 52, 958, 1067 (1949).

[5]L. D. Landau and E. M. Lifshitz, Fluid Mechanics (Pergamon Press, New York, 1959).

[6]M. Schwarzschild, Structure and Evolution of the Stars (Princeton University Press, Princeton, New Jersey, 1958).

[7]S. F. Singer, in Progress in Elementary Particle and Cosmic-Ray Physics, edited by J. G. Wilson and S. A. Wouthuysen (Interscience Publishers, Inc., New York, 1958), Vol. IV.

[8]L. Biermann has pointed out that the cosmic-ray spectrum is known considerably more accurately than the errors in the equipment might indicate. However, our present calculations are uncertain by more than the indicated errors; L. Biermann and L. Davis, Z. Naturforsch. 13a, 909 (1958).

[9]The average density includes the "galactic halo" of trapped cosmic rays. An extensive review is given by V. L. Ginzburg, in Progress in Elementary Particle and Cosmic-Ray Physics, edited by J. G. Wilson and S. A. Wouthuysen (Interscience Publishers, Inc., New York, 1958), Vol. IV.

[10]E. N. Parker and D. A. Tidman, Phys. Fluids 3, 369 (1960).

PLASMA RESONANCE IN A RADIO-FREQUENCY PROBE

K. Takayama and H. Ikegami
Electrical Communication Laboratory, Musashino-shi, Tokyo, Japan

and

S. Miyazaki
Radio Research Laboratory, Kokubunji, Tokyo, Japan

(Received July 21, 1960)

As the frequency of a low-voltage rf signal superposed on a probe is swept within an adequate frequency range, the dc component[1] of the electron current due to the nonlinearity of the sheath impedance is measured. It has been found that a resonant increase appears in the current at the electron plasma frequency,

$$\omega_p = (4\pi N_0 e^2/m)^{1/2}, \qquad (1)$$

where N_0 is the electron density.

The schematic diagram of the apparatus used is shown in Fig. 1(a). The rf probe does not necessarily have to be a cathode-probe system, where the rf voltage is applied between the cathode and the probe. The experimental results are qualitatively unaffected by the shape or dimensions of the probe. In this experiment a plane probe consisting of a nickel disk 2 cm in diameter is

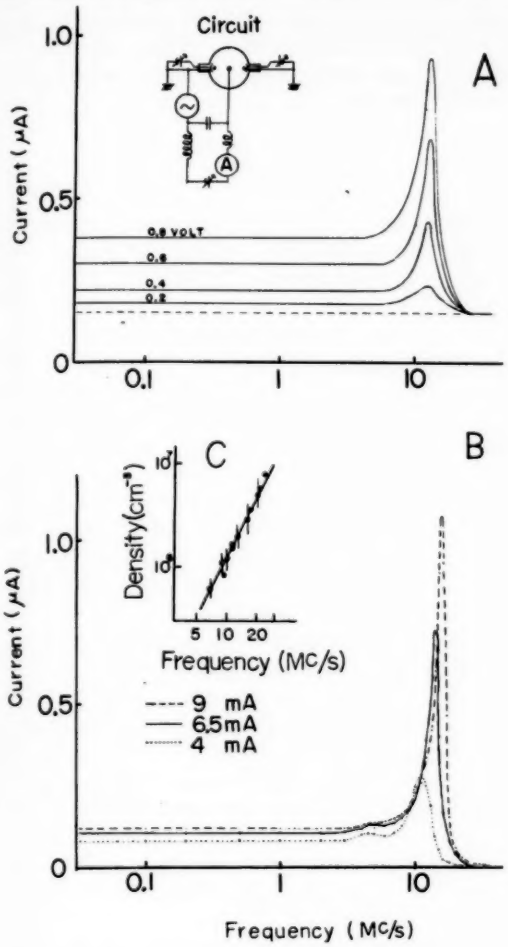

FIG. 1. (A) Characteristic curves of the rf probe with a constant discharge current of 5 ma, corresponding to 5.6×10^{6} electrons per cc, for various rf voltages ranging from 0.2 to 0.8 volt. The electron temperature is 1800°K. (B) Characteristic curves for various discharge currents corresponding to 1.2×10^{6}, 6.6×10^{6}, and 7.9×10^{6} electrons per cc. (C) Resonance frequency versus electron density determined by the Langmuir probe method. The solid line denotes Eq. (1).

used. It is biased relative to the cathode so as to be always negative with respect to the plasma potential, even when the rf voltage is superposed on the probe.

The discharge tube[2] is a Pyrex glass sphere 30 cm in diameter filled with mercury vapor at a pressure of 10^{-4} mm Hg. Two anode-hot cathode systems are arranged in such a way as to produce a very low density and homogeneous plasma, and the discharge currents can control the electron density. The plasma in the tube being of a diffusive type, there is no beam present.

The relation between the frequency of the rf voltage and the corresponding dc component of electron current to the probe is shown in Fig. 1(a) for various amplitudes of rf voltage with a constant discharge current of 5 ma, and with the probe set 0.5 volt below the plasma potential. In Fig. 1(b), however, the probe is set at the wall potential. The curves in this case are for various discharge currents with a constant rf potential difference of 0.4 volt.

Every characteristic curve in Fig. 1 consists of the following three frequency ranges: the first range where the electron current maintains a constant value independent of frequency, the second range where a resonance peak appears, and the third range where the superposed rf field has no effect on the dc current to the probe.

In the first frequency range, the electron current density at the probe surface for a superposed rf voltage $V\cos\omega t$ is given by

$$j = j_0\langle\exp(-eV\cos\omega t/kT)\rangle_{\mathrm{av}} = j_0 J_0(ieV/kT), \qquad (2)$$

where the average is taken over a long time. $J_0(iz)$ is the zeroth order Bessel function for a pure imaginary argument, and

$$j_0 = N_0 e(kT/2\pi m)^{1/2}\exp(-eV_0/kT).$$

T is the electron temperature, and V_0 is the potential difference between the plasma and the probe.

j_0 corresponds to the constant current in the third frequency range, since the Boltzmann distribution of electron density for the oscillating electric field in Eq. (2) is no longer valid when the frequency is higher than the electron plasma frequency. Accordingly Eq. (2) holds when the field changes slowly in a time interval of the order of ω_P^{-1}. The ratio of j to j_0 gives the electron temperature through the argument of the Bessel function.

In the second frequency range, it will be noted from Fig. 1(a) that the positions of the peaks along the frequency axis coincide with each other whenever the discharge current is the same. In Fig. 1(c) the values of resonance frequency are plotted against the electron density determined by the well-known Langmuir probe method. The solid line was calculated from Eq. (1). It is seen from the figure that the resonance occurs at the electron plasma frequency.

The height of a resonance peak depends not only on the magnitude of the rf voltage, but on the collision frequency of electrons with atoms. Thus this height decreases as the pressure is increased.

The mechanism of the resonance is interpreted in terms of the interaction between the electron beam and the plasma medium.[3-5]

In the experiment, the oscillating electric field applied between the plasma and the probe drives off some electrons from the positive ion sheath around the probe into the plasma during one half-cycle, and during the next half-cycle, because of the shielding effect of the plasma, the field cannot restore these electrons which were driven off. These electrons which are driven off can be regarded as an electron beam with its density modulated by the frequency of the oscillating field.

An electron beam of this kind is known to excite growing plasma waves[4] when the kinetic energy of the beam exceeds the thermal energy of the electrons of the medium.

This interpretation, in terms of a beam-plasma interaction, seems to be supported by the experiments shown in Fig. 2, where the resonance peak nearly vanishes when the energy supplied by the field to the electron beam becomes comparable to the thermal energy of the electrons.

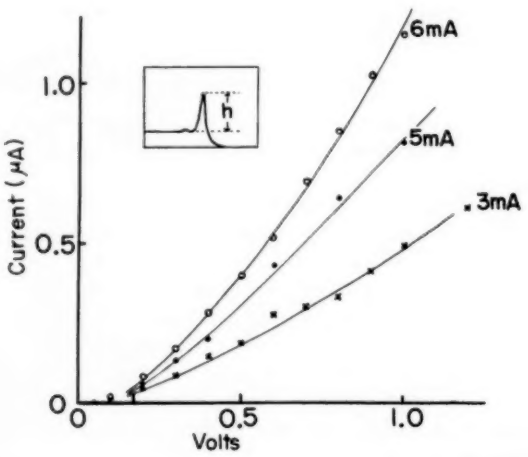

FIG. 2. The height of resonance peaks in μa versus rf potential difference in volts, for several discharge currents. The electron thermal energy is 0.17 ev which is shown by a short line on the abscissa.

The growing wave gives a density fluctuation $\tilde{N}_0$ of the following form:

$$\tilde{N}_0 = A \exp(\gamma d + i\varphi - i\omega t)$$
$$= \tilde{N} \exp(-i\omega t), \quad (3)$$

where d is a suitable distance; φ is a phase difference, expected to be π, given, in terms of the beam velocity u, by

$$\varphi \approx \omega d/u \approx \pi,$$

and γ is a growth rate which is a function of ω having a sharp maximum at $\omega = \omega_P$ and rapidly decreasing to zero for ω different from ω_P.[4,5]

The dc electron current in this case is given by

$$j = j_0 J_0(is)[1 - i\tilde{N} J_1(is)/N_0 J_0(is)], \quad (4)$$

where $s = eV/kT$, and J_1 is the first order Bessel function. In the first frequency range, $\tilde{N}$ is small enough that (4) reduces to (2).

At a frequency nearly equal to the electron plasma frequency, γ in (3) gives a maximum value of $\tilde{N}$, and j shows a resonant increase. Hence the resonance can be fully explained by the behavior of $\tilde{N}$.

The authors would like to thank Professor S. Kojima for his advice and encouragement, and also Dr. M. Sumi and many members of our Laboratory for their interesting discussions.

[1]S. Kojima, K. Takayama, and A. Shimauchi, J. Phys. Soc. (Japan) 8, 55 (1953).

[2]T. Ichimiya, K. Takayama, and Y. Aono, Proceedings of the Cospar Space Symposium (North Holland Publishing Company, Amsterdam, 1960).

[3]D. Bohm and E. P. Gross, Phys. Rev. 75, 1851 (1949); M. A. Lampert, J. Appl. Phys. 27, 5 (1956); J. H. Piddington, Phil. Mag. 46, 1037 (1955), and Phys. Rev. 101, 9, 14 (1956); J. R. Pierce and L. R. Walker, Phys. Rev. 104, 306 (1956); M. Sumi, Phys. Rev. Letters 2, 37 (1959); D. H. Looney and S. C. Brown, Phys. Rev. 93, 965 (1954); H. J. Merrill and H. W. Webb, Phys. Rev. 55, 1191 (1939).

[4]G. D. Boyd, L. M. Field, and R. W. Gould, Phys. Rev. 109, 1393 (1958); M. Sumi, J. Phys. Soc. (Japan) 14, 653 (1959).

[5]J. R. Pierce, J. Appl. Phys. 19, 231 (1948).

INFRARED MAGNETOREFLECTION IN BISMUTH. I. HIGH FIELDS

B. Lax, J. G. Mavroides, H. J. Zeiger, and R. J. Keyes
Lincoln Laboratory,* Massachusetts Institute of Technology, Lexington, Massachusetts
(Received August 4, 1960)

The pulsed-field infrared experiments on bismuth reported by Keyes et al.[1] at wavelengths between 10 and 22 μ and at room temperature, were originally interpreted as transitions corresponding to cyclotron resonance. Well-defined dispersion curves were obtained by reflection techniques. The value of the magnetic field at the center of each line and the measured wavelength were utilized to obtain an apparent effective mass from the well-known cyclotron equation $m^* = eH/\omega_c c$. Three distinct sets of mass values obtained from the strongest absorption data[1] yielded apparent effective masses for electrons which showed a large variation with magnetic field, with mass values above and below those deduced from the de Haas-van Alphen effect[2] and microwave cyclotron resonance.[3] This suggested that the large change in the effective masses was due to a rapid change in the curvature of the energy bands. To explain this a theoretical expression was developed for the energy-momentum relation, assuming only two sets of interacting energy bands which are located near the edge of the zone. The derivation uses the $\vec{k}\cdot\vec{p}$ perturbation method, following the work of Kane[4] on InSb and that of Cohen and Blount[5] on bismuth. We showed that the nonparabolic energy dependence of the bands could be represented by the expression[6]

$$\epsilon\left(1+\frac{\epsilon}{\epsilon_g}\right)=\vec{p}\cdot\frac{\alpha}{2}\cdot\vec{p}, \qquad (1)$$

where ϵ_g is the energy gap and α is the inverse mass tensor at the bottom of the conduction band and (with a minus) at the top of the valence band. When a magnetic field is applied, the Hamiltonian including spin becomes

$$\mathcal{H}_{\text{eff}}=\left[\vec{\Pi}\cdot\frac{\alpha}{2}\cdot\vec{\Pi}+\frac{\beta}{2}\vec{\sigma}\cdot g\cdot\vec{H}\right]\frac{1}{1+\epsilon/\epsilon_g}, \qquad (2)$$

where $\vec{\Pi}=\vec{p}+e\vec{A}/c$, $\vec{A}$ is the magnetic vector potential, β is the Bohr magneton, and g is the effective spectroscopic splitting tensor[5] at the bottom of the bands. The solution of Eq. (2) with the magnetic field taken in the z direction yields an equation for the eigenvalues for the valence and conduction bands,

$$\epsilon_n\left(1+\frac{\epsilon_n}{\epsilon_g}\right)=(n+\tfrac{1}{2})\hbar\omega_c+\frac{\hbar^2k_z^2}{2m_z}\pm\tfrac{1}{2}\beta g_{\text{eff}}H, \qquad (3)$$

where

$$\epsilon_n=-\tfrac{1}{2}\epsilon_g\pm\left\{(\tfrac{1}{2}\epsilon_g)^2+\left[(n+\tfrac{1}{2})\hbar\omega_c+\frac{\hbar^2k_z^2}{2m_z}\pm\tfrac{1}{2}\beta g_{\text{eff}}H\right]\epsilon_g\right\}^{1/2}, \qquad (4)$$

$\omega_c = eH/m^*c$, cyclotron mass $m^*=[\alpha_1\alpha_2\alpha_3 m_z]^{-1/2}$, $m_z=\alpha_1^{-1}\lambda_1^2+\alpha_2^{-1}\lambda_2^2+\alpha_3^{-1}\lambda_3^2$, and $g_{\text{eff}}=[g_1^2\lambda_1^2+g_2^2\lambda_2^2+g_3^2\lambda_3^2]^{1/2}$; the α_i are the components of the inverse mass tensor α and the λ_i are the directional cosines of the magnetic field relative to the principal ellipsoidal axes. The plus sign in front of the radical in Eq. (4) gives the energy of the conduction band and the minus sign, that of the valence band.

In attempting to fit the experimental curves for bismuth with Eq. (4), assuming cyclotron resonance, it was necessary to choose very small values for the energy gap ϵ_g (~0.01 ev) and also for the effective masses; at room temperature the data yielded masses at the Fermi level approximately one quarter of those found at low temperatures.[2,3] In addition, two other dilemmas were present. The first involved the existence of well-defined "resonant" reflection traces, such as shown in Fig. 1. This was in contradiction

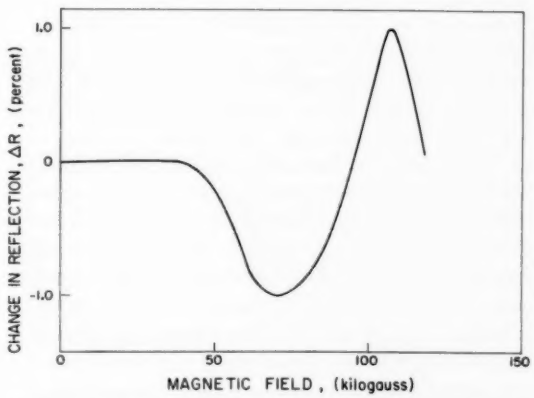

FIG. 1. Trace of the "resonance" dispersion curve for bismuth obtained by reflection using pulsed magnetic fields at infrared wavelength, $\lambda = 13.0$ microns.

with the expected magnetoplasma effect for bismuth at room temperature, where the plasma wavelength occurs at ~10 μ for a carrier concentration of $n \approx 10^{18}/\text{cm}^3$ as derived from galvanomagnetic data.[7] From theoretical considerations, a resonant reflection trace should not have been observed over at least part of the wavelength range (i.e., near 20 μ). The second puzzle involved the appearance of two resonances with the magnetic field in the binary direction $[11\bar{2}0]$, where only one was expected. The intensity of the extra line appeared greater than that of the line which agreed best with known values of masses.

These difficulties all seem to be resolved if it is assumed that the observed transitions do not correspond to intraband cyclotron resonance but are interband transitions between magnetic levels of the valence and conduction bands near the edge of the Brillouin zone. Such direct transitions are known to have high absorption coefficients from similar studies in semiconductors.[8] The estimated penetration depth for this process in bismuth is of the order ~0.1 μ, whereas that for free carrier penetration due to the presence of a plasma (for $\omega\tau \gg 1$) would be one order of magnitude larger, i.e., ~1 μ.

The explanation of the first dilemma can be considered in a more general context as suggested by Dresselhaus.[9] The argument is similar to that of Anderson[10] for the direct observation of cyclotron resonance of minority carriers in the presence of majority carriers even at a frequency well below the plasma frequency. If the complex conductivity of the medium consists of a large part $\sigma(\omega, H)$ which varies slowly with magnetic field and a small part $\Delta\sigma(\omega, H)$ which varies "resonantly" with magnetic field, then the "resonance" line will be observable, modified in shape only slightly by the background absorption. Thus a trace as in Fig. 1 of reflection versus magnetic field will represent the "resonance" due to $\Delta\sigma(\omega, H)$. In the particular case of bismuth the dominant contributions to $\sigma(\omega, H)$ are the nonresonant background interband transitions and $\Delta\sigma(\omega, H)$ is due to the small "resonant" interband transitions between Landau levels. The analysis for such a situation in the absence of a plasma has been treated for semiconductors.[11] The important conclusion for other metals is that the presence of a large plasma contribution $\sigma(\omega, H)$ due to the conduction electrons should not interfere with the observation of "resonant" interband transitions between Landau levels, although the frequency at which these observations are made is below the plasma frequency. However, the intensity of the magnetoreflection lines in a more highly conducting metal would probably be smaller than that in bismuth.

In order to test the hypothesis that interband transitions have been observed, the pulse data reported were replotted in terms of photon energy as a function of magnetic field. The three sets of lines converged to a value at zero field of 0.040 $\pm$ 0.005 ev, corresponding to the energy gap near the edge of the zone at room temperature. Had these been cyclotron resonance transitions the lines would have converged to the origin. Furthermore, upon re-examining the original photographic traces, we found additional weak lines corresponding to what we believe to be transitions between higher quantum states. With this in mind, it is now possible to interpret the data from a model of the energy level diagram shown in Fig. 2, including spin splitting.[5] However, since the scatter of the present data was large, only a semiquantitative interpretation was possible. It appears that some of the points in the $[11\bar{2}0]$ direction can be explained as transitions between the large mass levels corresponding to the resonance mass value $m^* \sim 0.2m_0$. These appear as reasonably well-defined lines.

We again attempted to interpret the data, this time assuming interband transitions and using the theory for nonparabolic bands since on theoretical grounds Eq. (4) should apply; however, the pulsed data and those in the following Letter indicate that the deviation from parabolicity is not as large as that predicted by this equation. It is possible that an analysis similar to the pres-

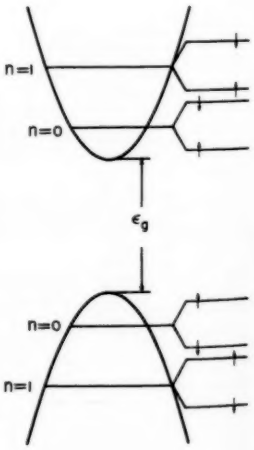

FIG. 2. Model for bismuth of the energy levels near the edge of the Brillouin zone in a magnetic field. For the low-mass directions, the spin splitting of the Landau levels is determined from $g_{\text{eff}} \approx 2m_0/m^*$. The arrows indicate $\vec{j}$ states rather than pure spin states.

ent one, but modified to take into account the effects of other bands, would provide a better model for the quantitative treatment of the data. The effective Hamiltonian given in Eq. (2) can be readily extended to the case of a band interacting with a number of other bands, but the location and character of other bands near the zone edge in bismuth are not at present known.

This experiment indicates the power of the method of interband magnetoreflection measurements in exploring the energy band structure of metals. Masses and g values for both conduction and valence bands can be studied. In addition, bands can be studied not only at the Fermi surface (as with de Haas-van Alphen effect and cyclotron resonance) but at energies above the Fermi energy; and information about lower lying bands can be obtained. Furthermore, the temperature dependence of the band parameters can be studied up to room temperature and possibly higher. It is interesting that the detection of transitions due to a mass as large as $\sim 0.2m_0$ is possible at room temperature and with transient pulse techniques. This lends encouragement to experiments in other metals with high carrier masses at low temperatures, with steady magnetic fields. By using magnetic fields of the order of 100 kilogauss and higher, this method could be applicable to the investigation of a number of metals.

The pulse experiments logically suggested the possibility that this phenomenon could be observed at lower fields and at low temperatures with photon energies well above those used in the pulse experiments, thereby permitting the observation of interband transitions to higher quantum numbers. Such experiments were indeed successfully realized and are discussed in the following Letter.

We wish to thank Dr. L. M. Roth and Professor G. F. Koster for valuable discussion in connection with the theory for two interacting bands in a magnetic field.

---

*Operated with support from the U. S. Army, Navy, and Air Force.

[1]R. J. Keyes, S. Zwerdling, S. Foner, H. H. Kolm, and B. Lax, Phys. Rev. 104, 1804 (1956). In this experiment damped oscillatory magnetic fields up to 150 kgauss, with a half period of approximately 150 microseconds, were used.

[2]B. Lax, K. J. Button, H. J. Zeiger, and L. M. Roth, Phys. Rev. 102, 715 (1956).

[3]J. K. Galt, W. A. Yager, F. R. Merritt, B. B. Cetlin, and A. D. Brailsford, Phys. Rev. 114, 1396 (1959).

[4]E. O. Kane, J. Phys. Chem. Solids 1, 249 (1957).

[5]M. H. Cohen and E. I. Blount, Phil. Mag. 5, 115 (1960).

[6]B. Lax, Bull. Am. Phys. Soc. 5, 167 (1960); B. Lax and J. G. Mavroides, Advances in Solid-State Physics, edited by F. Seitz and D. Turnbull (Academic Press, New York, 1960), Vol. 9. Recently P. A. Wolff has also obtained the above result (private communication).

[7]B. Abeles and S. Meiboom, Phys. Rev. 101, 544 (1956).

[8]W. C. Dash and R. Newman, Phys. Rev. 99, 1151 (1955).

[9]G. Dresselhaus (private communication).

[10]P. W. Anderson, Phys. Rev. 100, 749 (1955).

[11]B. Lax, Phys. Rev. Letters 4, 511 (1960).

INTERBAND MAGNETOREFLECTION IN BISMUTH. II. LOW FIELDS

R. N. Brown, J. G. Mavroides, M. S. Dresselhaus, and B. Lax
Lincoln Laboratory,* Massachusetts Institute of Technology, Lexington, Massachusetts
(Received August 4, 1960)

Magnetoreflection measurements in bismuth have been carried out at liquid air temperatures and below with static magnetic fields up to 38 kilogauss. The measurements were made using a magnetospectrometer similar to that of Zwerdling et al.,[1] except that infrared reflection techniques were used. Best results were obtained by sweeping the magnetic field at a fixed wavelength. This was done at wavelengths between 6 and 14 μ, using an NaCl prism.

Single-crystal specimens were grown from Bi of "99.999" % purity. Surfaces were obtained by cleaving at nitrogen temperature along a trigonal plane. A diamond saw was used to cut two samples 2 mm × 3 mm × 25 mm from the crystal. The cuts were made so that the magnetic field parallel to the exposed trigonal surface was in one case along the bisectrix axis $[10\bar{1}0]$, and in the other case along the binary axis $[11\bar{2}0]$. The surface was then polished with Buehler No. 3 grit to obtain a good reflecting surface. The surface strains were removed by electropolishing.[2] Back-reflection Laue patterns gave the crystal orientation and revealed minor strains. The samples

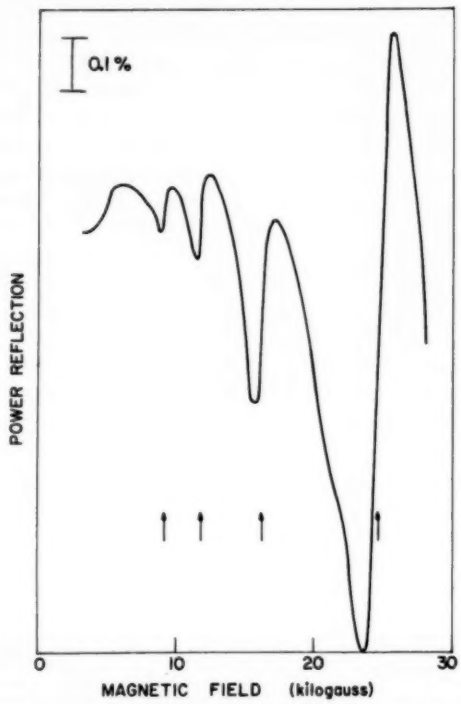

FIG. 1. Variation of power reflection with magnetic field on bismuth for photon energy $\Delta\epsilon = 0.1041$ ev. The arrows indicate the field for which interband transitions of this photon energy occur. The magnetic field is along $[11\bar{2}0]$ and the inner Dewar is at 4.2°K.

were freely mounted with Teflon tape in a copper sample holder attached by a copper rod to the bottom of the inner Dewar which contained either liquid helium or liquid air.[3]

A typical trace of the variation of power reflection with magnetic field at constant photon energy is shown in Fig. 1. The line shape is characteristic of dispersion curves. The center of the straight portions of trace, indicated by arrows, is taken as the value of the magnetic field for which the infrared photon induces an interband transition between a magnetic level of the valence band to one of the conduction band. The resolution was sufficient to identify lines with peak to peak intensities from 3% to 0.05%. The intensity of a given line was found to increase with increasing magnetic field and to decrease with increasing quantum number.

Each interband transition appearing in the magnetic field trace (as in Fig. 1) was identified, and the results plotted in terms of photon energy $\Delta\epsilon$ vs magnetic field H, as in Fig. 2 $[11\bar{2}0]$ and Fig. 3 $[10\bar{1}0]$. These measurements were obtained near liquid helium temperature. Quantitatively, the results at liquid air temperature were essentially the same except that the lines sharpened and increased in intensity as the temperature was lowered. For H along $[11\bar{2}0]$, only the light-mass ($\sim 0.01 m_0$) transitions are seen. For H along $[10\bar{1}0]$, both light ($\sim 0.01 m_0$) and heavy ($\sim 0.02 m_0$)

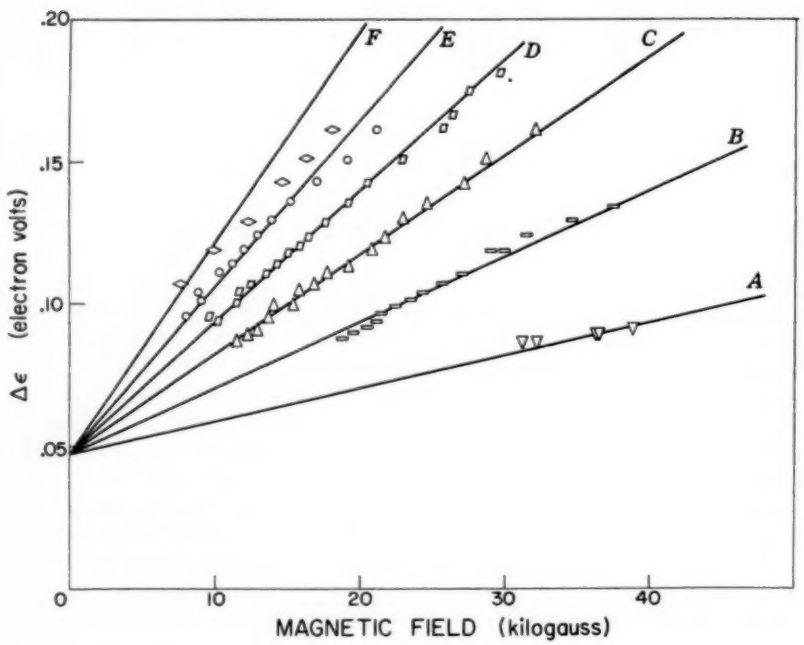

FIG. 2. Photon energy for interband transition vs magnetic field on bismuth. The magnetic field is along $[11\bar{2}0]$ and the inner Dewar is at 4.2°K. The various transitions are identified by A, $(0\uparrow 0\downarrow)$; B, $(0\downarrow 0\downarrow)$ and $(1\uparrow 1\uparrow)$; C, $(1\uparrow 1\downarrow)$ and $(1\downarrow 1\uparrow)$; D, $(1\downarrow 1\downarrow)$ and $(2\uparrow 2\uparrow)$; E, $(2\uparrow 2\downarrow)$ and $(2\downarrow 2\uparrow)$; and F, $(2\downarrow 2\downarrow)$ and $(3\uparrow 3\uparrow)$. (See Fig. 2 of preceding Letter.)

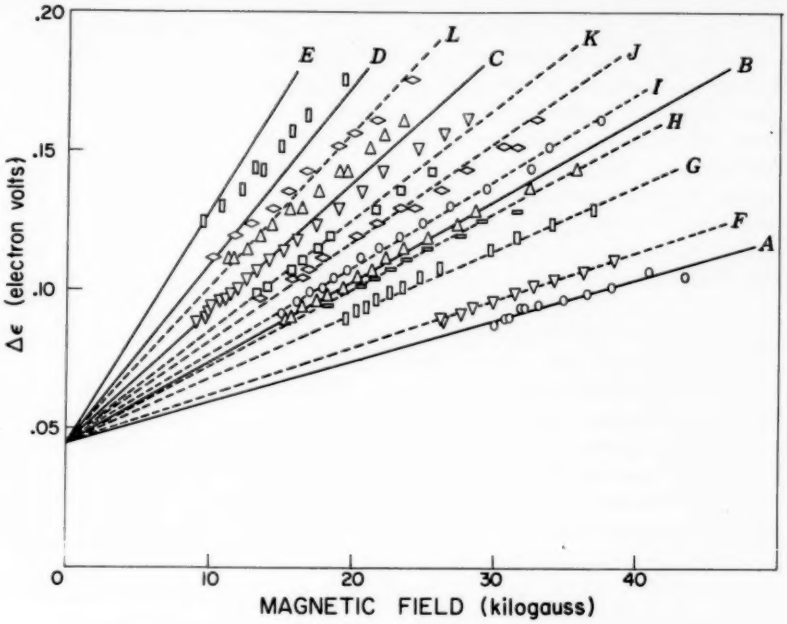

FIG. 3. Photon energy for interband transition vs magnetic field on bismuth. The magnetic field is along [10$\bar{1}$0] and the inner Dewar is at 4.2°K. The light-carrier transitions follow the solid lines and the heavy-carrier transitions follow the dashed lines. The identification for the light mass is A, (0↑0↓); B, (0↓0↓) and (1↑1↑); C, (1↑1↓) and (1↓1↑); D, (1↓1↓) and (2↑2↑); E, (2↑2↓) and (2↓2↑). The identification for the heavy mass is F, (0↓0↓) and (1↑1↑); G, (1↑1↓) and (1↓1↑); H, (1↓1↓) and (2↑2↑); I, (2↑2↓) and (2↓2↑); J, (2↓2↓) and (3↑3↑); K, (3↑3↓) and (3↓3↑); L, (3↓3↓) and (4↑4↑). (See Fig. 2 of preceding Letter.)

masses are observed. Experimentally, the light masses are distinguished from the heavy masses by their relatively greater intensity and by the disappearance of some of the light-mass transitions when polarized radiation is used.

For both orientations, the points identified with a given transition follow straight lines, particularly for transitions with low quantum number. As in the pulsed-field experiments,[4] the results of Figs. 2 and 3 show a convergence of the straight lines for different transitions to an energy gap $\epsilon_g = 0.047 \pm 0.003$ ev.[5] The value for ϵ_g was determined in each case by drawing the best straight line through the experimental points associated with low quantum number. The lines drawn through the experimental points for high quantum number were joined to this value of the gap. The deviation from linearity for the higher transitions may be an indication of nonquadratic energy surfaces at these high energies.

In order to interpret the interband transitions, the model illustrated by Fig. 2, of the preceding paper was adopted. The energy of an interband transition is written as

$$\Delta\epsilon = \epsilon_g + (n_c + \tfrac{1}{2})\hbar\omega_c{}^c \pm \tfrac{1}{2}\beta g_{\text{eff}}{}^c H + (n_v + \tfrac{1}{2})\hbar\omega_c{}^v \pm \tfrac{1}{2}\beta g_{\text{eff}}{}^v H, \quad (1)$$

in which c and v refer to the conduction and valence bands, respectively, g_{eff} is the spectroscopic splitting factor, and β is the Bohr magneton. Using this expression, one can in principle determine from the four lowest transitions the masses and g values for both the valence and conduction bands. From Eq. (1), we find that the experimental results are consistent with approximately equal masses for the two bands and g factors approximately as given by Cohen and Blount,[6]

$$g_{\text{eff}} \approx 2m_0/m^*. \quad (2)$$

For H in the [11$\bar{2}$0] direction, the value $m_c{}^*/m_0 = 0.010$ is obtained for the mass of the conduction band. The effective mass of the valence band $m_v{}^*/m_0$ differs from $m_c{}^*/m_0$ by less than 10%. For H in the [10$\bar{1}$0] direction, we find the effective mass of the light electron to be $m_c{}^*/m_0 = 0.0080 \pm 0.0002$ with $|(m_c{}^* - m_v{}^*)/m_0| < 0.0003$. For the heavy electrons in this orientation there are two possibilities. Either the valence and conduction masses are approximately equal, with $m_c{}^*/m_0 = 0.019$ and $|(m_c{}^* - m_v{}^*)/m_0| < 0.002$; or, $m_c{}^*/m_0$ and $m_v{}^*/m_0$ are quite different, $m_c{}^*/m_0 = 0.019$ and $m_v{}^*/m_0 = 0.011$. This ambiguity can be resolved by using higher fields to look for the lowest observable transition (0↑0↓). The conduction band masses are in agreement with those

deduced from Shoenberg's[7] de Haas-van Alphen data and Galt et al.[8] (cyclotron resonance).

These results definitely indicate that the theoretical expression, Eq. (4) of the preceding paper, does not give a good fit. The curvature for the theoretical curves of energy versus magnetic field is much sharper than that indicated in Figs. 2 and 3. Extension of these measurements to higher magnetic fields will permit the study of the departure from parabolicity and the added resolution will allow the independent determination of the masses for the valence and conduction bands together with the g values associated with them.

We are grateful of Dr. G. B. Wright for his generous loan of the apparatus for carrying out these experiments, Mr. E. Warekois for x-ray studies of the samples, Mr. D. F. Kolesar for his capable assistance with the experimental work, and Dr. G. Dresselhaus and Dr. H. J. Zeiger for many fruitful discussions.

*Operated with support from the U. S. Army, Navy, and Air Force.

[1]S. Zwerdling, B. Lax, L. M. Roth, and K. J. Button, Phys. Rev. 114, 80 (1959).

[2]G. E. Smith, Phys. Rev. 115, 1561 (1959).

[3]Measurements on this apparatus indicate that the temperature of the sample holder differed by no more than 2°K from the bath temperature using the liquid air refrigerant. The temperature of the sample was not measured when liquid helium was used, but it is believed that the sample was somewhat above 4°K.

[4]B. Lax, J. G. Mavroides, H. J. Zeiger, and R. J. Keyes, preceding Letter [Phys. Rev. Letters 5, 241 (1960)].

[5]A crude attempt to estimate this gap was made by W. S. Boyle and K. F. Rodgers, Phys. Rev. Letters 2, 338 (1959). They stated that the "edge at 20 microns would set the lower lying states at about 0.05 ev below the Fermi surface." If $\mathcal{E}_F$ (≈ 0.018 ev) were subtracted this would give $\mathcal{E}_g \approx 0.03$ ev, which is too small.

[6]M. H. Cohen and E. I. Blount, Phil. Mag. 5, 115 (1960).

[7]D. Shoenberg, Physica 19, 791 (1953); B. Lax, K. J. Button, H. J. Zeiger, and L. M. Roth, Phys. Rev. 102, 715 (1956).

[8]J. K. Galt, W. A. Yager, F. R. Merritt, B. B. Cetlin, and A. D. Brailsford, Phys. Rev. 114, 1396 (1959).

DIFFERENCE IN LATTICE SPECIFIC HEATS IN THE NORMAL AND SUPERCONDUCTING PHASES*

H. A. Boorse, A. T. Hirshfeld, and H. Leupold
Pupin Physics Laboratories, Columbia University, New York, New York
(Received August 18, 1960)

A series of measurements of the heat capacity of annealed niobium in the normal and superconducting phases, carried out in this laboratory, was reported at the 1958 International Conference on the Electronic Properties of Metals at Low Temperatures.[1] One of the principal objectives of the investigation was the determination of the temperature dependence of the superconducting electronic specific heat C_{es}, and its comparison with the detailed predictions of the Bardeen, Cooper, Schrieffer[2] (BCS) theory. Although an exponential dependence of C_{es} with temperature was observed as required by the theory, it was not possible to make measurements below $0.2T_c$ and hence the predicted change to the lower temperature exponential[3] could not be investigated. A new cryostat was therefore constructed for this and other investigations and the research on niobium was resumed.

According to current ideas, the determination of C_{es} requires a measurement of C_n, the specific heat of the metal in the normal phase, and of C_s, the specific heat in the superconducting phase. Values of C_n were found to follow the relation:

$$C_n = \gamma T + A(T/\Theta)^3,$$

with $\gamma = 7.62$ millijoules/mole deg^2 and $\Theta = 231$°K. Values of the normal lattice term, $A(T/\Theta)^3$, were subtracted from C_s at the same temperature to yield values of C_{es} which, down to 1.7°K, were found to satisfy the following relation:

$$C_{es} = \gamma T_c[10 \exp(-1.63T_c/T)],$$

with $T_c = 9.09$°K. It should be pointed out that this procedure assumes that the superconducting specific heat consists of independent lattice and electron contributions and that the lattice specific heat is identical in the normal and superconducting phases.

The validity of this method for determining C_{es} was discussed some time ago by Chester[4] who pointed out that it could be proved only for those superconductors which obey the similarity rule for critical magnetic fields. Critical field studies of isotopic mixtures are limited, but where they have been made it has been found that the similarity principle holds. On the basis of this evidence it seems to have been assumed that the principle holds generally and that therefore the phonon spectrum in the normal and superconducting phases, at least for superconductors of several isotopes, is the same. Further, the current theoretical point of view as provided by the BCS theory presents no contradiction to these ideas.

The recent specific heat measurements of Bryant and Keesom[5] on indium now indicate that the phonon spectrum in that superconductor at least is not the same in the normal and superconducting phases.

The purpose of this Letter is to present evidence that in niobium also the lattice specific heat is different in the two phases. When our measurements were taken at temperatures less than 1.7°K the <u>total</u> superconducting specific heat was found to be less than the corresponding lattice heat in the normal state as shown in Fig. 1. After another independent set of measurements had confirmed this result, a complete remeasurement of the superconducting and normal heat capacities was made using as a thermometer a 1-watt Allen-Bradley carbon resistor. This resistor was carefully recalibrated by comparing the resistance with (1) the vapor pressure of helium from 1.02°K to 4.2°K, (2) the transition temperature of a sample of very pure lead taken as 7.17°K,[6] and (3) the triple point of normal hydrogen, 13.96°K. The results gave a complete confirmation of the 1958 measurements and also confirmed that C_s at the lowest temperatures was smaller than the normal lattice heat in the

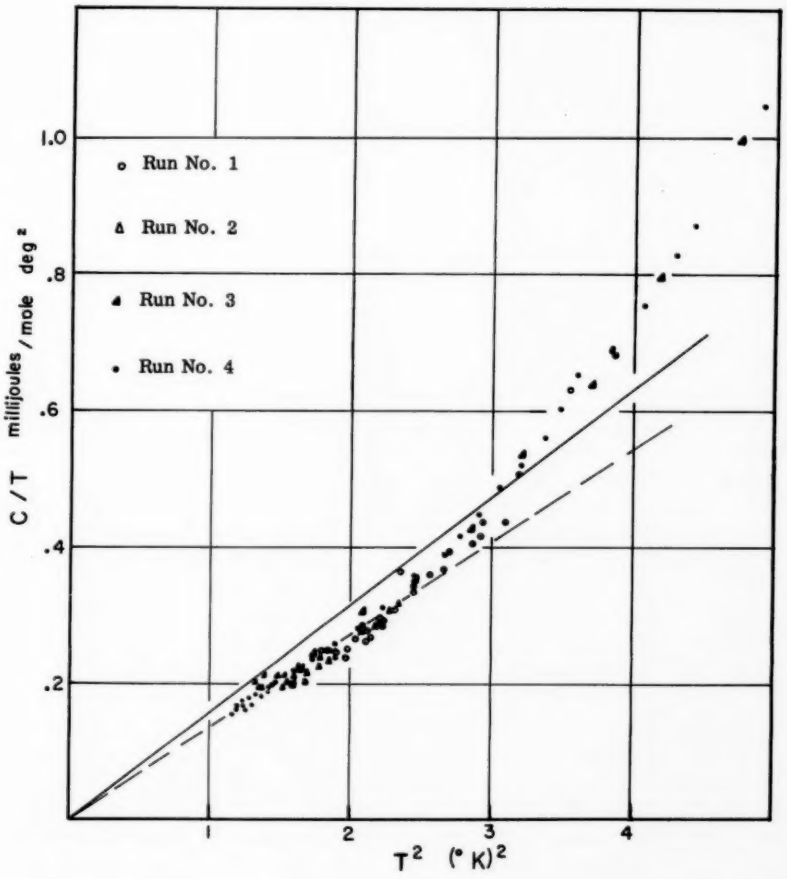

FIG. 1. Values of C/T vs T^2 for niobium in the superconducting phase at low reduced temperatures. The full line represents the lattice heat taken from the normal data. The dashed line is drawn to show the tentative assumption of a linear relation for C_S at the lowest temperatures.

same range. Figure 1 shows the results of the four separate measurements below $T^2 = 5.0$. If less weight is given to the first and less precise set of data represented by the open circles, then below $T^2 = 2.2$ ($T = 1.48°K = 0.163T_C$) the individual determinations fall along a straight line which passes through the origin. A possible interpretation would be that the electronic specific heat at this temperature is inconsiderable in comparison with the superconducting lattice specific heat and that the latter can be represented by a T^3 term with an altered value of Θ which may be evaluated from the data as 243°K.

We regard this interpretation as provisional since a number of small corrections must be made to these data to account for the thermal capacities of the heater wires wound around the sample, for the Allen-Bradley carbon resistor, and for the glyptal adhesive. These corrections, now being investigated, would all be subtracted and their influence, if significant, could only increase the discrepancy with the normal line. A detailed report of the measurements will be submitted in the near future.

We wish to thank Mrs. Claire Metz, Mrs. Sarina Hirshfeld, and Dr. Truly C. Hardy for their kind assistance in taking these measurements.

*This research was supported in part by the National Science Foundation, the Office of Naval Research, and Linde Air Products Company.

[1]International Conference on the Electronic Properties of Metals at Low Temperatures, Geneva, New York, August 25-29, 1958 (unpublished).

[2]J. Bardeen, L. N. Cooper, and J. R. Schrieffer, Phys. Rev. 108, 1175 (1957).

[3]H. A. Boorse, Phys. Rev. Letters 2, 391 (1959).

[4]G. V. Chester, Phys. Rev. 104, 883 (1956).

[5]C. A. Bryant and P. H. Keesom, Phys. Rev. Letters 4, 460 (1960).

[6]W. B. Pearson and I. M. Templeton, Phys. Rev. 109, 1094 (1958).

CHANGES IN SUPERCONDUCTING CRITICAL TEMPERATURE PRODUCED BY ELECTROSTATIC CHARGING*

R. E. Glover, III and M. D. Sherrill
University of North Carolina, Chapel Hill, North Carolina
(Received June 16, 1960; revised manuscript received August 29, 1960)

In the process of charging a parallel plate condenser, electrons are added to one plate and removed from the other one. Using a film 100 A thick as one of the condenser plates, it is possible to add or subtract about one electron for each 10^4 atoms. The maximum charge that can be added is limited by the breakdown strength of dielectrics, typically on the order of 10^6 v/cm. The effect of electrostatic charging on the conductivity of a metal film has been investigated repeatedly over the last fifty years.[1-3] Recent measurements by Deubner and Rambke[4] and by Bonfiglioli, Coen, and Malvano[5,6] have shown that the normal-state conductivity of metals can be modified by electrostatic charging (field effect). Changes of relative conductivity on the order of one in 10^4 have been produced. The conductivity of the films can be increased or lowered depending on the sign of the added charge.

We have made measurements of the effect of charging on the normal-state conductivity of films of gold and have examined the effect on both the superconducting transition temperature and the normal-state conductivity of tin and indium. Charging resulted in a change in the normal-state conductivity of all metals tried. It caused a change in the transition temperature of the superconducting materials.

Ruby (muscovite) mica substrates about 5 μ thick were used for the experiments. A gold coating was evaporated onto the back side to serve as one plate of the condenser, and gold potential and current contact patches were placed on the front. The substrates were then placed in a vacuum system and the film to be studied was evaporated so as to form the second plate of the condenser. Charging voltages of 150 volts were applied giving a maximum electric field of 3×10^5 v/cm. The conductivity of the film was measured using a 1000-cycle bridge. Film thickness was estimated from the temperature-dependent part of the resistance.

Of the metals examined, gold would be expected to have the simplest conductivity mechanism. Our gold films were condensed at room temperature. Negative charging resulted in an increase in conductivity while positive charging caused a decrease. The relative change in conductivity was

of the same order of magnitude as the ratio of added or subtracted electrons to the number of atoms in the film. Measurements made at room temperature and at 77°K gave essentially the same results. The magnitude of the change in conductivity was the same for positive and negative charging.

Tin and indium films were prepared by evaporation onto mica substrates held at liquid nitrogen temperature. The films were annealed to about 200°K. Measurements were made of the normal-state field effect as the films were cooled down to liquid helium temperature. The effect in both indium and tin was opposite in direction to that found for gold. Negative charging decreased the conductivity while positive charging increased it. For tin the effect was very much larger than for indium.

For the superconducting measurements the film temperature was slowly lowered through the transition region. Resistance vs temperature curves for an indium and a tin film are shown by the dashed curves in Figs. 1 and 2. The next step was to stabilize the temperature at various points in the transition region and measure the change of resistance caused by charging. The results are shown by the solid curves of Figs. 1 and 2. The displacement of the transition curve necessary to cause the observed resistance changes was calculated from the slope of the R vs T traces.

Qualitative measurements made in the superconducting transition region for five indium films showed in every case an increase in resistance with negative charging and a corresponding decrease with positive charging. This effect is the same in sign but much larger than that found for normally conducting indium. The measured resistance changes correspond to a decrease in transition temperature with negative charging. Quantitative measurements were made on three indium films. Thicknesses ranged from 60 to 120 A. The results of Fig. 1 are typical. A field of 2.6×10^5 v/cm produced a shift in transition temperature on the order of 10^{-4}°K. Approximately 3×10^{-5} electron were added for each atom of the film. The amount of added charge was obtained from capacity measurements and the charging voltage. The number of atoms was calculated from the thickness estimate using the normal density of indium. To an accuracy of 10% the decrease in transition temperature caused by negative charging was equal to the increase caused by adding positive charge.

The effect of charging on the transition temperature of tin was opposite to that found for indium. Qualitative measurements on seven films all showed an increase in transition temperature with negative charging. Quantitative results were obtained with four tin films having thicknesses from 70 to 110 A. Results typical of three of these are shown in Fig. 2. Here again the mag-

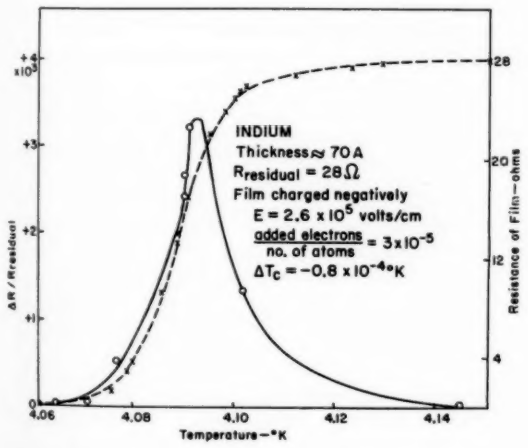

FIG. 1. Transition curve and change of resistance caused by negative charging of an indium film. Positive charging causes a change in resistance of the same size but in the opposite direction.

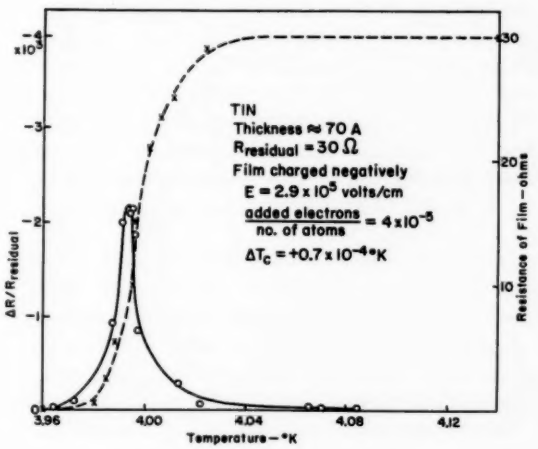

FIG. 2. Transition curve and change of resistance caused by negative charging of a tin film. Positive charging produces a change in resistance of the same size but in the opposite direction.

nitudes of the shifts of transition temperature with positive and negative charging were equal. It should be noted that the effect of charging on the resistance of tin films is opposite in sign in the superconducting transition region to that found for normally conducting material. The fourth tin film showed a shift in transition temperature an order of magnitude larger. For this film, the size of the effect was not symmetrical with respect to charge, the increase in transition temperature being about six times larger than the decrease. However, the width of the transition region was also an order of magnitude larger than for the other films, perhaps indicating a lack of uniformity.

After the first experiments on tin had been made but before measurements on indium were started, Donald Seraphim pointed out to us that an effect similar to the one observed might result if the substrate were piezoelectric. Strains which would depend on the sign of the applied charge could cause changes in transition temperature. The space group $C_{2h}(2/m)$ usually quoted for muscovite[7] has a center of symmetry, a property that rules out the possibility of piezoelectric behavior. Unfortunately, a closer look at the literature indicates that the details of the muscovite structure are still in doubt since the proposed structure does not account for all of the x-ray diffraction lines.[8] Accordingly, experiments were made to try and detect piezoelectric behavior in muscovite. None was found. Strips of mica 3 mm by 19 mm were cut from material similar to that used for the field-effect measurements. Thin gold films were evaporated onto both sides of the strips. The specimens were then clamped at one end in a special vise which also made electrical contact to the gold films. The free end of the mica was observed in a microscope as fields of 3×10^5 v/cm were applied first in one direction and then in the other. A piezoelectric behavior capable of causing a charge-dependent raising and lowering of the superconducting transition temperature would have shown up as a deflection dependent on the direction of the applied field. No such effect was observed. Any such strain $(\Delta l/l)$ was less than 1×10^{-8}. Measurements of the effect of pressure on the transition temperature of tin give $\Delta T_c = 30.0\,\Delta V/V$.[9] Assuming $3\Delta l/l \approx \Delta V/V$, the change in transition temperature that could be produced by a still undetected piezoelectric effect would be less than 1×10^{-6} °K. This is two orders of magnitude smaller than the shifts in transition temperature reported here. A further reason for believing that the effects are not caused by strains in the substrate is that the shifts are in opposite directions for tin and indium. This is in contrast to measurements[9] which show that compression lowers the transition temperatures of both materials.

---

*Supported in part by the National Science Foundation, the Office of Naval Research, and the Department of Defense.

[1]E. Bose, Physik. Z. 7, 373 (1906).

[2]R. W. Pohl, Physik. Z. 7, 500 (1906).

[3]H. Mayer, Physik Dünner Schichten (Wissenschaftliche Verlagsgesellschaft M. B. H., Stuttgart, 1955), Vol. II, Chap. 2, p. 272. (Discussion and further references.)

[4]A. Deubner and K. Rambke, Ann. Physik 17, 317 (1956).

[5]G. Bonfiglioli, E. Coen, and R. Malvano, Phys. Rev. 101, 1281 (1956).

[6]G. Bonfiglioli, E. Coen, and R. Malvano, Phys. Rev. 115, 330 (1959).

[7]W. W. Jackson and J. West, Z. Krist. 76, 211 (1930).

[8]S. B. Hendricks and M. E. Jefferson, Am. Mineralogist 24, 729 (1939).

[9]L. D. Jennings and C. A. Swenson, Phys. Rev. 112, 31 (1958).

MAGNITUDE AND SIGN OF THE CONDUCTION ELECTRON POLARIZATION IN RARE-EARTH METALS

V. Jaccarino, B. T. Matthias, M. Peter, H. Suhl, and J. H. Wernick
Bell Telephone Laboratories, Murray Hill, New Jersey
(Received August 26, 1960)

From nuclear magnetic resonance (NMR) and electron paramagnetic resonance (EPR) measurements on rare-earth intermetallic compounds, we have determined the magnitude and sign of the conduction electron polarization. These results may be interpreted in terms of a negative exchange interaction of ~0.1 ev between the localized f electrons and conduction electrons.

The NMR of Al^{27} in the rare-earth intermetallic compounds having the cubic Laves structure[1] XAl_2 (X = La, Ce, Pr, Nd, Sm, Eu, Gd, Tb, Dy, Ho, Er, Tm, Yb, Lu, and as well, U)[2] was investigated as a function of field (8-14 koe) and temperature (4.2° - 300°K) using a Varian NMR spectrometer. The EPR of $EuAl_2$ and $GdAl_2$ was studied at 55 kMc/sec between 100° - 300°K.

Large, temperature-dependent, Knight shifts (k) were observed for all of the $4f$ magnetic compounds $CeAl_2$ through $TmAl_2$ and for UAl_2. The sign of k_{Al} obeyed the following simple rule: If we denote by $\vec{S}$, $\vec{L}$, and $\vec{J}$ the spin, orbital, and total angular momentum of the ground state of the rare-earth ion, then

$$k_{Al} > 0 \text{ for } \vec{J} = \vec{L} - \vec{S},$$
$$k_{Al} < 0 \text{ for } \vec{J} = \vec{L} + \vec{S}. \quad (1)$$

For the nonmagnetic compound $LaAl_2$, $k_{Al} = +0.13 \pm 0.02\%$. The Knight shift results from the contact hyperfine interaction $A\vec{I}\cdot\vec{s}$ between the Al^{27} nuclear spin $\vec{I}$ and the s conduction electron spin $\vec{s}$.

An explanation for the magnitude, sign, and temperature dependence of k_{Al} in the magnetic compounds may be found in the enhanced conduction electron polarization that results from the exchange interaction between the localized f electrons and the conduction electrons; i.e.,

$$\mathcal{H}_{ex} = -\mathcal{J}_{sf}\vec{S}\cdot\vec{s}. \quad (2)$$

By virtue of $\mathcal{J}_{sf}$ an additional hyperfine interaction, $A'\vec{I}\cdot\vec{S}$, exists, which we assume for simplicity to be isotropic. The fact that $\vec{J}$ is a good quantum number necessitates projecting $\vec{S}$ on to $\vec{J}$; hence $A'\vec{I}\cdot\vec{S} \to A'\vec{I}\cdot\vec{J}\,\langle\vec{S}\cdot\vec{J}\rangle/J(J+1)$. We may then express the Knight shift at a temperature T,

$$k = k_0\left[1 + \frac{\mathcal{J}_{sf}\chi_f}{g_f g_s n_f \beta^2}\frac{\langle\vec{S}\cdot\vec{J}\rangle}{J(J+1)}\right], \quad (3)$$

where k_0 is the Knight shift in the absence of f-electron polarization effects and χ_f/n_f is the f-electron susceptibility (at T) per rare earth ion.

Since

$$\langle\vec{S}\cdot\vec{J}\rangle < 0 \text{ for } \vec{J} = \vec{L} - \vec{S},$$
$$\langle\vec{S}\cdot\vec{J}\rangle > 0 \text{ for } \vec{J} = \vec{L} + \vec{S}, \quad (4)$$

the observed relations (1) for k are consistent with a negative $\mathcal{J}_{sf}$. The values of $\mathcal{J}_{sf}$ derived from the observed k and measured values[3] of χ using (2) are given in Fig. 1. The value of $k_{Al}(LaAl_2)$ was assumed for k_0.

For $PrAl_2$ the temperature independence of $\mathcal{J}_{sf}$ was established by measurements between 77° and 300°K. Since k_{Al} ($PrAl_2$:300°K) is but 4 times k_0, it was possible to verify that k is not proportional to χ, as a function of T, but is given by Eq. (3). For all but Ce, Pr, Sm, and Gd, the magnitude and field dependence of the linewidth at 300°K indicated that the Knight shift was anisotropic and could not be accounted for by electronic dipolar broadening. The large linewidths result from either an anisotropic exchange interaction or partial quenching of the orbital angular momentum (anisotropic g) or both.

We briefly mention certain other results of these experiments. Large Al^{27} quadrupole interactions were observed, the magnitudes of which are given in Table I. The La^{139} NMR in $LaAl_2$ was studied as a function of temperature and k_{La} was found to be weakly temperature dependent (see Table I). The relative broadening of the La^{139} and Al^{27} NMR vs either Gd or Dy impurity concentration in $LaAl_2$ was studied and found to be consistent with the Ruderman-Kittel-Yosida[4,5] conduction electron polarization description.

Yosida[5] has shown that the conduction electron

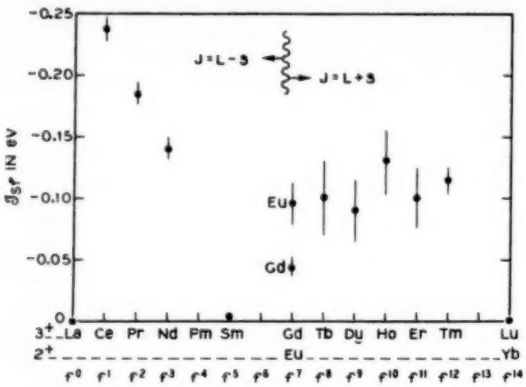

FIG. 1. The magnitude and sign of the exchange interaction in the rare earth-aluminum intermetallic compounds of the cubic Laves structure XAl_2 as determined from the Knight shift of the Al^{27} NMR and the measured susceptibilities. The number of $4f$ electrons and the corresponding valence is that which is usually given for the free ion. [C. Kittel, Introduction to Solid-State Physics (John Wiley & Sons, Inc., New York, 1956).] X-ray data and susceptibility measurements support the assignment given in the figure for these quantities. The relative size of the anisotropic interaction observed is indicated by the vertical line. Neither the inconstancy of ϑ_{sf} nor its magnitude and sign are understood at present. The anomalously small value of ϑ_{sf} ($SmAl_2$) derived probably results from the assumption that the state $^6H_{5/2}$ for the Sm^{3+} ion is pure. Due to the close spacing of the fine structure levels and the importance of crystal field and exchange interactions in admixing states for which $J \neq \frac{5}{2}$, this assumption is questionable.

polarization gives rise to an electronic g shift of the EPR of the magnetic ions in metals. The fractional change in the g value expected is

$$\Delta g/g = 3n\vartheta_{sf}/2n_f g\epsilon_f. \quad (5)$$

Here, $2n/n_f$ is the number of conduction electrons per atom, and ϵ_f is the Fermi energy.

The observed shift $\Delta H = H_{res} - H_0$ was only a fraction of the half-power linewidth ($\delta H \sim 900$ oe in $GdAl_2$). The resonance line shows a Lorentz shape as would be expected in the case of strong exchange narrowing.[6] The observed line profile indicated a mixture of the real and imaginary parts of the rf susceptibility.[7] The relative admixture was determined for each measurement. The field for resonance showed a temperature dependence which results from demagnetizing effects.

Table I. The Al^{27} nuclear electric quadrupole interaction constants e^2qQ^{27} as determined from the field dependence of the broadening of the $1/2 \longleftrightarrow -1/2$ transition. The temperature dependence of the Knight shift of the La^{139} NMR in $LaAl_2$ is given in the lower portion of Table I. No measurable temperature dependence was found for the Al^{27} Knight shift in $LaAl_2$: $k_{Al} = 0.13 \pm 0.02\%$. (Reference solutions: $LaNO_3$ and $KAlSO_4$.)

Compound	Valence	e^2qQ^{27} (Mc/sec)
$LaAl_2$	3+	4.63
$CeAl_2$	3+	4.54
$PrAl_2$	3+	4.54
$YbAl_2$	2+	2.30
UAl_2	?	4.31

Temp(°K)	4.2	20	295
$k_{La}(LaAl_2)$, %	0.65	0.64	0.60

This dependence was eliminated by linear extrapolation to zero magnetization.

Using these procedures, we obtained the values

$$GdAl_2: g = 1.982 \pm 0.003, \ \Delta g = 0.010,$$

$$EuAl_2: g = 1.994 \pm 0.003, \ \Delta g = 0,$$

where Δg is obtained from a comparison with the ionic value for Gd of $g = 1.992$ estimated by Lacroix.[8] A comparison with published measurements on ionic crystals[9] indicates that crystalline field effects on the g value are negligible. The measured $\Delta g/g$ in $GdAl_2$ leads to a value of $\vartheta_{sf} = -0.03$ ev if we assume $\epsilon_f = 5$ ev and $n/n_f = 1$. No polarization was detected within our accuracy in $EuAl_2$.

It remains in interpreting the NMR results to justify the statement [Eq. (3)] that the conduction electron polarization at the aluminum sites due to the exchange interaction with the rare earth ions is proportional to ϑ_{sf} as though the rare earth ion spins imposed a uniform magnetic field on the conduction electrons. In actual fact the s-f interaction is highly localized. Suppose that $\chi(\vec{r} - \vec{r}_i)$ is the conduction electron magnetization at $\vec{r}$ due to a localized "field" of unit strength at $\vec{r}_i$ (in this case the exchange field). Then the total magnetization at $\vec{r}$ is proportional to

$$\sum_{\substack{\text{rare earth} \\ \text{sites } \vec{r}_i}} \chi(\vec{r} - \vec{r}_i) = \sum_{\vec{r}_i, \vec{q}} \chi(\vec{q}) e^{i(\vec{r} - \vec{r}_i)\cdot\vec{q}},$$

where the $\chi(\vec{q})$'s denote the Fourier coefficients in the expansion of χ, assuming the usual boundary conditions. The sum over $\vec{r}_i$ gives zero unless $\vec{q}$ is zero or one of the reciprocal lattice vectors $\vec{K}$. Thus the magnetization is

$$\chi(0)+\sum_{\vec{K}}\chi(\vec{K})e^{i\vec{r}\cdot\vec{K}}.$$

The leading term is, of course, the magnetization due to a spatially uniform field of unit strength. Assuming that χ is simply the Ruderman-Kittel susceptibility, $\chi(\vec{q})$ decreases from $\chi(0)$ to zero at $q=2k_f$. Therefore, unless $2k_f$ is comparable with one of the $\vec{K}$'s the sum will be negligible, and Eq. (3) is justified. The internal consistency of the data suggests that no such special conditions prevail.

Only for a naive model would one expect a detailed agreement between ϑ_{sf} as derived from the NMR and EPR experiments since the former gives the polarization at the Al site while the latter that at the Gd site. The fact that both measurements show a negative polarization is strong evidence for assuming $\vartheta_{sf}<0$.

To our knowledge this is the first determination of the sign of conduction electron polarization in a magnetic metal.[10]

We are particularly indebted to H. J. Williams and R. C. Sherwood for the measurements of the susceptibilities, to A. M. Clogston for many critical discussions, and to Mrs. V. B. Compton for x-ray analyses.

[1]The cubic Laves structure AB_2 belongs to the space group $O_h^7=Fd3m$; the point symmetry for the A site is $\bar{4}3m$ and the B site $\bar{3}m$. An axial quadrupole interaction is possible for the B site. All NMR measurements were made above the Curie point.

[2]The compounds were prepared by induction heating of stoichiometric amounts of the pure metals in silica or alumina crucibles in an argon atmosphere. J. H. Wernick and S. Geller, Trans. Am. Inst. Mining, Met. Petrol. Engrs. (to be published). S. E. Haszko, Trans. Am. Inst. Mining, Met. Petrol. Engrs. (to be published). For the NMR and EPR experiments, the samples were pulverized and sieved (400 mesh).

[3]H. J. Williams and R. C. Sherwood (private communication).

[4]M. A. Ruderman and C. Kittel, Phys. Rev. 96, 99 (1954).

[5]K. Yosida, Phys. Rev. 106, 893 (1957).

[6]P. W. Anderson and P. R. Weiss, Revs. Modern Phys. 25, 269 (1953). Assuming dipolar broadening, this theory predicts $\delta H=500$ oe in $GdAl_2$.

[7]M. Peter and B. T. Matthias, Phys. Rev. Letters 4, 449 (1960).

[8]R. Lacroix, Helv. Phys. Acta 30, 374 (1957).

[9]J. W. Orton, Reports on Progress in Physics (The Physical Society, London, 1959), Vol. 22, p. 204.

[10]J. Owen, M. E. Browne, V. Arp, and A. F. Kip, J. Phys. Chem. Solids 2, 85 (1957), have found no shift for the EPR of Mn^{++} in copper but have detected a broadening of the Cu NMR.

OPTICAL OBSERVATION OF SPIN-ORBIT INTERACTION IN GERMANIUM

Jan Tauc and Emil Antončík
Institute of Technical Physics, Czechoslovak Academy of Sciences, Praha, Czechoslovakia
(Received August 12, 1960)

Philipp and Taft[1] have recently determined the optical constants of germanium from the measurement of reflectivity in a broad wavelength range. In the reflection spectrum they observed near 2 ev a characteristic peak which Phillips[2] from an analysis of the absorption curve ascribed to the transition $L_3'\rightarrow L_1$ (see also Roth and Lax[3]). Our measurements of the reflection spectrum on etched single crystals of germanium have shown that this peak is split into two peaks, a at 2.1 ev and b at 2.3 ev (see Fig. 1). Using the optical constants as determined by Philipp and Taft[1] and considering the splitting $a-b$ as a small perturbation of the reflectivity reproduced in reference 1, it is possible to show that in the absorption

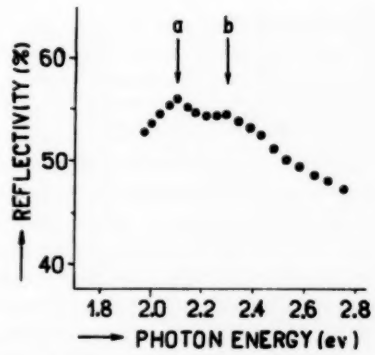

FIG. 1. Reflection spectrum of germanium (at 300°K) near 2 ev.

spectrum a similar splitting appears (naturally with the peaks somewhat shifted).[4]

The double peak may be explained by the splitting of the state L_3' by spin-orbit interaction. The observed value of about 0.2 ev agrees well with the theoretical estimate by Roth and Lax.[3]

The correctness of this interpretation is supported by measurements on Ge - Si alloys: the splitting diminishes with increasing content of Si (e.g., in an alloy with 22% atomic percent of Si the energy interval of the peaks a, b in the reflection curve is only 0.15 ev; in Si it was not observable at all).[5] Similar double peaks were also found[5] in the reflection spectra of GaAs (the peak a is at 2.94, b at 3.20 ev), GaSb (2.00; 2.48), InAs (2.53; 2.82), InSb (1.82; 2.38); the general features of our interpretation are here in good accord with theoretical expectations as was kindly pointed to us by Phillips.[6]

It may be expected that the corresponding spin-orbit splitting in the Γ point should also be observable optically; however, in the absorption spectrum of Ge determined by Dash and Newman[7] this is not apparent. This point deserves further experimental investigations.

For help in our work and valuable discussions we thank A. Abrahám, F. Lukeš, J. C. Phillips, Z. Trousil, and B. Velický.

[1]H. R. Philipp and E. A. Taft, Phys. Rev. 113, 1002 (1959).

[2]J. C. Phillips, J. Phys. Chem. Solids 12, 208 (1960).

[3]L. M. Roth and B. Lax, Phys. Rev. Letters 3, 217 (1959).

[4]At our suggestion F. Lukeš from the University of Brno determined the absorption index k of germanium by the method of D. G. Avery [Proc. Phys. Soc. (London) B65, 425 (1952)]; his preliminary results confirm our observations. He found the peaks in the k curve at about 2.11 and 2.32 ev (private communication).

[5]J. Tauc and A. Abrahám, Proceedings of the Conference on Semiconductor Physics, Praha, 1960 (to be published).

[6]J. C. Phillips (private communication).

[7]W. C. Dash and R. Newman, Phys. Rev. 99, 1151 (1955).

PROTON HELICITY FROM Λ DECAY

Robert W. Birge and William B. Fowler*
Lawrence Radiation Laboratory, University of California, Berkeley, California
(Received August 22, 1960)

When Λ hyperons are produced with K^0 mesons in $\pi^- - p$ reactions there is a large up-down asymmetry of the decay products with respect to the production plane.[1] The angular distribution of the decay pion from a completely polarized hyperon at rest can be written as[2]

$$dN = (1/4\pi)(1 + \alpha \cos\chi)d\Omega,$$

where $d\Omega$ is the solid angle of the pion momentum vector $\vec{P}_\pi$, and χ the angle between $\vec{P}_\pi$ and the spin of the hyperon. The constant α is given by

$$\alpha = 2\,\mathrm{Re}(A^*B)/(|A|^2 + |B|^2),$$

and characterizes the degree of mixing of parities in the decay. A and B are the amplitudes for decay into $s_{1/2}$ and $p_{1/2}$ final states of the pion-nucleon system. The quantity $\alpha\bar{P}$, which has the possible values $0 \leq |\alpha\bar{P}| \leq 1$, is a measure of the up-down asymmetry and has been experimentally shown[3] to be $\geq 0.73 \pm 0.14$. This large asymmetry can exist only if the Λ's are highly polarized in the production process and if there is nonconservation of both parity and charge conjugation in the decay process.

Another necessary consequence of parity nonconservation in the decay process is a longitudinal polarization of the decay proton from unpolarized Λ's decaying at rest. It can be shown that this longitudinal polarization equals $-\alpha$.[4]

Fortunately, this longitudinal polarization of the proton, referred to the center of mass of the Λ, appears as a partial transverse polarization in the laboratory system when a Λ decays in flight and, hence, can be measured by a suitable scattering experiment. In this way the helicity of the proton can be obtained, whereas in the $\alpha\bar{P}$ experiments only the lower limit to the magnitude can be determined. The sign of α was determined in an experiment of Boldt et al.,[5] who found $\alpha = +0.85^{+0.15}_{-0.21}$, based on 54 selected events from a total of 257 in a multiplate cloud chamber.

In the course of an experiment designed to produce Ξ particles[6] from a high-momentum (1.1-Bev/c) K^- beam[7] impinging on the Berkeley

30-inch propane chamber, about 20 000 Λ's were produced. A fraction of these (about 800 events) were observed to decay and have a subsequent scattering of the proton within the liquid of the chamber. This constituted a considerably larger sample of events than had been obtained by Boldt et al.; hence it seemed worth while to repeat the experiment because of its fundamental nature. Preliminary and incomplete results of this experiment have already appeared elsewhere.[8]

All events visually identified as Λ's were measured, and the relevant data were then calculated on an IBM-650 computer. A constraint program was used to find the best fit to the data, taking into account transverse momentum balance and coplanarity of the Λ's with respect to the production origin as well as the "Q" of the decay. In addition, the ionization of all tracks was visually checked for consistency with measured momentum and particle assignments. Above about 800 to 900 Mev/c there was difficulty separating θ^0's from Λ's, and those events were deleted.

A major difficulty was encountered because the proton track, prior to scattering, was often too short to measure the momentum accurately. Because very large errors were assigned to these tracks, the constraint program could not readily compute reliable values for the momenta, yet these values were needed to obtain the asymmetry parameter in the scattering process. For this reason, we assumed an elastic scattering and used the momentum obtained from the scattered prong instead. The events were accepted only when the proton momenta calculated by this method (after appropriate corrections for energy loss by ionization) were consistent with the values needed to give the right Q for the Λ. In most cases the scattered proton stopped in the chamber and a very accurate momentum determination could be made; unfortunately, however, these low-momentum events are just those where the asymmetry from scattering by carbon is quite small. Therefore these events do not help to measure the initial polarization of the proton. In order to eliminate possible inelastic scattering events an acceptance cutoff was made in the scattering angle at a point where the elastic scattering cross section still dominates the inelastic processes. Even in those events in which both the incoming and outgoing momenta could be well measured, it was impossible to detect excitation into the low-lying levels of carbon; therefore, the cutoff procedure was used for all events. This procedure was necessary because the asymmetry parameter for inelastic scattering can be of opposite sign to that of elastic scattering in certain angular regions. Those events with two prongs that appeared to be hydrogen scatterings were subjected to an additional constraint program to determine whether they were indeed elastic hydrogen scatterings.

As a result of rejecting θ-like events, inelastic scattering, poorly measured events, events with large kinks in the tracks, and events in which all tracks were too short to be measured accurately or the momentum was obviously too low for analysis, only 212 events remained for further analysis. Finally, all single Λ's without visible production origins were eliminated from the sample, leaving 183 events. Of these, 36 were cases in which the proton was scattered by hydrogen in the propane and the remainder were elastic carbon scatterings.

It is difficult to see how any bias can creep into the selection of these events even with such a high filtering factor, because the sign of the polarization is not an obvious quantity when the event is viewed in a bubble chamber picture.

The following procedure was then used to analyze the selected events. First, for each event the angle between the spin of the proton and the direction of motion of the proton in the laboratory system was computed in a manner prescribed by Stapp.[9] The sine of this angle multiplied by the magnitude of the original longitudinal polarization ($-\alpha$) is the magnitude of the transverse polarization. Second, correction was made for the precession of the proton spin in the magnetic field of the bubble chamber prior to the scattering event. The rate of precession of the spin was computed according to the equations derived by Ford and set forth in the paper by Nelson et al.,[10] namely,

$$\omega_s = \frac{e\vec{B}}{m_0\gamma c}[1+(\tfrac{1}{2}g-1)\gamma] - \frac{\vec{v}}{v}(\gamma-1)(\tfrac{1}{2}g-1)\frac{e\vec{B}\cdot\vec{v}}{m_0\gamma c v},$$

where $\vec{B}$ = magnetic field, $\vec{v}$ = velocity of the proton, and $\frac{1}{2}g = 2.79275$. Third, because of spin-orbit forces, the scattered intensity is proportional to $1+(-\alpha\vec{P}_1)\cdot\vec{P}_2(\theta)$, where $-\alpha\vec{P}_1$ is the transverse polarization of the incoming proton at the position of the scattering (as determined by the above transformation) and $P_2(\theta)$ is the asymmetry parameter in the scattering process. The direction of $P_2(\theta)$ is along the normal to the scattering plane, $\vec{\eta}_2 = \vec{k}\times\vec{k}'/|\vec{k}\times\vec{k}'|$. The magnitude of $P_2(\theta)$ is a function of incoming momentum and scattering angle and has been determined

experimentally elsewhere. For example, with an initial transverse polarization downwards, $P_2(\theta)$ is determined as

$$P_2(\theta) = (N_R - N_L)/(N_R + N_L),$$

where N_R and N_L are the number of protons scattered to the right and to the left. (The angle ϕ between P_1 and P_2 is 0 deg and 180 deg, respectively.) In. Figs. 1 and 2 the values of $P_2(\theta)$ are summarized as a function of laboratory-system momentum and scattering angle for protons scattered by carbon and hydrogen, obtained from references available in the literature and by private communication. A list of references from which these data were taken is available on request. Data from these charts were put into the memory of the computer and intermediate values obtained by interpolation. A dashed line in Fig. 1 indicates the elastic cutoff. Below 300 Mev/c the asymmetry parameter P_2 was set equal to 0, even though at very low momenta P_2 again becomes finite. This condition eliminated another 63 events and left only 120 events of significance.

Finally, the probability that a proton scatter to the right is $N_R/(N_R+N_L) = \frac{1}{2}(1 - \alpha P_i)$, where $P_i = P_1 P_2 \cos\phi$ for the ith event. The product of all of these independent probabilities is the likelihood function

$$L = \prod_i (1 - \alpha P_i),$$

which may be plotted as a function of α to obtain the most likely value for the magnitude and sign of α.

In Fig. 3 the natural logarithm of L is plotted for 120 events.

Although these data indicate that $\alpha = -0.45 \pm 0.4$,[11] the relevant question to be answered here is the sign of α and not the magnitude (which is already known to be $\geq 0.73 \pm 0.14$). Hence one may state that our value is three standard deviations away from $\alpha = +0.73$. The ratio of the likelihood function at $\alpha = -0.73$ to that at $\alpha = +0.73$ is 65:1; for $\alpha = \mp 0.45$ the ratio is 12:1. The negative sign for α implies positive helicity for the proton in contradiction to theoretical speculations[12] based on the universal Fermi interaction, and to the experimental findings by Boldt et al.,[5] whose results are plotted in the same graph as a dashed

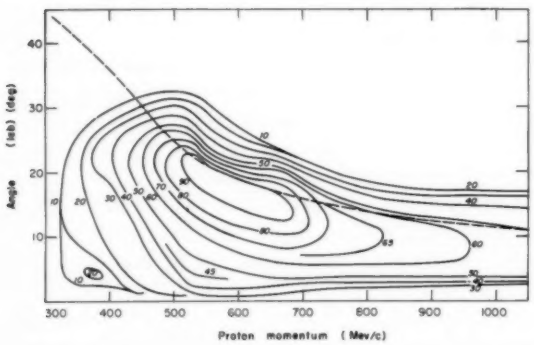

FIG. 1. Curves of constant asymmetry for elastic scattering of protons from carbon as a function of laboratory-system momentum and scattering angle. Dashed line indicates cutoff where elastic-scattering cross section still dominates inelastic scattering.

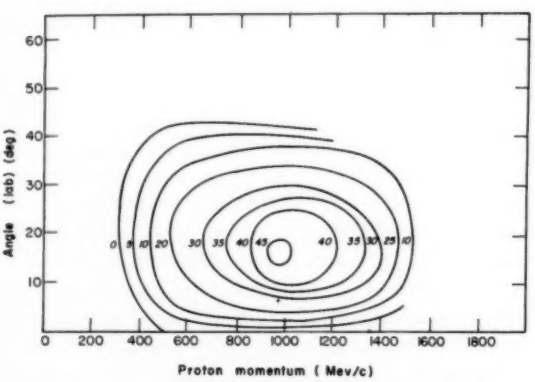

FIG. 2. Curves of constant asymmetry for proton-proton scattering as a function of laboratory-system momentum and scattering angle.

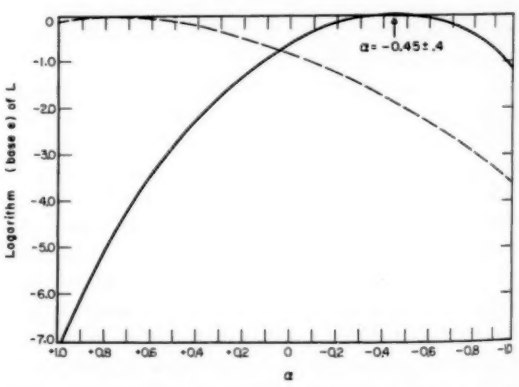

FIG. 3. Natural logarithm of the likelihood function L as a function of α. The longitudinal polarization of the proton from Λ^0 decay is $-\alpha$. Solid curve is this work. Dashed line is that of Boldt et al.[5] This experiment indicates $\alpha = -0.45 \pm 0.4$.

line, and contrary to our own preliminary results.[8]

A second way of determining the sign of α is to measure the right-left asymmetry directly. The result obtained in this manner is $(N_R - N_L)/(N_R + N_L) = 20/120 = 0.16 \pm 0.091$. The computed value for this ratio, $(-2\alpha\langle P_1 P_2\rangle_{\text{av}}/\pi)$, based on the average of the product of the input polarization $-\alpha P_1$ and the asymmetry parameter $P_2(\theta)$, is 0.16 for $\alpha = 1.0$, and 0.07 for $\alpha = -0.45$. The experimental asymmetry is in agreement with both of these values.

Finally, we have computed the quantity $D = -\sum_i P_i \cos\phi_i$ as suggested by Bowen et al.,[13] so that these data may be combined with other results. The value obtained here is $D = -2.79$, to which may be added Bowen's -0.142.

Every effort has been made to detect errors in the experiment, to the extent that the signs and magnitude of the polarization of the individual events making up the most significant part of the data have been checked numerous times. Although these data disagree with previous measurements of the sign of α, we have no other choice but to present the results as they now stand.

It is with pleasure that we acknowledge the work done by Howard White and his group in programming the computer and processing all the data. Dr. Cyril Henderson collaborated with us on a preliminary version of this experiment. We are indebted to Dr. Wilson Powell and to all the members of the 30-inch propane chamber group, and to the staff of the Bevatron for their part in making a successful run of the chamber.

We thank the many scanners and technicians for their help in the analysis. Discussions with Dr. Francis Muller and Dr. Oreste Piccioni were most helpful, as well as discussions with many other people too numerous to list.

*Now at Brookhaven National Laboratory, Upton, New York.

[1]F. S. Crawford, M. Cresti, M. L. Good, K. Gottstein, E. M. Lyman, F. T. Solmitz, M. L. Stevenson, and H. K. Ticho, Phys. Rev. 108, 1102 (1957); F. Eisler, R. Plano, A. Prodell, N. Samios, M. Schwartz, J. Steinberger, P. Bassi, V. Borelli, G. Puppi, G. Tanaka, P. Woloschek, V. Zoboli, M. Conversi, P. Franzini, I. Mannelli, R. Santangelo, V. Silvestrini, D. A. Glaser, C. Graves, and M. L. Perl, Phys. Rev. 108, 1353 (1957).

[2]T. D. Lee, J. Steinberger, G. Feinberg, P. K. Kabir, and C. N. Yang, Phys. Rev. 106, 1367 (1957).

[3]Frank S. Crawford, Jr., Lawrence Radiation Laboratory (private communication), results from experiments in reference 1.

[4]T. D. Lee and C. N. Yang, Phys. Rev. 108, 1645 (1957); R. Gatto, University of California Radiation Laboratory Report UCRL-3795, June, 1957 (unpublished); J. Leitner, Nuovo cimento 8, 68 (1958).

[5]E. Boldt, H. S. Bridge, D. O. Caldwell, and Y. Pal, Phys. Rev. Letters 1, 256 (1958).

[6]W. B. Fowler, R. W. Birge, P. Eberhard, M. L. Good, W. M. Powell, and H. K. Ticho, reported at the Ninth Annual International Conference on High-Energy Physics, Kiev, 1959 (unpublished).

[7]P. Eberhard, M. L. Good, and H. K. Ticho, Lawrence Radiation Laboratory Report UCRL-8878, August, 1959 (unpublished).

[8]R. W. Birge and W. B. Fowler, Bull. Am. Phys. Soc. 4, 355 (1959). The results reported at the meeting from a larger sample of events already indicated a negative value of α, inconsistent with the value given in the Abstract.

[9]Henry Stapp, University of California Radiation Laboratory Report UCRL-8096, December, 1957 (unpublished).

[10]D. F. Nelson, A. A. Schupp, R. W. Pidd, and H. R. Crane, Phys. Rev. Letters 2, 492 (1959).

[11]The error was obtained by taking the value of α when the logarithm of the likelihood function equals -1/2.

[12]R. P. Feynman and M. Gell-Mann, Phys. Rev. 109, 193 (1958); E. Sudarshan and R. Marshak, Phys. Rev. 109, 1860 (1958); J. J. Sakurai, Nuovo cimento 7, 649 (1958).

[13]T. Bowen, C. R. Sun, and A. E. Werbrouck, Princeton University Report NP-7079, December, 1958 (unpublished).

POSSIBLE ANOMALY IN MESON PRODUCTION IN $p+d$ COLLISIONS*

Alexander Abashian, Norman E. Booth, and Kenneth M. Crowe
Lawrence Radiation Laboratory, University of California, Berkeley, California
(Received August 11, 1960; revised manuscript received August 22, 1960)

Several authors have proposed the existence of new particles and π - π resonances.[1-5] Along these lines we are studying the reactions

$$p+d- \begin{cases} \mathrm{He}^3+\pi^0 & \text{(1a)} \\ \mathrm{He}^3+\omega^0 & \text{(1b)} \\ \mathrm{He}^3+\pi^+ +\pi^- & \text{(1c)} \\ \mathrm{He}^3+\pi^0+\pi^0 & \text{(1d)} \end{cases}$$

$$p+d- \begin{cases} \mathrm{H}^3+\pi^+ & \text{(2a)} \\ \mathrm{H}^3+\omega^+ & \text{(2b)} \\ \mathrm{H}^3+\pi^+ +\pi^0, & \text{(2c)} \end{cases}$$

where ω may be a particle of mass intermediate between that of a π meson and a K meson. Our first experiment consists of measuring at a fixed laboratory-system angle of 11.7 deg the He^3 momentum spectrum from 1.0 Bev/c to 1.6 Bev/c for incident proton energies ranging from 624 Mev to 743 Mev.

Figure 1 is a schematic drawing of the experimental arrangement. Protons extracted from the 184-inch cyclotron impinged upon a Y-shaped gaseous deuterium target operated at a pressure of 320 psi and at liquid-nitrogen temperature. He^3 nuclei produced at an angle of 11.7 ± 0.2 deg passed through the collimators C_2 through C_4 into the magnet spectrometer and were detected by scintillation counters S_1 through S_7. Q_1, an 8-inch triplet quadrupole magnet, focused the particles initially at f_1, and Q_2 (a lens similar to Q_1) focused them finally at S_3. The slit at f_1 was 0.5 in. wide at full proton energy of 743 Mev and 2.0 in at reduced proton energies, thereby yielding momentum intervals of ± 0.6% and ± 2.5%, respectively.

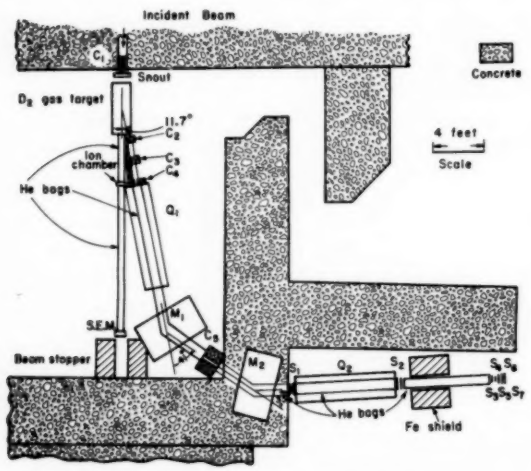

FIG. 1. Experimental arrangement.

Identification of He^3 was made by requirements of momentum, time of flight, range, and dE/dx in S_3. For He^3 momenta greater than 1200 Mev/c, $S_1S_2S_3S_4S_5\bar{S}_6\bar{S}_7$ coincidences were required, while below 1100 Mev/c, $S_1S_3S_4\bar{S}_6\bar{S}_7$ were required. The momentum interval between 1100 and 1200 Mev/c was measured with both arrangements to check that they agreed. Backgrounds were measured by using H_2 gas of the same stopping power as the D_2 in the target. The backgrounds thus measured agreed with target-empty measurements when corrections were made for energy losses. At the full proton energy the backgrounds were always less than 1% of the maximum counting rates. However, at reduced energies they amounted to as much as 20% of the peak rate because the greater dimensions of the incident proton beam due to scattering in the energy degrader increased the production of He^3 in the walls of the target.

Figure 2 shows the He^3 momentum spectra corrected for energy loss and for the change in momentum interval, Δp, with momentum p. The assigned errors are statistical and constitute the major part of the error. Each spectrum has a high-momentum peak due to single π^0 production and a lower momentum continuum associated with double meson production. The solid curves drawn for the π^0 peaks are the calculated momentum-resolution functions of the system, normalized to the area under the experimental points.

For comparing the continua with theory, we have chosen a simple phase-space calculation as a first approximation. The expression used for the phase-space volume element ϕ_S is

$$\phi_S = \frac{d^2\rho}{dp_3\,d\Omega} = \frac{p_3^2}{\omega_3}\left(\frac{t-4}{t}\right)^{1/2}, \qquad (3)$$

where ρ is the relativistically invariant three-body phase-space volume, ω_3 and p_3 are the total

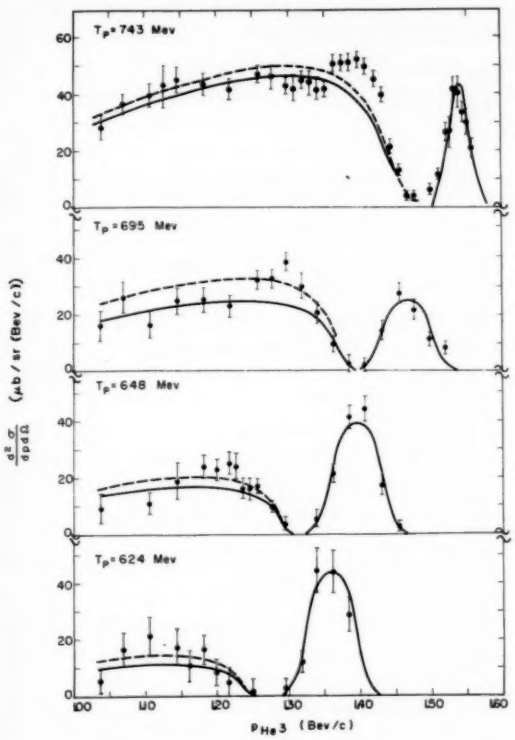

FIG. 2. He^3 momentum spectra for various incident proton energies. (See text for description of curves.) Ordinate scale is correct to within a factor of two.

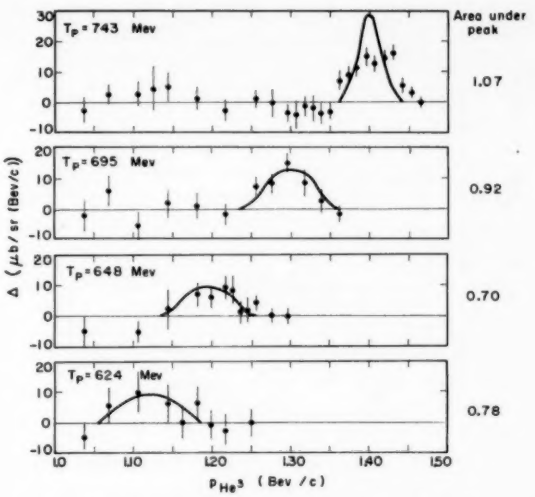

FIG. 3. Difference between He^3 data and solid curves of Fig. 2 for various incident proton energies. (See text for description of curves.)

energy and momentum of the He^3, respectively, and t is the square of the total energy of the two pions in their own c.m. system in units of the pion mass. The dashed curves drawn in the continua are these calculations fitted by the method of least squares to all of the experimental points.

It is clear that these calculations alone cannot reproduce the peaks that occur in the continua. We have investigated some of the conventional mechanisms for extending these calculations: for example, the effects of Bose statistics for the two pions, pion-nucleon interaction, and final-state wave function for the He^3 nucleus. Our crude calculations of these effects do not give quantitative agreement with the data. We have therefore attempted to fit only that part of the data outside the peaks with ϕ_S; the results are shown as the solid curves in Fig. 2. In Fig. 3, Δ, the differences between the data and the solid curves of Fig. 2, have been plotted as a function of He^3 momentum. The curves are the calculated resolution functions for a particle or a resonance of zero width and located according to kinematics for a mass or total energy of 310 Mev. The areas under the curves have been normalized to the areas under the points.

Some caution must be exercised before firm conclusions are drawn about the rather broad observed peak at full energy, as contrasted to the more narrow distribution expected. First, since the peak resides so close to the sharply changing edge of the continuum, the subtraction is sensitive to errors in momentum settings and the exact shape of ϕ_S. Second, the data have been combined over many runs, so that errors in settings from run to run tend to smear out any narrow peaks. We think that it is unlikely that these two possibilities are the entire explanation for the width observed. We therefore fitted the widths of the peaks with a simple Breit-Wigner one-level formula with experimental resolution folded in. The results of these calculations gave, for the natural linewidth, $\Gamma_{BW} = 10 \pm 6$ Mev. No definite conclusion on the linewidth can be drawn at this time.

Information on the isotopic spin assignments for the particle or resonance may be obtained from a study of Reactions (2a), (2b), and (2c), which proceed via pure $I = 1$ production. Figure 4 shows our attempts to measure these reactions at the highest proton energy. Because our spec-

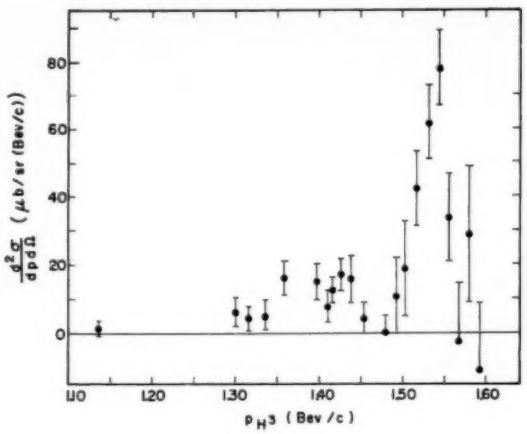

FIG. 4. H^3 momentum spectrum for incident proton energy of 743 Mev. Ordinate scale is arbitrary.

trometer was designed for the He^3 measurements, we had to degrade the H^3 with Be to a momentum of 800 Mev/c. The small number of points and the large errors assigned are results of the large backgrounds and low counting rates. Experimentally, we find that the ratio of the cross sections of (2a)/[(2b)+(2c)] is about 2.3:1. We expect from charge independence the same ratio for the $I=1$ part of (1a)/[(1b)+(1c)] or (1a)/peaks if the He^3 peaks are $I=1$ and the remainder of the continuum is $I=0$. From our fits, we find the ratio (1a)/peaks to be 1.9:1. Thus, within the large errors involved, an $I=1$ assignment for the peak is possible.

Upon the suggestion of Chew we attempted to fit the full-energy He^3 data with a combination of an S-wave ($I=0$) ϕ_S and a P-wave ($I=1$) resonant ϕ_p given by

$$\phi_p = c_1\phi_S[(t-4)/t]|F_\pi|^2, \qquad (4)$$

$$|F_\pi|^2 = [(t-t_\gamma)^2 + (t-4)^3\Gamma^2/t]^{-1},$$

where $(t_\gamma)^{1/2}$ is the position of the resonance in units of the meson mass and Γ is a parameter appearing in the expression for the pion form factor F_π of Frazer and Fulco.[3] We obtained reasonable agreement for $c_1 \approx 3$, $t_\gamma = 5.0 \pm 0.2$, and $\Gamma = 1.0$ to 2.0. These values of t_γ and Γ do not agree with those of Frazer and Fulco, who predict t_γ between 12 and 16 and $\Gamma = 0.4$ in fitting the nucleon form factors and magnetic moments.

In concluding, we can summarize the following:

1. The data are inconsistent with the relativistically invariant phase space assumed. The discrepancy appears in the form of a narrow peak which kinematically behaves like a system with a mass or total energy of 310 ± 10 Mev. The natural linewidth of this system is not more than about 16 Mev.

2. Plausible explanations of the line are the existence of a new neutral particle or a resonant π-π system. The possible isotopic spin assignments are $I=1$ or $I=0$. The H^3 data crudely support the $I=1$ assignment.

3. Alternate explanations may be possible although we have not found any in quantitative agreement with the data. Further experimental work, particularly on the H^3 reactions, is clearly essential. Our present conclusions therefore must be regarded as tentative.

A more complete discussion of the experiment and any new results will be forthcoming shortly in a more extensive article.

We would like to thank Professor Geoffrey Chew, Professor Kenneth Watson, and Professor Emilio Segrè for several enlightening discussions of the experiment and the results. We also wish to thank Mr. Morris Pripstein for his assistance during the early phases of the experiment, and Mr. James Vale and the cyclotron crew for their cooperation.

---

*Work carried out under the auspices of the U. S. Atomic Energy Commission.

[1]Y. Nambu, Phys. Rev. 106, 1366 (1957).

[2]S. N. Gupta, Phys. Rev. 111, 1436 (1958); Phys. Rev. 111, 1698 (1958); Phys. Rev. Letters 2, 124 (1959).

[3]W. R. Frazer and J. R. Fulco, Phys. Rev. Letters 2, 365 (1959); Phys. Rev. 117, 1609 (1960).

[4]G. F. Chew, Phys. Rev. Letters 4, 142 (1960).

[5]J. J. Sakurai, Nuovo cimento 16, 388 (1960).

ELECTRON SCATTERING FROM THE PROTON*

F. Bumiller, M. Croissiaux,† and R. Hofstadter
Department of Physics and High-Energy Physics Laboratory, Stanford University, Stanford, California
(Received August 25, 1960)

We have recently put into operation a new large double-focusing magnetic spectrometer capable of analyzing electrons or other singly-charged particles up to a momentum value of 1000 Mev/c. This spectrometer is of the 180° type previously used in this laboratory and has a mean radius of curvature of 72 in. We have employed this spectrometer in electron-scattering work on the proton between incident electron energies of 650 Mev and 900 Mev and between scattering angles of 45° and 145°. A typical value of the solid angle employed in detecting electrons is 5.6×10^{-3} steradian. The higher energies (>650 Mev) have been realized by virtue of the recent extension in the length of the Stanford linear accelerator.

The 72-in. spectrometer forms part of a two-magnet system; the second part is the 36-in. spectrometer described previously.[1] Figure 1 is a schematic drawing of the two spectrometers in a position in which they are 120° apart. Both spectrometers are arranged so that they can be rotated independently about a common scattering center. We have taken data simultaneously with both spectrometers, usually employing the 36-in. magnet at large angles, e.g., up to 145°. The 36-in. spectrometer can handle scattered electrons only up to 500 Mev/c without excessive deterioration of focusing and we have used the 36-in. spectrometer in these experiments only in the very safe region below 370 Mev/c. Such a procedure limits, and has limited in the past, the ability of this spectrometer in obtaining scattering data at high energies and small angles,[1,2] i.e., in those circumstances where the energy of the scattered electron is high.

We have begun to carry out a series of experiments on the proton at various energies and angles with these spectrometers. In both instruments we used Čerenkov counters as detectors. In. Fig. 2(a) we show a typical electron-scattering

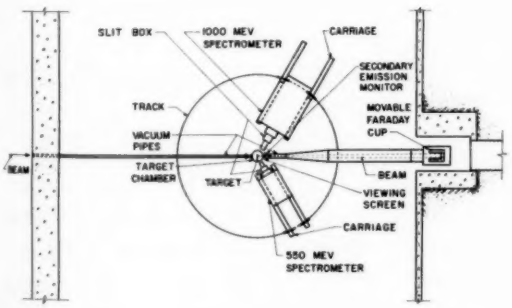

FIG. 1. The double spectrometer system used in these experiments.

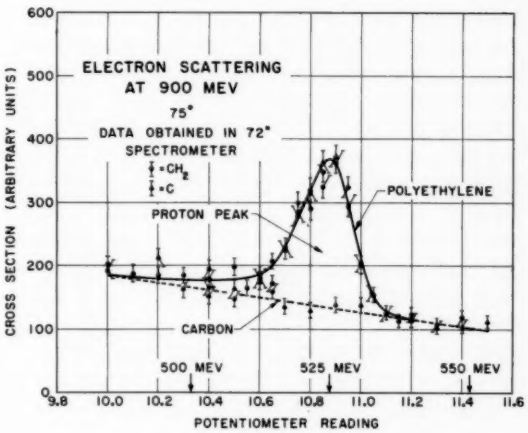

FIG. 2. (a) Electron-scattering peak obtained with a 0.237-in. polyethylene target at an incident energy of 900 Mev and a scattering angle of 75°. The target was at 45° with respect to the incident beam. (b) Same except parameters are 850 Mev, 145°, 36-in. spectrometer, and target at 0°.

peak obtained with the 72-in. spectrometer at an incident energy of 900 Mev and a scattering angle of 75°. The target material was polyethylene and we have subtracted the carbon background in analyzing the data to obtain the proton-scattering peak. The carbon data were obtained in the same run with a separate graphite target. In Fig. 2(b) we show a corresponding peak obtained in the 36-in. spectrometer at 850 Mev and 145°.

The cross sections obtained in this work are absolute cross sections and are based on the readings of the Faraday cup shown in Fig. 1 which gives the number of electrons in the main beam. The secondary emission monitor was an adjunct used as a monitor for the 72-in. spectrometer and was calibrated during each run with reference to the Faraday cup. The Faraday cup was the same unit used in previous experiments.[2] In our present experiments the vacuum pipe leading to the Faraday cup was not used.

It is difficult at the present time to estimate the errors associated with our absolute cross sections. The main uncertainty is the detection efficiency of our Čerenkov counters. These counters have been tested carefully but it is still possible that a 10% or smaller error remains in our efficiency measurements. Our efficiency measurements differ very little from 100% and we have therefore used this figure as the detector efficiency. Statistical errors are usually small compared with possible systematic errors and perhaps a measure of our errors should be the differences between individual measurements made under the same conditions of energy and angle. These differences are always less than ±10%. Another small source of uncertainty is the value of the dispersion constant of the 72-in. spectrometer. We have measured the dispersion constant to an accuracy of about 5%.

Our results are presented in Table I and include standard radiative corrections.[1] In addition to the cross sections in the Table we give the values of the square of the momentum transfer. In many cases we have given a single value as an average of several measured cross sections. As a general rule we believe our results are accurate to about ±10% because of the aforementioned possible errors. Relatively speaking, errors are probably less than ±5%. Our interpretation of the above results will be given in an accompanying paper.[3]

We understand that the Cornell group[4] is investigating the same electron-scattering problem. Unfortunately we have no firm data of that group to compare with our results.

Table I. Summary of results.

E (Mev)	θ (deg)	q^2 (fermi^{-2})	$(d\sigma/d\Omega)\times10^{33}$ (cm^2/sr)
597	60°	6.96	67.9
597	90°	11.20	8.76
597	120°	14.06	2.65
650	135°	16.97	1.51
700	60°	9.16	38.0
700	75°	12.01	11.2
700	135°	18.90	0.955
700	145°	19.43	0.778
750	45°	6.86	136
750	75°	13.45	10.0
750	90°	16.06	4.08
750	135°	20.86	0.728
750	141.5°	21.24	0.735
750	145°	21.42	0.580
775	135°	21.86	0.644
800	45°	7.70	104
800	60°	11.53	23.5
800	75°	14.93	8.19
800	90°	17.75	2.99
800	120°	21.64	0.888
800	135°	22.86	0.605
800	145°	23.44	0.360
850	45°	8.59	80.6
850	60°	12.77	17.8
850	75°	16.46	5.62
850	120°	23.60	0.711
850	135°	24.88	0.509
850	145°	25.50	0.371
875	40°	7.56	127
875	45°	9.05	82.0
875	60°	13.42	15.7
875	145°	26.54	0.376
900	45°	9.51	61.5
900	60°	14.06	14.3
900	75°	18.03	5.35
900	90°	21.24	2.09
900	145°	27.58	0.347

We wish to acknowledge most gratefully the cheerful cooperation and assistance we have received from D. Aitken, P. Auvil, C. Buchanan, G. Burleson, B. Chambers, H. Collard, E. Dally, P. Gram, T. Janssens, M. Ryneveld, and W. Wadensweiler.

*This work was supported in part by the Office of Naval Research and the U. S. Atomic Energy Com-

mission, and by the U. S. Air Force, through the Office of Scientific Research of the Air Research and Development Command.

†Visitor from University of Strasbourg, Strasbourg, France.

[1]E. E. Chambers and R. Hofstadter, Phys. Rev. 103, 1454 (1956).

[2]R. Herman and R. Hofstadter, High-Energy Electron Scattering Tables (Stanford University Press, Stanford, California, 1960), and the work of F. Bumiller and R. Hofstadter shown in Fig. 8 of this reference.

[3]R. Hofstadter, F. Bumiller, and M. Croissiaux, following Letter [Phys. Rev. Letters 5, 263 (1960)].

[4]K. Berkelman and J. Cassels (private communication).

SPLITTING OF THE PROTON FORM FACTORS AND DIFFRACTION IN THE PROTON*

R. Hofstadter, F. Bumiller, and M. Croissiaux†
Department of Physics and High-Energy Physics Laboratory, Stanford University, Stanford, California
(Received August 25, 1960)

Electron-scattering studies of the proton obtained in the last few years have been summarized recently.[1] The measurements showed that the proton form factors (F_1, F_2) were less than unity, implying a finite structure, and lay in a region in which they were approximately equal to each other at momentum transfers (q) as high as $q^2 = 9.3$ in units of squared inverse fermis. At this value of the momentum transfer the measured ratio was $F_1/F_2 = 1.23 \pm 0.20$.[2] The experiments were confined to angles larger than 60° at the highest energies then obtainable (650 Mev) because of the limitation imposed by the energy-handling ability of the 36-in. spectrometer. It was therefore not possible to solve for F_1 and F_2 separately at values of $q^2 \geq 9.3$. Several independent experiments[2,3] indicated that the F_1 values were slightly greater than the F_2 values at the same momentum transfer, but for simplicity and ease of calculation, in the past, the ratio of form factors was usually taken to be unity.

We have now succeeded in splitting apart the two proton form factors. Because of the great interest in the proton form factors and because our data appear to be internally consistent, we wish to present in this paper some conclusions drawn from the experimental results given in the accompanying paper.[4]

Our procedure has been to solve for the separate form factors (F_1, F_2) at conditions lying between $7.7 \leq q^2 \leq 25$ by choosing a pair of experimentally measured cross sections at the same value of q^2 but at different correlated values of energy and angle. We have used the method of intersecting ellipses[5] to find the form factors.

Table I shows the values selected and the form factors found by combining the results. In a few cases, indicated by asterisks, we have used older data and combined the older values with the newly-measured cross section at the same value of q^2. In two cases (866 Mev, 75°; 675

Table I. Form factors F_1 and F_2.

q^2 (f^{-2})	E_1 (Mev)	θ_1 (deg)	$(d\sigma/d\Omega)_1$ (cm^2/sr)	E_2 (Mev)	θ_2 (deg)	$(d\sigma/d\Omega)_2$ (cm^2/sr)	F_1	F_2
7.70	800	45°	1.04×10^{-31}	400	124°	*1.06×10^{-32}	0.520	0.490
9.16	700	60°	3.80×10^{-32}	464	135°	*6.26×10^{-33}	0.500	0.420
11.50	800	60°	2.35×10^{-32}	500	135°	*4.18×10^{-33}	0.451	0.341
14.06	900	60°	1.43×10^{-32}	597	120°	2.65×10^{-33}	0.423	0.214
16.97	866	75°	5.56×10^{-33}	650	135°	1.51×10^{-33}	0.430	0.160
18.03	900	75°	5.35×10^{-33}	675	135°	1.23×10^{-33}	0.451	0.108
21.24	900	90°	2.09×10^{-33}	750	141.5°	7.35×10^{-34}	0.405	0.087

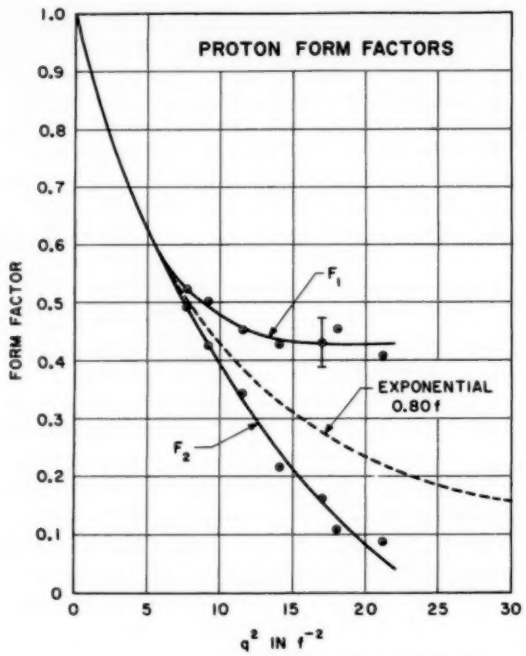

FIG. 1. The proton form factors obtained in Table I, plotted against q^2. F_2 may be approaching a diffraction zero.

Mev, 135°) we have interpolated between two newly-measured results in order to obtain properly matched pairs of cross sections.

The form factor results now show the behavior plotted in Fig. 1. The dashed line is the form factor corresponding to the exponential model and $F_1 = F_2$. Apparently our new F_2, which is seen to approach zero, indicates qualitatively that the Pauli magnetic moment cloud is a "soft," spread-out distribution. On the other hand, the constancy of F_1 suggests qualitatively that the Dirac electric/magnetic cloud has a small, perhaps point-like, core.

The form factors found in the above manner were then put back into the well-known Rosenbluth Eq. (40) of reference 1:

$$d\sigma/d\Omega = \sigma_{NS}\{a_{11}F_1^2 + a_{12}F_1F_2 + a_{22}F_2^2\}, \quad (1)$$

where the values of the coefficients a_{11}, a_{12}, and a_{22} are taken from the tables[1] at the appropriate energies and angles. When this is done we obtain the results shown in Fig. 2. Notice that in Fig. 2(c) the cross section appears to be going through a diffraction dip, so characteristic of electron-scattering studies on heavier nuclei. The experimental data indeed show this diffraction dip and we believe that this is the first time diffraction has been observed in the proton.

Within experimental error the new experimental results appear to be in agreement with the split form factor curves. It is very interesting to observe that the new form factors account for an increase of the cross section above the exponential case at small angles, merge approximately with the exponential case at 120°, and drift below the exponential case at the large angles 135° and 145°. This is what the experiments appear to indicate and the result is a rather complicated pattern of cross sections which the form factors must satisfy. The experimental data appear to fit the calculated curves for separate form factors absolutely as well as relatively.

The data are in excellent agreement with the earlier experimental results.[1] The measurements of a proton root-mean-square radius appear to remain undisturbed because those measurements were made at low q values. However, we are aware that at higher values of q^2 the conclusions about the neutron's form factors may be influenced slightly.[1,6] This question is now under investigation by R. Herman and the authors. It may be pointed out that the inelastic electron-scattering studies on the deuteron should perhaps yield new information on the F_1 form factor of the neutron when combined with these results. It is interesting to speculate on whether the proton's F_2 factor rises again after approaching zero at about $q^2 \cong 24$ or whether it becomes negative at that point. In our analysis we assumed $F_2 \cong 0$ at $q^2 > 24$.

By use of these results new information on F_2 of the neutron should result from a study of the deuteron's elastic scattering at large angles.

We wish to thank Mr. Francis Lewis for his help in making some of the calculations with intersecting ellipses.

---

*This work was supported in part by the Office of Naval Research and the U. S. Atomic Energy Commission, and by the U. S. Air Force, through the Office of Scientific Research of the Air Research and Development Command.

†Visitor from University of Strasbourg, Strasbourg, France.

[1]R. Herman and R. Hofstadter, High-Energy Electron Scattering Tables (Stanford University Press, Stanford, California, 1960).

[2]F. Bumiller and R. Hofstadter; see Fig. 8, p. 28,

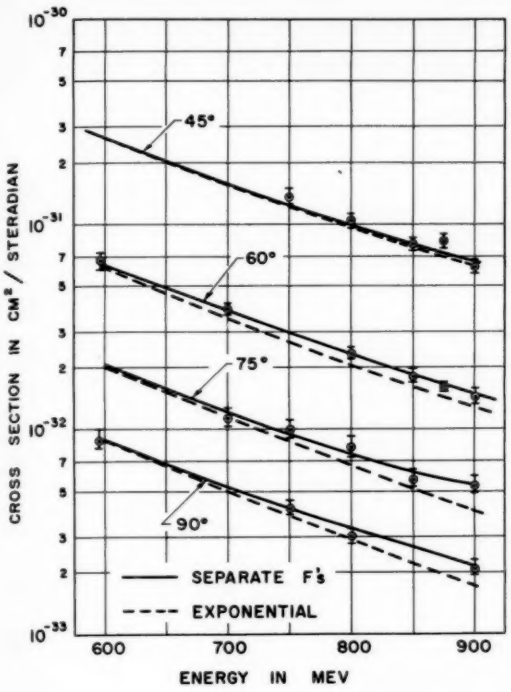

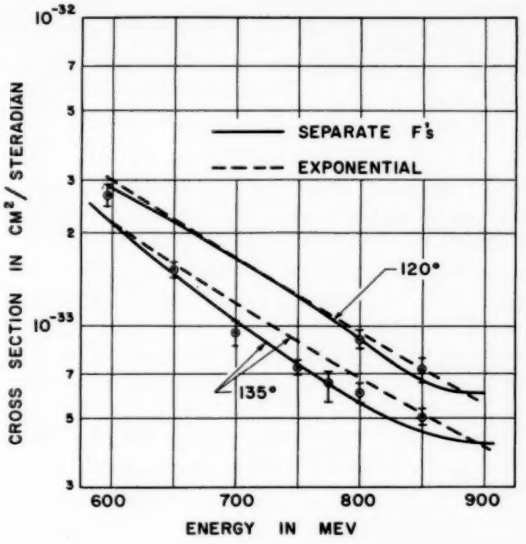

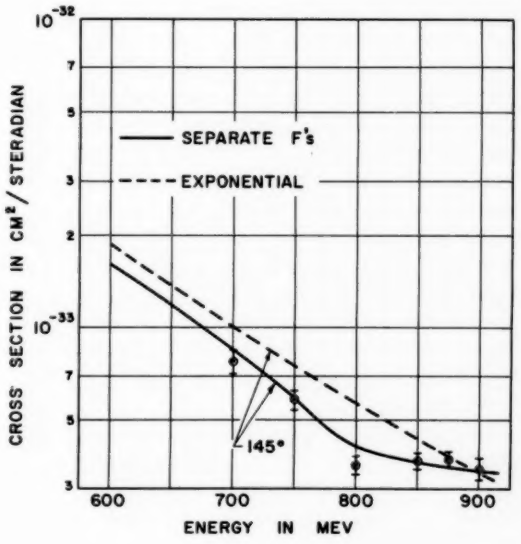

FIG. 2. Comparison of observed and calculated cross sections. The experimental points are shown by hollow circles. The dashed line refers to the case $F_1 = F_2$ and corresponds to the form factors deduced from the old exponential model.[1] The solid line is obtained from Eq. (1) and the newly-obtained form factors of Table I and Fig. 1.

of reference 1.

[3]E. E. Chambers and R. Hofstadter, Phys. Rev. 103, 454 (1956).

[4]F. Bumiller, M. Croissiaux, and R. Hofstadter, preceding Letter [Phys. Rev. Letters 5, 261 (1960)].

[5]R. Hofstadter, Ninth Annual International Conference on High-Energy Physics, Kiev, July, 1959 (unpublished). See also reference 1, pp. 30-32.

[6]R. Hofstadter, F. Bumiller, and M. R. Yearian, Revs. Modern Phys. 30, 482 (1958).

BOUNDARY CONDITION MODEL FOR PROTON-PROTON SCATTERING

D. P. Saylor, R. A. Bryan, and R. E. Marshak
Physics Department, University of Rochester, Rochester, New York
(Received July 18, 1960)

An interesting feature of the potential model devised by Bryan[1] for proton-proton scattering is that in the triplet states there is a region of great strength between $0.6\hbar/\mu c$ (μ is the pion mass) and the radius of the infinite core, $0.38\hbar/\mu c$, and that outside this region the potential is comparatively weak, and closely resembles most one- and two-pion theoretic calculations. These features made it seem likely that a boundary condition model with meson-theoretic potential tails could give a good description of nucleon-nucleon scattering in the 40- to 310-Mev energy range.

The boundary condition model without potential tails was first suggested and applied to S-wave scattering by Breit and Bouricius.[2] Later, Feshbach and Lomon[3] extended the model to higher waves, but their predicted phase shifts resembled the No. 6 solution of Stapp, Ypsilantis, and Metropolis[4] which has since been ruled out. The possibilities of the boundary condition model with potential tails were then explored by Tubis and Feshbach,[5] though the analysis has not been carried out to the extent of securing really good fits to the experimental data as yet. We have found that such a boundary condition model, using the Taketani-Machida-Ohnuma (TMO) potential,[6] indeed yields a very good description of the p-p data up to 310 Mev consistent with the MacGregor, Moravcsik, and Stapp phase shift solution No. 1 (MMS No. 1).[7]

We have applied the boundary conditions at the same radius for all states of a given spin angular momentum S. Preliminary values of the boundary conditions were obtained by inward stepwise calculation of the wave functions for each state, starting in the asymptotic region with values corresponding to the MMS No. 1 phase shifts at 310 Mev. The energy-independent boundary conditions used in the model are given in Table I. Some of the resulting phase shifts appear in Table II and the predictions of this model are compared with experiment[8] in Fig. 1. It is seen that r_0 differs only slightly for the singlet ($r_0 = 0.53\hbar/\mu c$) and triplet ($r_0 = 0.56\hbar/\mu c$) states. Applying the boundary conditions at the same radius ($r_0 = 0.53\hbar/\mu c$) for all states regardless of spin gives a slightly less good fit.

Table I. Energy-independent boundary conditions used in conjunction with the TMO potential. The notation is that of Feshbach and Lomon.[a]

	Singlet f_j			r_0 ($\hbar/\mu c$)
$^1S_0$	0.716			0.53
$^1D_2$	1.52			0.53
	Triplet uncoupled f_j			r_0 ($\hbar/\mu c$)
$^3P_0$	19.2			0.56
$^3P_1$	4.19			0.56
$^3F_3$	-0.313			0.56
	Triplet coupled $f_{j,j-1}$	$f_{j,j+1}$	f_j^t	r_0 ($\hbar/\mu c$)
$^3P_2$-$^3F_2$	1.32	4.71	4.54	0.56
$^3F_4$-$^3H_4$	-0.644	22.5	-0.0815	0.56

[a]See reference 3.

Table II. Phase shifts predicted by TMO+boundary condition model. The phase shifts are the nuclear bar phase shifts of reference 4 in degrees.

E (Mev)	$^1S_0$	$^1D_2$	$^3P_0$	$^3P_1$	$^3P_2$	ϵ_2	$^3F_2$	$^3F_3$	$^3F_4$	ϵ_4	$^3H_4$
40	43.1	0.8	11.2	-7.3	3.8	-1.2	0.1	-0.2	0.0	0.0	0.0
150	15.9	5.9	5.8	-17.5	14.6	-3.2	1.2	-2.3	0.7	-0.8	0.1
210	5.3	7.6	-0.6	-21.6	17.0	-2.8	1.7	-3.0	1.4	-1.3	0.2
310	-9.1	11.9	-11.5	-27.8	17.0	-1.6	2.2	-3.63	3.5	-1.5	0.4

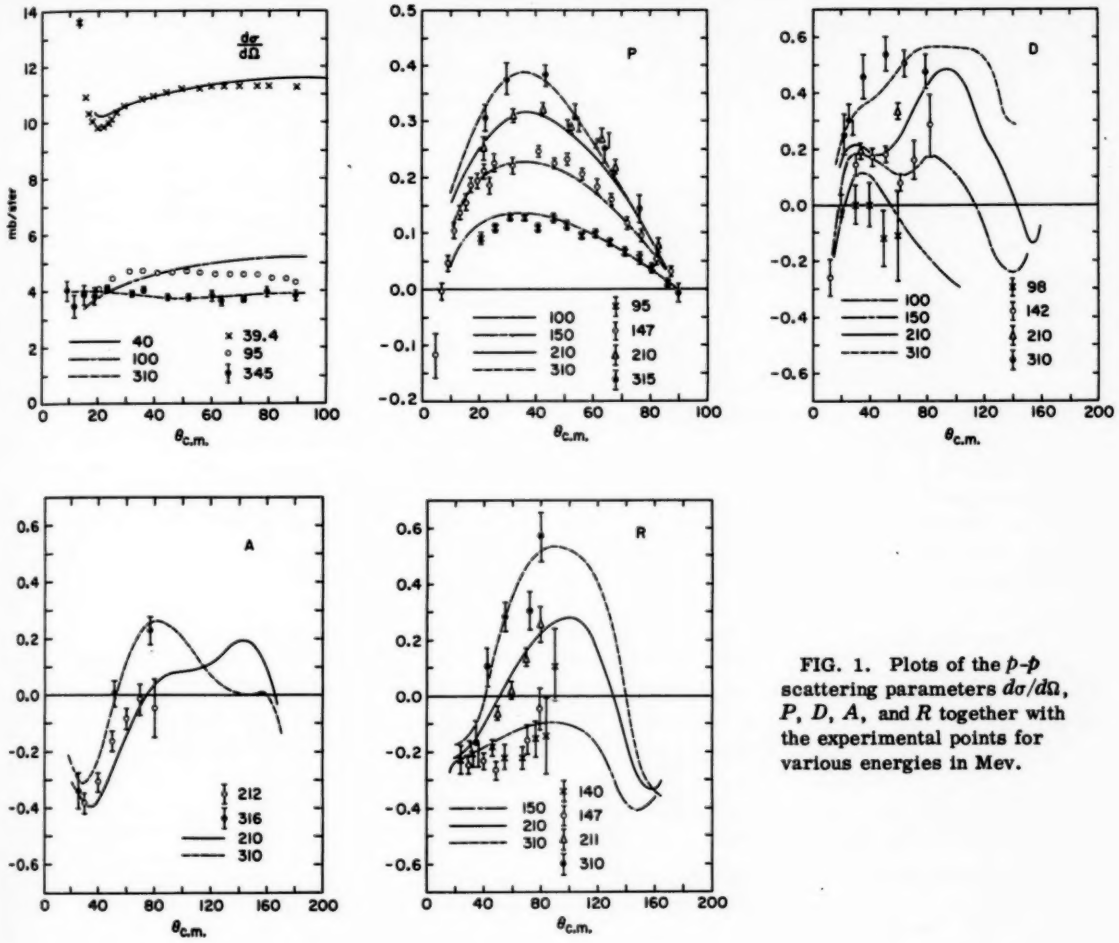

FIG. 1. Plots of the p-p scattering parameters $d\sigma/d\Omega$, P, D, A, and R together with the experimental points for various energies in Mev.

Because the computer program used in this work only takes the Coulomb force into account in an approximate way, this model is not compared with low-energy experiments (less than 40 Mev) or with experimental data in the Coulomb interference region at the higher energies. It should be noted, however, that the boundary condition model will probably also give too large a scattering length (and a fortiori a negative shape parameter) a feature which has plagued most models to date.[9]

The boundary condition method was also tried with the one-pion exchange potential (OPEP) in the outer region. Figure 2(a) shows the 150-Mev cross section with OPEP and TMO. The $^1D_2$ phase shift is 4° for OPEP and 5.1° for TMO when the 310-Mev MMS No. 1 value is matched. This difference is largely responsible for the difference in cross sections exhibited in Fig. 2(a). Figure 2(b) shows the extra strength of the TMO potential in singlet states which brings about this larger phase shift. A defect of this model is the tendency of the cross section to dip too low in the forward direction. As can be seen from the trend of the curves shown in Fig. 2, one can improve the fit if one uses a potential which has more long-range attraction for the $^1D_2$ state than is given by OPEP or TMO.

Beyond the boundary radius r_0, the wave functions predicted by our model are very similar to those given by the Bryan potential. Evidently, a boundary condition model with static potential tails may simulate a more general velocity-dependent interaction than a potential model based on a combination of central, tensor, and spin-orbit forces. Furthermore, the present boundary

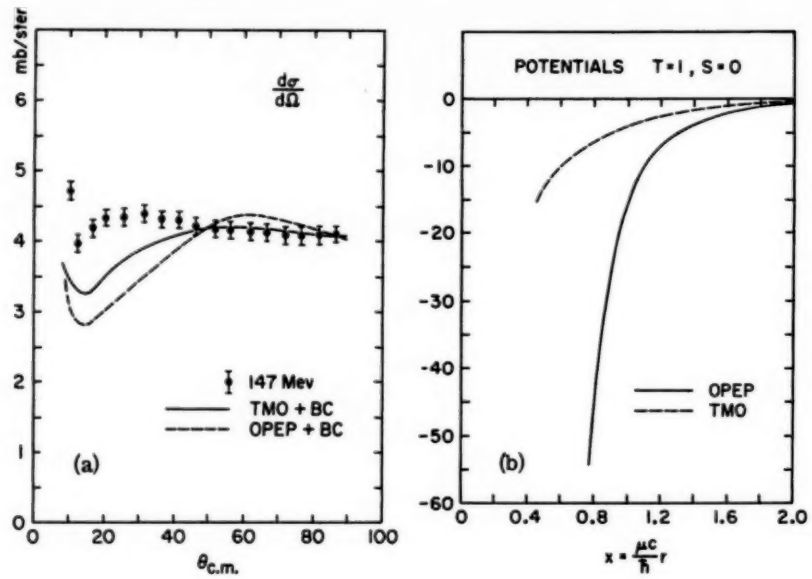

FIG. 2. (a) Plot of the $d\sigma/d\Omega$ as predicted by OPEP and TMO models. (b) The singlet, even-parity OPEP and TMO potentials.

condition model has the advantage, apart from its simplicity, of not requiring a knowledge of the meson-theoretic two-nucleon interaction below one-half of a pion Compton wavelength. This advantage may be considerable from the point of view of existing dispersion techniques.

[1]R. A. Bryan, Nuovo cimento (to be published).

[2]G. Breit and W. G. Bouricius, Phys. Rev. 79, 1029 (1949).

[3]H. Feshbach and E. Lomon, Phys. Rev. 102, 891 (1956).

[4]H. P. Stapp, T. J. Ypsilantis, and N. Metropolis, Phys. Rev. 105, 302 (1957).

[5]A. Tubis (private communication). See also A. M. Saperstein and L. Durand, III, Phys. Rev. 104, 1102 (1956).

[6]M. Taketani, S. Machida, and S. Ohnuma, Progr. Theoret. Phys. (Kyoto) 6, 638 (1951).

[7]M. H. MacGregor, M. J. Moravcsik, and H. P. Stapp, Phys. Rev. 116, 1248 (1959).

[8]$d\sigma/d\Omega$, 39.4 Mev: L. H. Johnston and D. A. Swenson, Phys. Rev. 111, 212 (1958); $d\sigma/d\Omega$ and $P(\theta)$, 95 Mev and 147 Mev: J. N. Palmieri, A. M. Cormack, N. F. Ramsey, and R. Wilson, Ann. Phys. 5, 299 (1958); $D(\theta)$, 98 Mev: E. H. Thorndike and T. R. Ophel, Phys. Rev. 119, 362 (1960); $D(\theta)$, 142 Mev: C. F. Hwang, T. R. Ophel, E. H. Thorndike, and R. Wilson, Phys. Rev. 119, 352 (1960); 147 Mev: C. F. Hwang et al. (to be published); $R(\theta)$, 140 Mev: A. E. Taylor (private communication); $P(\theta)$, 210 Mev: E. Baskir, E. M. Hafner, A. Roberts, and J. H. Tinlot, Phys. Rev. 106, 564 (1957); $D(\theta)$, 210 Mev: K. Gotow (private communication); $R(\theta)$, 210 Mev: J. Tinlot, E. Heer, A. England, and W. Gibson, Bull. Am. Phys. Soc. 4, 252 (1959); $d\sigma/d\Omega$, 345 Mev, $P(\theta)$, 315 Mev, $D(\theta)$, 310 Mev, $R(\theta)$, 310 Mev: as compiled in reference 4.

[9]M. H. MacGregor, M. J. Moravcsik, and H. P. Noyes, University of California Radiation Laboratory Report, UCRL 5582-T (unpublished).

RAPID REDUCTION OF COSMIC-RADIATION INTENSITY MEASURED IN INTERPLANETARY SPACE*

C. Y. Fan,† Peter Meyer, and J. A. Simpson
Enrico Fermi Institute for Nuclear Studies, University of Chicago, Chicago, Illinois
(Received August 10, 1960)

In a recent Letter[1] we showed that the mechanism responsible for the rapid decreases of galactic cosmic-ray intensity was located beyond 8 Earth radii, and that this result excluded all existing geocentric theories for this phenomenon. We have extended these experiments out to distances of 8×10^6 km and now can prove that there is no possible association of this phenomenon with the earth and its magnetic field. We also find strong evidence that there is a bulk motion outward from the sun of conducting solar plasma ejected in association with a solar flare which either carries magnetic fields within itself, or manipulates an interplanetary magnetic field to remove convectively the galactic cosmic radiation from a limited volume of the inner solar system.

The experimental apparatus was carried in the space probe Pioneer V launched March 11, 1960 on a trajectory inside the orbit of the earth and towards the orbit of Venus. The apparatus is identical with equipment on Explorer VI; namely, a wide-angle, triple coincidence counter telescope surrounded by 5 g/cm² lead which detects protons with energies in excess of 75 Mev and electrons of more than 13 Mev. Bremsstrahlung due to electrons in the energy range 0.2 - 13 Mev is measured independently. The details of the experiment have been described in earlier communications.[1,2] To compare simultaneously the changes of cosmic-ray intensity at the earth and at the position of the vehicle in interplanetary space, the recordings of nucleonic component intensity monitors were used. The telemetry limitations for Pioneer V confined the data recording to relatively short intervals several times each 24-hour period. Therefore, the correlation method used previously for Explorer VI data[1] cannot be applied to Pioneer V results. Consequently, averaged, simultaneous observations in the space probe and at the earth are used to determine the relative change in galactic intensity at the probe and at the earth both before the intensity decrease, and after the decrease reached its full extent.

Although several intensity decreases have been detected in the Pioneer V data,[3] the largest and most readily analyzed event occurred on March 31, 1960, at which time the probe was nearly on the Sun-Earth line and 5.2×10^6 km inside the orbit of Earth. The changes in the nucleonic component at the earth—representing changes in the primary beam of particles with magnetic rigidities > 2.4 Bv—are shown in Fig. 1. The corresponding data for Pioneer V are shown in Fig. 2(a).

It is almost certain that the ejection of plasma from the solar flare[4] of importance 2 at 1455 - 1858 U. T. on March 30 led to the commencement of the geomagnetic storm and the beginning of the cosmic radiation intensity decrease at about 1200 U. T. on March 31. From this time delay we compute an average radial velocity of 2000 km/sec for the advancing "front" of conducting plasma. The expected time difference of ~40 - 50 minutes between the arrival of the plasma at Pioneer V and at the earth could not be observed due to the intermittent reception of data.

After extrapolating the neutron intensity monitor data of Fig. 1 to the top of the atmosphere,[1] we compute the ratio of the relative intensity change at the space probe and at the earth as

$$\frac{\text{Relative change in Pioneer V detector}}{\text{Relative change at the earth}} = 1.3 \pm 0.15$$

on April 1, 1960.

The larger decrease measured by the Pioneer

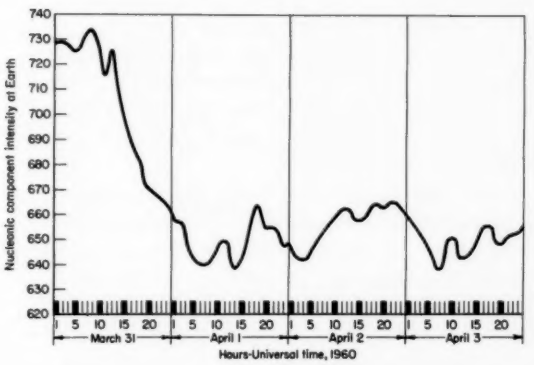

FIG. 1. The changes in galactic cosmic-ray intensity for particles above 2.4-Bv magnetic rigidity. The neutron monitor is located at Climax, Colorado.

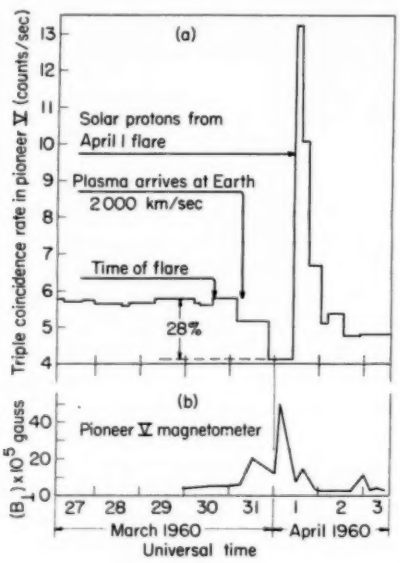

FIG. 2. Telemetered data from the space probe Pioneer V at distances $4-5.5\times10^6$ kilometers from the earth. The errors for each bar are less than 1%. The time for the first arrival of solar protons April 1 was determined by the onset of enhanced ionization from protons at the polar cap.[8] The magnetometer measurements in Pioneer V are published by Coleman et al.[7]

V detector arises from the removal of cosmic radiation with magnetic rigidities below the cutoff for the detector at the earth (2.4 Bv) but not below the threshold of the probe detector. Indeed, this removal of low-energy particles persisted for more than 30 days after April 1 although the relativistic particle flux by that time had returned to the intensity prevailing before the decrease.[5] From analysis of our neutron monitor data extending to the geomagnetic equator where the cutoff reaches ~15 Bv, we find independent evidence that the intensity decrease was more strongly dependent upon particle magnetic rigidity than for the event of August 19 - 20, 1959 previously reported.[1]

These results prove that the rapid reduction in galactic cosmic radiation is a phenomenon of solar origin taking place in interplanetary space and is not related to the presence of the earth or its magnetic field. Since the observed intensity decreases only follow solar flares on the visible side of the sun, the reduction of cosmic-ray particle intensity is confined to a limited volume of the inner solar system. We also eliminate all electrostatic field deceleration models for this effect.

From the simultaneous measurements in Pioneer V and at the earth we may also deduce some of the properties of these modulating magnetic fields:

(a) It has been known for many years that the rate of decrease of cosmic-ray intensity may be as high as 5% per hour for some events. On the basis of our Explorer VI studies[1] and the present results, we now conclude that this high rate applies to the removal rate of particles and, hence, to the transient magnetic field parameters in the interplanetary medium. Since telemetered data from Pioneer V on March 31, 1960 did not provide details on the rate of intensity change, we refer to the neutron data in Fig. 1 for these measurements. Approximately 28% of the particle flux detected by Pioneer V disappeared in less than 20 hours, with half of this decrease occurring in less than six hours. From these data and the computed radial velocity of 2000 km/sec for the advancing "front" of solar plasma, it is clear that a penetration to ~0.3 a.u. behind the front is required to reduce the intensity by 14%—half the full intensity decrease. For other events of this kind where the rate of decrease may be as high as 5 to 6% per hour the corresponding depth of penetration may be smaller by a factor of 3. This requires the rapid appearance of enhanced interplanetary magnetic field intensities; the magnitude of the changes and the degree of disordering of the required fields depends upon initial conditions and specific models which are not discussed here. Whereas our results describe large-scale transient magnetic fields over great distances from Pioneer V, the magnetometer in Pioneer V registers field changes at the position of the vehicle perpendicular to its spin axis.[6,7] These data[7] are shown in Fig. 2(b) where magnetic field increases of a factor 10 - 20 times the quiescent field conditions occur at the time for which we deduce the existence of large-scale magnetic fields from the changes in cosmic-ray flux. Both kinds of observations show that magnetic fields are being moved or generated in interplanetary space as a consequence of the solar flare on March 30. The only known way by which these transient fields could be established, or existing fields manipulated, is by moving, conducting plasma of solar flare origin. Therefore, we believe these Pioneer V results provide the most direct evidence to date for the existence of conducting gas ejected at high velocity from solar flares—a concept

strongly supported already by many solar and terrestrial observations. Convective removal of galactic cosmic radiation by particle collisions with advancing magnetic field irregularities, such as a shock front, is the most likely explanation at this time. We do not discuss here the many models which may fulfill some of these conditions.

(b) By 0600 April 1 the advancing region which produced the full decrease of intensity had passed outward beyond Pioneer V and the earth. What were the magnetic field conditions remaining immediately thereafter in space between the sun and Pioneer V, i.e., behind the advancing "front"? This question may be investigated by examining the propagation of solar flare protons on April 1 which penetrated the volume of space between the sun and Pioneer V only four hours after the full reduction of galactic cosmic-ray intensity. The solar flare was observed to begin at 0845 and extend through 1222 U. T., with the first solar particles arriving to produce ionization in the polar ionosphere at 0945 U. T.[8] Thus the upper limit for the transit time is one hour. The solar particle increase is shown in Fig. 2(a) for protons >75 Mev (but less than 1 Bev since no increases were observed by neutron monitors at the earth). Maximum intensity was reached within 50 minutes.[8] The subsequent decline of intensity with time t closely follows a power law $1/t$.

These data show that the interplanetary magnetic field conditions behind the advancing front are either smooth and radial or weak, irregular fields ($B_{rms} < 5\times10^{-6}$ gauss), otherwise the low-energy solar protons would not penetrate to the orbit of the earth in less than one hour.

Bremsstrahlung-producing radiation was also observed by our single, lead-shielded counter in Pioneer V[3] and by the University of Minnesota detectors[9] beginning about two days before and during the Forbush decrease. The measurement of detector efficiency is under way and these results will be reported at a later date.

For their contributions to the engineering and construction of our apparatus we wish to thank Mr. J. Jezewski, Mr. J. Lamport, Mr. L. Petraitis, and Mr. R. Takaki of the Laboratories for Applied Science, University of Chicago. We also appreciate the over-all engineering and management of the Pioneer V project by Dr. A. Thiel, Dr. J. Lindner, and the staff of Space Technology Laboratories. The assistance of Dr. J. Lindsay of the N.A.S.A. for the Pioneer V project and the use of the Jodrell Banks radio telescope by Professor A. C. B. Lovell enhanced greatly the results of these experiments.

---

*This research was supported principally by the National Aeronautics and Space Administration, and in part by the Air Force Cambridge Research Center, Geophysics Research Directorate, and the Air Force Office of Scientific Research.

†Also Laboratories for Applied Science, University of Chicago, Chicago, Illinois.

[1]C. Y. Fan, P. Meyer, and J. A. Simpson, Phys. Rev. Letters 4, 421 (1960), and references therein.

[2]C. Y. Fan, P. Meyer, and J. A. Simpson, Proceedings of the First International Conference on Space Research (North-Holland Publishing Company, Amsterdam, 1960); I.G.Y. Satellite Report No. 11, p. 115, June, 1960 (World Data Center A).

[3]C. Y. Fan, P. Meyer, and J. A. Simpson, J. Geophys. Research 65, 1862 (1960).

[4]Solar and Geophysical Data, National Bureau of Standards, Central Radio Propagation Laboratory Series-F, Part B (1960).

[5]See C. Y. Fan, P. Meyer, and J. A. Simpson, following Letter [Phys. Rev. Letters 5, 272 (1960), Fig. 3.

[6]P. J. Coleman, Jr., L. Davis, and C. P. Sonett, Phys. Rev. Letters 5, 43 (1960).

[7]P. J. Coleman, Jr., C. P. Sonett, D. L. Judge, and E. J. Smith, J. Geophys. Research 65, 1856 (1960).

[8]H. Leinbach [private communication and preprint, June 21, 1960 (unpublished)].

[9]J. R. Winckler (unpublished communication).

EXPERIMENTS ON THE ELEVEN-YEAR CHANGES OF COSMIC-RAY INTENSITY USING A SPACE PROBE*

C. Y. Fan,† Peter Meyer, and J. A. Simpson
Enrico Fermi Institute for Nuclear Studies, University of Chicago, Chicago, Illinois
(Received August 10, 1960)

The total intensity of cosmic radiation reaching the earth changes with the 11-year solar activity cycle.[1] The energy spectrum of relativistic particles up to at least 20 Bev changes approximately from $E^{-2.7}$ (1954) to $E^{-2.0}$ at maximum solar activity (1957-8) with the intensity being reduced at solar maximum by a factor 2 for the relativistic particle flux,[2] and by a factor in excess of 4 for the integral flux down to ~100 Mev for protons.[3] Figure 1 shows the change in nucleonic component intensity between 1954 and 1960. Experimental evidence strongly supports the view that the spectrum at solar minimum approximates the full galactic spectrum outside the solar system, and that through an electromagnetic modulation mechanism, initiated by solar activity, the galactic particle flux having access to the inner solar system, or the earth, is greatly reduced at solar activity maximum.[2] We have performed direct experiments which prove that any mechanism changing the cosmic-ray intensity over 11 years is centered about the sun, and the scale size is >1 astronomical unit (a.u.) for the volume of space in which the cosmic-ray intensity is reduced at this period of the solar activity cycle. We also find that the gradient of cosmic-ray intensity near the orbit of Earth is so small as to suggest that modulation of galactic intensity occurs at distances much greater than the orbit of Earth.

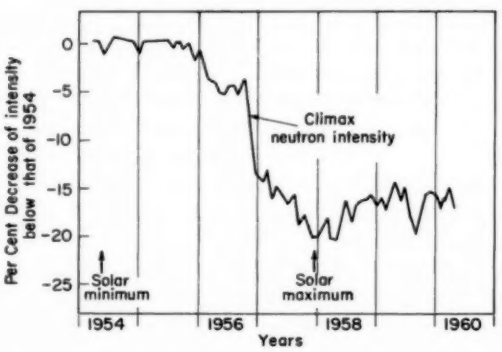

FIG. 1. Changes in the nucleonic component intensity between 1954 and 1960 at Climax, Colorado (~2.4 Bv magnetic rigidity cutoff).

The experiment consists in carrying a cosmic radiation detector from the earth to great distances in interplanetary space near the time of solar maximum. The detector measures protons above 75 Mev and, hence, integrates over that part of the cosmic-ray spectrum which changes by a factor of 2 to 4 in intensity between solar maximum and solar minimum. If the reduced intensity is restricted to the vicinity of the earth, the flux measured in interplanetary space will be greater by a factor of 2 to 4. If the volume in which there is reduced intensity is heliocentric, then there will be an intensity gradient in the direction of the sun, the magnitude of which depends greatly upon the model adopted for the solar origin of the 11-year cosmic-ray intensity variations.

Identical cosmic-ray detectors were carried by the satellite Explorer VI (launched August 7, 1959) and the space probe Pioneer V (launched March 11, 1960), and are described elsewhere.[4,5] Since this detector was not sensitive to bremsstrahlung[4] from trapped electrons in the outer radiation belts of the earth, the cosmic-ray flux was measured from less than 10 000 km to 48 000 km from Earth by Explorer VI. The data for August 9, 1959 are shown in Fig. 2. Between

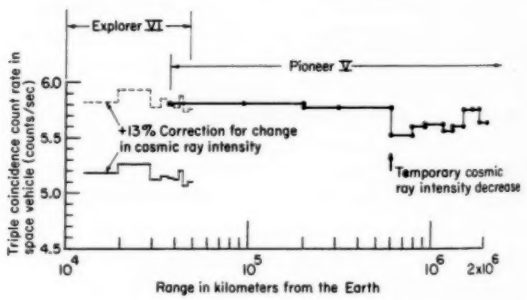

FIG. 2. Counting rate of triple coincidence events in Explorer VI satellite (August 9, 1959) and Pioneer V space probe (March, 1960). The 13% correction in Explorer VI data arises from intensity changes known to take place outside the atmosphere between August, 1959 and March, 1960 due to the 11-year cycle (see Fig. 1). Assigned errors on each interval of data are less than 1%. Pioneer IV (March, 1959) also observed constant intensity between 92 000 and 658 000 km.[8]

this date and the launching of Pioneer V on March 11, 1960, the integrated cosmic-ray intensity at the earth increased by +13% as deduced from nucleonic component monitors. The August 9, 1959 rates in Fig. 2 have, therefore, been increased by 13% for comparison with the Pioneer V data. We note that the cosmic-ray flux was approximately constant from inside the terrestrial field far into the interplanetary medium. Therefore the 11-year depression of cosmic-ray intensity is not geocentric.

We know from analysis of nucleonic component data such as shown in Fig. 1 that the cosmic-ray intensity measured at the earth as the earth moves in its orbit about the sun is not significantly dependent upon solar system longitude. Thus, at solar maximum the cosmic-ray intensity is not only depressed within the inner solar system but the depression is roughly concentric about the sun in the ecliptic plane.

Provided these intensity changes are brought about by solar modulation of the galactic flux, these results lead to the conclusion that there must be a cosmic-ray intensity gradient somewhere between interstellar space and the inner solar system. This gradient will exist in the regions of space where the electromagnetic modulation is taking place.

On the one hand, if the modulating region lies beyond the orbit of Earth (>1 a.u.) then the gradient between Sun and Earth will be very small. A model in this category would be convective removal of particles by advancing magnetic field irregularities arising from instabilities of a solar wind.[6] On the other hand, if the earth lies inside the modulation region the cosmic-ray flux will decrease as one approaches the sun. Several models, including a recent proposal of Elliot,[7] require a large, negative gradient between Sun and Earth.

One of the objectives for the space probe Pioneer V was to examine this problem. At this time we have data over the initial 50 days representing a change in solar radial distance of 0.1 a.u. (10% of the distance to the sun) which sets upper limits on the radial gradient of cosmic-ray intensity in interplanetary space. To remove the time-dependent changes of cosmic-ray intensity, we determined the ratio of the intensities in Pioneer V to the intensities at the earth represented by the nucleonic component monitor at Chicago. This ratio, normalized to unity at time of launch, March 11, is shown in Fig. 3 as a function of solar radial distance, and time. We have averaged data over intervals of two to three days for this analysis.

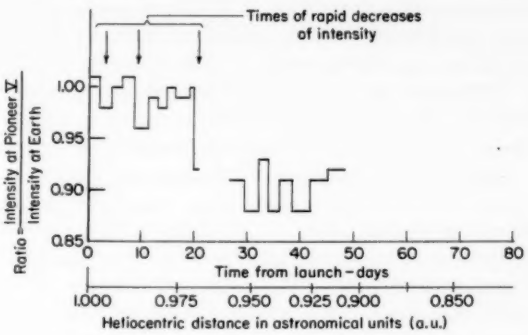

FIG. 3. The change of cosmic-ray intensity radially along the sun-earth line and relative to the intensity at the orbit of Earth. The errors assigned to these averaged intervals of data are less than 0.5%. The arrows indicate the existence of known perturbations in the low-energy portion of the cosmic-ray spectrum and data for these periods are not used in determining the intensity gradient.

It is immediately apparent from Fig. 3 that there was a sudden loss of flux of nonrelativistic particles at the time of the rapid, Forbush intensity decrease of March 31 - April 1.[5] This change in the primary spectrum persisted to the last available measurements 30 days later. The stepwise decrease in the very low energies was also detected in the Explorer VI data,[4] and will be discussed in a later publication. Smaller intensity decreases occurred at the times shown by arrows in Fig. 3. This effect is a change in spectrum which must be taken into account in measuring the gradient. There also exists the possibility that the negligible gradient observed from 0.95 a.u. to 0.90 a.u. (25th to 50th day) is the result of a space gradient plus a compensating gradual return of the low-energy particles. However, such a coincidence of effects is not likely to continue over so long a period.

We obtain a radial omnidirection intensity gradient of $-(15 \pm 20)\%$/a.u. measured near the orbit of the earth and in the direction of the sun. This value is inconsistent with the existence of a positive gradient such as required for an appreciable, steady solar production of the radiation. This small but negative gradient shows that (during the period of this measurement) any electromagnetic modulating mechanism required to account for the eleven-year intensity variations is located principally outside the orbit of Earth. Such re-

sults from Pioneer V place strong constraints upon acceptable heliocentric models for the eleven-year cosmic-ray intensity variation.

We hope that additional data at later times in May may be extracted from the noisy data arising from the low signal level at these great distances.

For their contributions to the engineering and construction of our apparatus we wish to thank Mr. J. Jezewski, Mr. J. Lamport, Mr. L. Petraitis, and Mr. R. Takaki of the Laboratories for Applied Science, University of Chicago. We also appreciate the over-all engineering and management of the Pioneer V project by Dr. A. Thiel, Dr. J. Lindner, and the staff of Space Technology Laboratories. The assistance of Dr. J. Lindsay of the N.A.S.A. for the Pioneer V project and the use of the Jodrell Banks radio telescope by Professor A.C.B. Lovell enhanced greatly the results of these experiments.

*This research was supported principally by the National Aeronautics and Space Administration, and in part by the Air Force Cambridge Research Center, Geophysics Research Directorate, and the Air Force Office of Scientific Research.

†Also Laboratories for Applied Science, University of Chicago, Chicago, Illinois.

[1]S. E. Forbush, J. Geophys. Research 59, 525 (1954).

[2]P. Meyer and J. A. Simpson, Phys. Rev. 106, 568 (1957); J. Simpson, Astrophys. J. Suppl. Series No. 44, 4, 378 (1960).

[3]H. V. Neher, Phys. Rev. 107, 588 (1957); J. R. Winckler and L. Peterson, Nature 181, 1317 (1958).

[4]C. Y. Fan, P. Meyer, and J. A. Simpson, Proceedings of the First International Conference on Space Research (North-Holland Publishing Company, Amsterdam, 1960); I.G.Y. Satellite Report No. 11, p. 115, June, 1960 (World Data Center A).

[5]C. Y. Fan, P. Meyer, and J. A. Simpson, preceding Letter [Phys. Rev. Letters 5, 269 (1960)].

[6]E. N. Parker, Phys. Rev. 109, 1874 (1958).

[7]H. Elliot, Nature 186, 299 (1960).

[8]J. A. Van Allen and L. A. Frank, Nature 184, 219 (1959).

FORM OF THE ONE-PION EXCHANGE POTENTIAL*

G. Breit, M. H. Hull, Jr., K. Lassila, and H. M. Ruppel
Yale University, New Haven, Connecticut
(Received August 18, 1960)

The one-pion exchange potential (OPEP) has been used in calculations in nucleon-nucleon scattering by various authors employing the theoretical expression as a whole.[1] In connection with fits to data by means of adjustable phase-parameters it proved possible to make tests on the correctness of the mathematical form of the OPEP, and a brief report appears desirable. The tests were made by modifying the form of the OPEP through the introduction of additional terms multiplied by dimensionless parameters, q. Varying one of the q together with the pion-nucleon coupling constant g, an adjustment was made to a minimum value of the mean weighted square deviation from experimental data, D, resulting in the determination of the most probable values of g_0 and of the q. Three types of variation have been studied. The first two, a and b, differ only in detail, both having the approximate meaning of changing the coefficient of the spin-spin term of the OPEP containing the factor $(\vec{\sigma}_1\cdot\vec{\sigma}_2)$ from the value 1 to $1+q$. For q_a this was literally the case. For q_b the added term was $(g_0^2/14)q_b$ times the usual spin-spin term. In the units used, $g_0^2\cong 14$. The object in using two ways of introducing q was to provide a check. The two q are denoted below by q_S when the distinction between a and b is immaterial. A third type of variation consists in the introduction of a central potential equal to q_C times $(-1/3)$ of the singlet-even OPEP. The computation of D for various values of g_0 and of the q gave the following results for the combined determination of g_0 and one of the q at a time.

A preliminary form of p-p scattering data fit[2] YLAM gave the pairs of values $q_S=-0.23\pm0.17$, $g_0^2=14.0\pm1.3$ and $q_C=-0.04\pm0.33$, $g_0^2=13.6\pm1.4$. In this test the parameters not varied as OPEP phase parameters were all those for $J\leq 3$ and in addition $\theta^{\overline{F}}_4$, ρ_4, and K_4. The p-p data and their analysis are more accurate than their n-p counterparts and the above values may be supposed to be the more significant among those reported here.

The n-p data fit[2] YLAN2M gave the pairs of values $q_S=0.23\pm0.19$, $g_0^2=12.8\pm1.8$ and $q_C=-1.0\pm1.2$, $g_0^2=15.0\pm1.6$. The one-pion parameters varied in this search were the same for $T=1$ as in YLAM while for $T=0$ the quantities not varied

were those with $J \leq 3$ and in addition δ^3G_4, θ^3G_5, and ρ_5. In this test the T = 0 and T = 1 parameters were varied together.

The n-p data fit[3] YLAN3 gave the pairs of values $q_S = -0.15 \pm 0.18$, $g_0^2 = 13.3 \pm 1.8$ and $q_C = -3.5 \pm 2.6$, $g_0^2 = 13.3 \pm 1.8$ for variations of the OPEP with T = 0 alone. The same fit was used also varying the OPEP parameters for T = 0 and 1 together. In this case the pairs of values $q_S = -0.12 \pm 0.13$, $g_0^2 = 14.2 \pm 1.8$ and $q_C = -4.5 \pm 1.0$, $g_0^2 = 11.8 \pm 0.8$ were obtained. For test YLAN3 the phase parameters which were not varied as OPEP quantities for T = 0 were all those with $J \leq 3$ and in addition those for $^3G_4$, $^3G_5$, and ρ_5 while for T = 1 they were all those with $J \leq 3$ and in addition $^3F_4$ and ρ_4. A later stage of YLAM was used for YLAN3 than for YLAN2M. In connection with the rather large q_C obtained in the last test, it is relevant that for it K_4 was included in the group of OPEP phase parameters subjected to the q, g_0 variations. The possibility that the phase shift K_4 is not sufficiently well represented by the OPEP is suggested by the fact that the other tests described here do not give a definite indication of a nonvanishing q_C.

This explanation of the large q_C is in agreement with the fact that the ^3G parameters change by amounts comparable to their OPEP values in the YLAN3 search. It should also be observed that K_4, having the smallest L, gives the largest contributions to the amplitudes of the OPEP group. For this reason the apparent accuracy of the determinations of q_C is high in the searches including K_4. The effect observed on q_C is of approximately the magnitude expected from other evidence since $-(1/3)(-4.5) = 1.5$ so that effectively the singlet-even long-range potential is roughly twice its OPEP value at the distances which matter most in this work.

A number of inaccuracies may be interfering with the validity of the numbers and error estimates given above. The data fits used are preliminary; there is an appreciable statistical error in the phase parameters of the non-OPEP group; the graphical determination of values of the q and of g_0 is not perfect and may be responsible for an inaccuracy of several units in the last digit of q_S. Nevertheless the tests indicate the absence of large deviations from the OPEP form and furnish a confirmation of it.

The results obtained are on the whole a corroboration of the tests of charge independence[4] which employed similar methods and of the approximate estimates of the internucleon distances beyond which the OPEP may be assumed responsible for the major part of the nucleon-nucleon interaction,[5] the OPEP groups of parameters being similar in the various sets of calculations. The procedure described above is capable of furnishing more definite information regarding the localization of long-range deviations from the OPEP. One of the objects of the present note is to report the possibility of at least a partial empirical analysis of the form of the potential. In future work it may prove possible to test the range constants and through that perhaps to ascertain whether the usual g or f are the more fundamental combinations. The tests themselves can be made to contain a more clean-cut spatial localization by including in the OPEP varied group additional parameters at the lower energies in accordance with the sensitivity curves calculated as in reference 5, and other extensions and improvements are possible. It may be hoped, in this manner, to provide quantitative evidence regarding the two-pion exchange term which is furnished qualitatively in the present study. The absence of definite spin-spin and tensor force modifications and the presence of a central force addition indicated by the numbers reported on is in accordance with expectation for the two-pion exchange.

The help of Mr. F. A. McDonald in performing some of the numerical reductions is gratefully acknowledged.

---

*This research was supported by the U. S. Atomic Energy Commission and by the Office of Ordnance Research, U. S. Army.

[1]M. Taketani, S. Nakamura, and M. Sasaki, Progr. Theoret. Phys. (Kyoto) 6, 581 (1951); J. Iwadare, S. Otsuki, R. Tamagaki, and W. Watari, Progr. Theoret. Phys. (Kyoto) 16, 455 (1956); P. Cziffra, M. H. MacGregor, M. J. Moravcsik, and H. P. Stapp, Phys. Rev. 114, 880 (1959). G. Breit, International Conference on Nuclear Forces and the Few Nucleon Problem, University College, London, July, 1959 (unpublished); this report was based on work done in collaboration with M. H. Hull, Jr., K. D. Pyatt, Jr., C. R. Fischer, K. Lassila, and T. Degges. No attempt to provide a complete bibliography is being made, only a few publications of each group of workers being cited.

[2]Fits obtained by gradient searches employing as a starting point the phase parameters of J. A. Gammel, R. S. Christian, and R. M. Thaler, Phys. Rev. 105, 311 (1957), and of J. A. Gammel and R. M. Thaler, Phys. Rev. 107, 1337 (1957) supplemented by additional values kindly supplied by Gammel and Thaler have designations with YLA for the first three letters. The YLAM set of fits is a modification of the original YLA

described in the last reference of reference 1. Further details regarding YLAM are contained in G. Breit, M. H. Hull, Jr., K. E. Lassila, and K. D. Pyatt, Jr., Phys. Rev. (to be published). A similar designation for n-p fits with YLAN as the first four letters has been partly described in G. Breit, M. H. Hull, Jr., K. Lassila, and K. D. Pyatt, Jr., Phys. Rev. Letters 4, 79 (1960).

[3]Fit YLAN3 is a development on fit YLAN2M with a major difference regarding the sign of ρ_1 through most of the energy range. It includes among other matters the employment of an improved mass treatment for the OPEP as described in the last reference of reference 2 and difference in treatment of OPEP values for $^3F_3$, $^3F_4$, and ρ_4 at different stages of the search.

[4]See last reference of reference 2.

[5]G. Breit and M. H. Hull, Jr., Nuclear Phys. 15, 216 (1960).

DEUTERON PRODUCTION IN HIGH-ENERGY COLLISIONS

R. Hagedorn
CERN, Geneva, Switzerland
(Received August 29, 1960)

The analysis of the beams of secondary particles resulting from 25-Gev protons hitting several different kinds of targets shows the presence of high-energy deuterons.[1] Deuterons have been observed also in cosmic-ray emulsion work[2] and were interpreted as belonging to the high-energy tail of evaporation.

Though the tail of evaporation and also the nuclear cascade may contribute to the total deuteron yield, it is very probable that the CERN deuterons are mainly due to elementary nucleon-nucleon interactions. If that is so, then deuterons should be produced even in a pure proton-proton collision (and, by the way, not only deuterons but also H^3, He^3, and antideuterons and He^4, if namely one or two antinucleons are created[3]).

It is the aim of the present note to explain this fact and give some numerical results.

We consider a p-p collision and calculate the deuteron production by means of the statistical theory. It can be shown[4] that the statistical theory is derivable from S-matrix theory with the result that (n-particle end state)

$$P_F = S(E, \eta_1 \cdots \eta_n) \times R_F(E, T, T_1 \cdots T_n, S_1 \cdots S_n, m_1 \cdots m_n) \quad (1)$$

is the probability of finding any one of the final states f contained in a set F. Here R_F is the total phase space of all $f \epsilon F$ including isospin, spin, and other statistical factors, whereas $S(E, \eta_1 \cdots \eta_n)$ is the average with respect to F of the matrix element squared. E is the total energy (center-of-mass system) and $\eta_1 \cdots \eta_n$ are those parameters of the n particles which survive the integration over final states (e.g., coupling strength, mass, isospin, structure) and therefore influence still the averaged matrix element squared. Considering the inverse reaction leads to some knowledge of S: Namely, for the inverse reaction the individual matrix elements squared are the same, only the sum over final states of the reaction proper goes over into the average over exactly the same states for the inverse reaction, since initial and final states are now interchanged. The function S is by definition this average, and consequently

$$P_F^{\text{inverse}} = S(E, \eta_1 \cdots \eta_n). \quad (2)$$

On the other hand, the inverse reaction can take place only if the n particles (contained in a normalizing box of volume V) meet in a small volume of order $\Omega = (4\pi/3)(1/\mu)^3$; μ = meson mass ($\hbar = c = 1$); hence $S(E, \eta_1 \cdots \eta_n) \propto (\Omega/V)^{n-1}$. Inserting this into (1) and taking into account the Lorentz contraction leads to the usual formula for the statistical theory, which—with certain refinements—seems to work quite well.

Suppose now that a deuteron appears in the final state. Looking at the reaction proper it seems hard to believe that in Ω a deuteron (which is so much bigger) could be born and escape without being destroyed. But certainly it has its legal place in the possible sets of final states. Now things look better in the inverse reaction: a deuteron comes in and has to join inside Ω the other $n-1$ particles. The condition for this is twofold: It has to be there and, at the same time, it has to be as small as Ω. In a way this "melting in" is a measurement of the size of the deuteron (which of course destroys it—in fact it has to disappear as deuteron) and the probability of

finding it as small as Ω (or smaller) is given by the integral over the deuteron wave function:

$$\int_{\Omega} |\psi_d|^2 dV.$$

Therefore, whereas each pion and nucleon is represented in S by a factor Ω/V, the deuteron gives rise to a factor

$$\frac{\Omega_d}{V} = \frac{\Omega}{V}\int_{\Omega} |\psi_d|^2 dV. \qquad (3)$$

Taking a Hulthén-type wave function with hard core (the latter has little influence) gives[5] $\int_{\Omega}|\psi_d|^2 dV \approx \frac{1}{5} - \frac{1}{10}$. With this value for Ω_d one finds the results given in Tables I and II. They show, though they do not apply directly to the experiments (no pp collisions have so far been analyzed with respect to deuterons), that this "elementary production" yields the correct orders of magnitude. The differences may be due to the presence of nuclear matter, to an anisotropy of nucleons in the center-of-mass frame (the transformation c.m. to lab involves the simplifying assumption of isotropy), and to "peripheral" collisions.

It is satisfying that the above picture, which treats the deuteron as a quasi-elementary particle (at least makes no assumptions about how it is formed), can be supported by a kinematical consideration. It can be shown that the above formula can be made plausible also by asking the condition that a neutron and a proton leave the interaction region with a relative momentum, which is "acceptable" as a deuteron internal momentum (it belongs to the Fourier transform of ψ_d). This

Table I. Relative cross sections for deuteron production in pure p-p collisions.

		2.3 Gev	25 Gev
$\sigma_d/\sigma_{\text{inel.}}$	$\Omega_d = \frac{1}{5}$	0.0125	0.024
	$\Omega_d = \frac{1}{10}$	0.006	0.012
$\sigma_{d+\pi}/\sigma_{\text{inel.}}$	$\Omega_d = \frac{1}{5}$	0.0072[a]	10^{-5}
	$\Omega_d = \frac{1}{10}$	0.0036[a]	10^{-5}
$\sigma_{d+\pi}/\sigma_{d+2\pi}$	$\Omega_d = \frac{1}{5}$, $\Omega_d = \frac{1}{10}$	1.73	not calculated

[a]This shows that at this primary energy a strong peak in the deuteron–as well as pion–c.m. spectrum should be observable.

Table II. The (deuteron/proton) ratio in the lab system at 15.9° in pp collisions with 25-Gev primary energy.

Momentum of d and p in Gev/c	$\Omega_d = \frac{1}{5}$	$\Omega_d = \frac{1}{10}$	Experiment p-Al[a]
2	0.002 %	0.001 %	approximately
4	0.6 %	0.3 %	constant, 2 %,[b]
6	2.8 %	1.4 %	between 2.6 and
8	7.8 %	3.9 %	5.5 Gev/c
10	8.2 %	4.1 %	

[a]See reference 1.

[b]Note that the experiment refers to p-Al collisions and the theory to pure p-p collisions.

will be explained elsewhere. Even a detailed final-state interaction treatment[6] leads back to essentially the statistical formula with Ω_d as in (3). The phase-space integrals are computed rigorously (apart from the statistical errors of a Monte Carlo method[7]). All computing work was done on Ferranti-Mercury computers[8] (partly by the author but) mainly by Dr. W. Laskar, University College, London. The author is very grateful to him for not only carrying out the machine runs but also writing up all data tapes.

Many thanks are due to the University College, London, for offering computing time on their Mercury, to Dr. J. von Behr, CERN, for transforming the c.m. spectra to the lab system, and to many colleagues for discussions, in particular to J. von Behr, G. Bernardini, F. Cerulus, G. Cocconi, G. Fidecaro, A. W. Merrison, A. Pais, L. I. Schiff, and Y. Yamaguchi. The last-named was the first to obtain a numerical estimate on the basis of an argument involving restricted relative momenta for the outgoing nucleons.

[1]V. T. Cocconi, T. Fazzini, G. Fidecaro, M. Legros, N. H. Lipman, and A. W. Merrison, Phys. Rev. Letters 5, 19 (1960).

[2]C. F. Powell, P. H. Fowler, and D. H. Perkins, Study of Elementary Particles by the Photographic Method (Pergamon Press, New York, 1959), p. 440.

[3]Calculations including these particles are in progress.

[4]R. Hagedorn, Nuovo cimento 15, 434 (1960).

[5]Y. Yamaguchi (private communication).

[6]L. I. Schiff (private communication), and CERN Report No. 60-32 (unpublished).

[7]F. Cerulus and R. Hagedorn, Suppl. Nuovo cimento 9, 646 and 659 (1958).

[8]R. Hagedorn, CERN Report No. 59-25 (unpublished).

PRODUCTION OF PARTICLE BEAMS AT VERY HIGH ENERGIES*

S. D. Drell
Institute of Theoretical Physics, Department of Physics, Stanford University, Stanford, California
(Received August 25, 1960)

We consider the production of beams of very-high-energy strongly interacting nuclear particles. By studying the transition amplitudes near their poles corresponding to "real" one-particle intermediate states, we show that photons are very effective in initiating collimated beams of high-energy charged pions and K mesons, (anti-) nucleons, etc. A photon of energy k incident on a nuclear target produces a high-energy charged pion, say, of energy $\omega_q > \frac{1}{2}k$ ($\hbar = c = 1$) in a forward cone of opening angle $\theta_{1/2} \sim \mu/\omega_q$ with a cross section that is reduced by roughly the fine structure constant, $\alpha = 1/137$, from geometric, $\sim 1/\mu^2 = 20$ mb. For nucleon-initiated processes, on the other hand, although one avoids the fine structure constant, the statistical model predicts that very high energy secondaries emerge in only a very small fraction of the collisions.

This result is of significance for predicting and comparing yields from very high energy electron and proton accelerators. Experiments can be performed on existing machines to check the validity of this "pole analysis" which, as applied here to general inelastic processes, is an extension of the work of Chew, Goebel, and particularly of Chew and Low.[1]

Figure 1 illustrates the process being considered, with X the nuclear target and (n) anything else produced in addition to the high-energy pion. Our basic approximation now, in calculating the cross section when the pion is produced with energy $\omega_q \sim k$ and within the forward angular cone at an angle $\theta_q \leq \theta_{1/2} \sim \mu/\omega_q$, is to assume that the amplitude corresponding to Fig. 2 makes the major contribution to this process. In Fig. 2 the photon produces a pair of charged pions, one of which emerges directly with ω_q, θ_q while the other ploughs into X initiating reactions to various final states (n). The cross section of interest is the sum of squares of the amplitudes for all possible states (n). The above approximation is made on the following grounds:

(i) We are near the pole in the production amplitude for Fig. 2 corresponding to a real pion in transit between (a) and (b). The propagator for this pion is

$$-[(k-q)^2 - \mu^2]^{-1} = (2q\cdot k)^{-1} = [2\omega_q k(1-\beta_q \cos\theta_q)]^{-1}, \quad (1)$$

where $k_\mu = (k, \vec{k})$ and $q_\mu = (\omega_q, \vec{q})$ are the photon and pion four-momenta, respectively. It is large for high energy $\omega_q \sim k \gg \mu$ and small angle $\theta_q \lesssim \mu/\omega_q$, equalling approximately

$$\{\mu^2(k/\omega_q)[1 + (\theta_q \omega_q/\mu)^2]\}^{-1} \approx 1/\mu^2.$$

This emphasizes the importance of this diagram relative to others for two or more pions or heavier particles propagating from (a) to (b). The next lightest state connecting (a) and (b) contains two pions and the continuous sequence of poles (the branch cut) for this state starts at a mass $(2\mu)^2$, so that the propagator for the two-pion state then is less than $1/4\mu^2$. Another way of saying this is that the emitted high-energy pion is distributed over a cone of broader angle $\theta' > 2\mu/\omega_q$ for heavier intermediate states and so the flux per solid angle at $\theta_q \sim \mu/\omega_q$ is reduced by a factor $< 1/4$.

(ii) We are led to a similar conclusion in considering processes in which more than one pion emerges directly from the electromagnetic

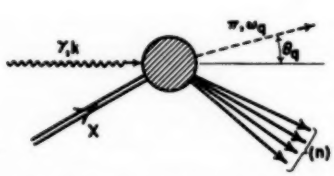

FIG. 1. Diagram for production amplitude $\gamma + X \to \pi + (n)$, where (n) denotes all particles produced in the final state, other than the observed π, from the target X.

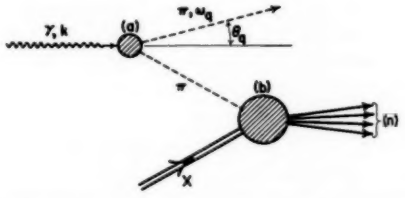

FIG. 2. Diagram for one-pion contribution to the production amplitude $\gamma + X \to \pi + (n)$. This dominates near the pole $(k-q)^2 \approx \mu^2$.

vertex (a). Integration over the undetected final-particle group (p) spreads the cone into which the observed pion emerges to a broad angle of width $\approx$ [energy in particle group (p)]$/\omega_q \gg \mu/\omega_q$.

(*iii*) Lastly we may consider the amplitude corresponding to one pion being exchanged between (a) and (b) but with the observed high-energy pion emerging from the nuclear part of the interaction (b). We come to the same conclusion as above, namely that the cone into which the observed pion emerges is spread over a larger angle than μ/ω_q.

For these reasons we consider Fig. 2 a first approximation to Fig. 1 for $\omega_q \sim k \gg \mu$ and $\theta_q \lesssim \mu/\omega_q$. We can then compute the production cross section in terms of the pion electromagnetic vertex for a real photon multiplied by the total cross section for a pion of energy $k - \omega_q$ incident on target X leading to all final states (n). This gives directly,[2] with $\beta_q \equiv |\vec{q}|/\omega_q \to 1$,

$$d^2\sigma_{\gamma,\pi^\pm}(k,\omega_q,\theta_q) = \frac{\alpha}{2\pi}\frac{\sin^2\theta_q}{(1-\beta_q\cos\theta_q)^2}\frac{d\Omega_q}{4\pi}\frac{\omega_q(k-\omega_q)d\omega_q}{k^3} \times \sigma_{\pi^\mp+X,\,\text{total}}(k-\omega_q), \quad (2)$$

for the cross section that a $\pi^\pm$ in energy interval $d\omega_q$ about ω_q and angle interval $d\Omega_q$ about θ_q is produced, along with anything else, by an incident unpolarized quantum of energy k on a target X.

Equation (2) leads to a sizable flux of pions of energy $\omega_q \sim k$ within a cone of angle $\theta_{1/2} = \mu/\omega_q$. Let us compare it with other electromagnetic and nonelectromagnetic mechanisms for producing a π beam. First consider the electromagnetic production of $\pi^\pm$ pairs in the Coulomb field of a charge Ze (Fig. 3). The cross section expressed in terms of the angle and energy distribution of one of the pions is[3]

$$d^2\sigma_{\gamma,\pi^+,\pi^-}(k,\omega_q,\theta_q) = \frac{\alpha}{2\pi}\frac{[(\mu/\omega_q)^4+\sin^4\theta_q]}{(1-\beta_q\cos\theta_q)^4}\frac{d\Omega_q}{4\pi}\frac{\omega_q(k-\omega_q)d\omega_q}{k^3} \times (Z\alpha)^2\frac{2\pi}{\omega_q^2}\ln(\omega_q/\mu). \quad (3)$$

In (3) we have neglected $1 < \ln(\omega_q/\mu)$ and taken the relativistic limit for the pions. Equations (2) and (3) are comparable in magnitude if in (2) we use $\sigma_{\pi+X,\,\text{total}} \approx 30$ mb, as is appropriate for total pion-nucleon cross sections in the Bev range, while in (3) we insert $Z = 82$. However, for any given target, process (2) will dominate for $\theta_q \sim \mu/\omega_q$ and $\omega_q \sim k$. Before leaving (3) we call attention to a difference in its derivation from that for (2). Both diagrams in Fig. 3 are necessary in order to arrive at the Pauli-Weisskopf cross section, whereas rescattering of the high-energy pion is not included in Fig. 2 and in the derivation of (2), on the basis of our earlier arguments. This is because the Coulomb scattering of the virtual pion in Fig. 3 concentrates both final pions in the forward cone of $\theta_{1/2} \sim \mu/\omega$ and the two diagrams there are of comparable magnitude and opposite sign.

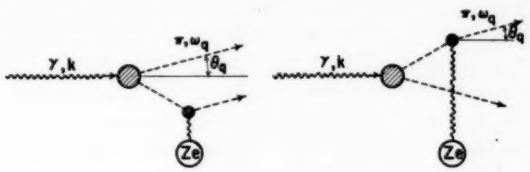

FIG. 3. Diagrams for electromagnetic production of $\pi^\pm$ pairs.

Next consider production of pions by an incident proton beam on a hydrogen target. Hagedorn and von Behr[4] have calculated pion yields from such collisions on the basis of the statistical model; they predict the fraction of interactions leading to pions produced in given angular and momentum intervals. Their results are presented in graphical form in the CERN tables.[4] Since we are primarily concerned here with the production of high-energy collimated pion beams, we want to compare (2) and the statistical model for $\theta_q \sim \mu/\omega_q$ and $k \sim \omega_q$. Choosing $k = 25$ Bev, $\omega_q = 20$ Bev, and $\theta_q = 1°$ to get an idea of the numbers, we find from (2)

$$d^2\sigma_{\gamma,\pi}/d\Omega_q d\omega_q \cong 10^{-2}\sigma_{\pi+X,\,\text{total}}(5\text{ Bev}) \cong 0.3\text{ mb/sr-Bev},$$

for X a target proton. This is a factor of ten larger than the prediction of the statistical theory,[5]

$$\cong 7\times10^{-4}\sigma_{p+p,\,\text{total}}(25\text{ Bev}) \cong 0.03\text{ mb/sr-Bev}.$$

To be sure the predictions of the statistical model are least reliable at the high-energy tip of the spectrum of produced particles. It is also true that quantitative validity of (2) can be established

by experiment alone. Equation (2) may be precise at the pole (1) in the nonphysical region $\cos\theta_q = (1/\beta_q) > 1$, but we cannot theoretically anticipate whether or not there are appreciable corrections in the physical region at $\theta_q \sim \mu/\omega_q$. At present the recent Cornell measurements[6] provide qualitative support for (2) in the energy-angle region of $k \sim 700$-1000 Mev, $\omega_q \sim 500$ Mev, and $\theta_q \sim 15°$. The peaking of their cross sections for mesons at forward angles is naturally explained by the retardation denominator in (2). Also, the total yields as well as the ratio of the π^- to the π^+ yield can be approximately accounted for by known $\pi^{\pm}$-nucleon cross sections occurring in (2). More detailed studies at larger ω_q and smaller θ_q are desirable.[7]

If the predictions of the statistical model for very high energy pion production in nucleon-nucleon collisions are verified, we conclude from (2) that a photon is more effective than a proton in initiating a high-energy beam of pions.[8]

Finally we turn to K-meson and baryon production. Equation (2) may be transcribed directly to the production of K^+ and K^- beams by changing the pion mass μ to μ_K for the K mesons, and the pion cross sections to $\sigma_{K^{\pm}+X}(k-\omega_q)$. Since K mesons are heavier than pions, several pions can accompany the K meson from (a) to (b) in Fig. 2 without appreciably broadening the cone of emission of the high-energy $K^{\pm}$. In this application to K mesons then, Eq. (2) is to be given only qualitative significance in predicting the K beam intensity. It can be checked experimentally in terms of known total $K^{\pm}$ cross sections at energies $k-\omega_q$. The ratio of intensities of high-energy K^+ to K^- mesons is just the ratio of K^- to K^+ interaction cross sections.

Going further and more recklessly afar from the pole, we can calculate also the production of nucleon and hyperon (anti-) particle beams by the mechanism of Fig. 2, obtaining in the high-energy limit

$$d^2\sigma_{\gamma,\eta}(k,\omega_q,\theta_q) = \frac{\alpha}{2\pi}\,\frac{\omega_q(k-\omega_q)d\omega_q}{k^3}\,\frac{d\Omega_q}{4\pi}\,\sigma_{\eta+X,\,\mathrm{total}}(k-\omega_q) \times\left\{\frac{(2-k/\omega_q)(a+\lambda)^2\sin^2\theta_q+\lambda^2\sin^2\theta_q\,[2-(k\omega_q/2M^2)\sin^2\theta_q]}{(1-\beta_q\cos\theta_q)^2}\right\}, \tag{4}$$

where M is the mass of the particle η, a is its charge in units of e, and λ its Pauli anomalous magnetic moment in units of the Bohr magneton ($a=+1$ for the proton, $\lambda=-1.91$ for the neutron, etc.). We wish to point out in connection with (4) only that it predicts a considerable yield. For example, the cross section to produce anti-neutrons at $\theta_q = M/\omega_q = 3°$, with $k = 25$ Bev and $\omega_q = 20$ Bev, is

$$5\times10^{-3}\,\sigma_{N+X,\,\mathrm{total}}(5\ \mathrm{Bev})\ \mathrm{sr}^{-1}\,\mathrm{Bev}^{-1},$$

and exceeds the prediction of the statistical theory calculation[4] for a proton-proton collision by a factor of ≈ 50. This is, however, a dangerous and perhaps misleading application.

Very valuable discussions, especially with D. Ritson and J. Ballam, have contributed to these remarks.

*Supported in part by the U. S. Air Force through the Air Force Office of Scientific Research.

[1]G. F. Chew, Phys. Rev. 112, 1380 (1958); C. J. Goebel, Phys. Rev. Letters 1, 337 (1958); G. F. Chew and F. E. Low, Phys. Rev. 113, 1640 (1959).

[2]The factors are arrived at as follows: $\frac{1}{2}\sum_{s=1}^{2}(2e\vec{\epsilon}_s\cdot\vec{q})^2 = 8\pi\alpha\beta_q^2\omega_q^2\sin^2\theta_q$ for the polarization average of the pion electromagnetic vertex, times $[(q-k)^2-\mu^2]^{-2} = [2\omega_q k(1-\beta_q\cos\theta_q)]^{-2}$ for the square of the propagator, times $d^3q/(2\pi)^3 2\omega_q = \beta_q\omega_q d\omega_q d\Omega_q/16\pi^3$ for the phase space of the observed pion, times $k^{-1}(k-\omega_q)\sigma_{\pi+X,\,\mathrm{total}}(k-\omega_q)$ for the absorption to all states (n) of the intermediate pion, where the factor $(k-\omega_q)/k$ takes into account that the normalization factor for the incident photon is $1/2k$, and $1/2(k-\omega_q)$ for the pion is missing in extracting the cross section $\sigma_{\pi+X,\,\mathrm{total}}(k-\omega_q)$.

[3]W. Pauli and V. Weisskopf, Helv. Phys. Acta 7, 709 (1934); the formula in this reference is a factor of 4 larger than Eq (3) above. W. Pauli, Revs. Modern Phys. 13, 203 (1941); the result in this reference is a factor of 2 larger than Eq. (3) above. Equation (3) is derived for a point Coulomb field and is valid only for small angles $\theta_q < \mu/\omega_q$ where the momentum transfers are $\approx\mu^2/k$. The Bethe-Heitler formula for the electromagnetic pair production of spin 1/2 Dirac par-

ticles of the same mass μ is larger by a factor ~6 at $\theta_q \sim \mu/\omega_q$ due to the spin degree of freedom.

[4]R. Hagedorn, Nuovo cimento 15, 434 (1960); J. von Behr and R. Hagedorn, CERN Report 60-20, 1960 (unpublished).

[5]Pion and nucleon total cross sections are comparable above a few Bev and both are ~30-40 mb for target protons. [See report of V. I. Veksler to Ninth Annual High-Energy Physics Conference, Kiev, U.S.S.R., 1959 (unpublished); also private communication from J. Adams to B. Cork.]

[6]B. M. Chasan, G. Cocconi, V. T. Cocconi, R. M. Schechtman, and D. H. White, Phys. Rev. 119, 811 (1960).

[7]An experiment is now in progress at Stanford University, by L. Hand and W. K. H. Panofsky.

[8]Using the equivalent photon spectrum for a high-energy electron, one can directly compare the yields of pions from incident electron and proton beams. These calculations have been made by J. Ballam, Stanford University High-Energy Physics Laboratory Report M200-8 (unpublished).

ERRATA

GENERALIZED BARDEEN-COOPER-SCHRIEFFER STATES AND ALIGNED ORBITAL ANGULAR MOMENTUM IN THE PROPOSED LOW-TEMPERATURE PHASE OF LIQUID He^3. P. W. Anderson and P. Morel [Phys. Rev. Letters 5, 136 (1960)].

In the paragraph after Eq. (8), we make the statements that "Δ_m decreases with m, but that the total (binding) energy increases; $m = l$ is always the best state." More careful computations show that this is not true. We find:

(a) When normalized Y_m^l are used in (7), the binding energy and Δ_m vary in the same direction.

(b) The variation with m is more complicated, and apparently no very general rule holds. The best states are: For $l = 1$, $m = 1$. For $l = 2$, $m = 1$ and 2 have identical energies, lower than $m = 0$. This agrees with reference 2. For $l = 3$, $m = 2$. One would guess, cautiously, that an intermediate m is the best state in most cases.

Since Fig. 1 is based on $m = l$, it, too, is not correct for $l \geq 3$. For $l \geq 2$ the density of states is linear in E, although the general appearance of curve 3 is maintained.

The conclusions about aligned angular momentum remain valid.

EVIDENCE OF THE NATURE OF ROTATING LIQUID HELIUM. J. R. Pellam [Phys. Rev. Letters 5, 189 (1960)].

In the first complete paragraph on page 190, the value of the apparent "rotation front" velocity radially inward should read "about 2 mm/min" instead of "about 2 mm/sec."

ABSTRACTS

In this section are printed the abstracts of Articles that have been forwarded to The American Institute of Physics for publication in THE PHYSICAL REVIEW. In quoting information obtained from this section before the appearance of the corresponding Article, reference should be made to "Physical Review (to be published)" rather than to this Journal.

CARTESIAN TENSOR SCALAR PRODUCT AND SPHERICAL HARMONIC EXPANSIONS IN BOLTZMANN'S EQUATION. T. Wyatt Johnston, RCA Victor Company, Ltd., Research Laboratories, Montreal, Canada (Received June 13, 1960).

The electron or ion distribution function, expanded in a sum of spherical harmonics, is shown to be equivalent to a tensor scalar product expansion. As such, it can be readily substituted into the Boltzmann equation to give transport equations integrated over angle and also the necessary equations for determination of the expansion coefficients. This has been done for terms up to order three, the order of the pressure transport tensor.

NUCLEAR SPIN RELAXATION IN LIQUID HELIUM 3. F. J. Low* and H. E. Rorschach, The Rice University, Houston, Texas (Received July 11, 1960)

The longitudinal relaxation time of liquid He^3 has been measured as a function of temperature above 1°K and of magnetic field below 13 kgauss in a number of sample containers. At a temperature of 2.0°K and in a magnetic field of 10 kgauss the longitudinal relaxation time, T_1, varied with the sample container from 60 seconds to 400 seconds. The transverse relaxation time, T_2, was measured by a new method and was approximately 30 seconds at a field of 10 kgauss in all sample containers. T_1 was determined as a function of magnetic field at 2.0°K in a single sample container; the values increased from less than 50 seconds in approximately zero field to 400 seconds at 13 kgauss. An impurity relaxation model is proposed to explain the T_1 results. By assuming both wall relaxation and a bulk relaxation given by the Bloembergen, Purcell, and Pound theory, the dependence of T_1 on pressure and temperature can be quantitatively understood. The low values of T_2 are inconsistent with the Bloembergen, Purcell, and Pound theory and may be due to the presence of paramagnetic impurities in suspension in the bulk liquid.

*Now at Texas Instruments Inc., Dallas, Texas.

RESONANCE ABSORPTION OF NUCLEAR GAMMA RAYS AND THE DYNAMICS OF ATOMIC MOTIONS. K. S. Singwi and A. Sjölander, Argonne National Laboratory, Argonne, Illinois (Received June 13, 1960).

The theory of resonance absorption of nuclear γ rays is generalized for an arbitrary system of interacting particles by expressing the relevant transition probability in terms of a space-time self-correlation function; and thus relating the resonance line shape to the incoherent differential scattering cross section for slow neutrons. Two limiting cases, (i) a gas and (ii) a solid, have been considered. Discussion regarding the justification of the use of a classical self-diffusion function for a liquid is given and expressions for the broadening of the resonance line due to diffusive motions of the atoms of the interacting system are derived. It is suggested how a Mössbauer-type experiment could be used to give information regarding the diffusive motions of atoms in a solid and also, under more favorable circumstances, in a liquid.

MEASUREMENTS OF TEMPERATURES AND DENSITIES IN SHOCK-HEATED HYDROGEN AND HELIUM PLASMAS. Wolfgang Wiese,* H. F. Berg, and H. R. Griem, University of Maryland, College Park, Maryland (Received July 5, 1960; revised manuscript received August 8, 1960).

Temperatures and densities in plasmas produced by strong magnetically driven shock waves in a "T tube" were measured spectroscopically. Local thermal equilibrium exists within the experimental accuracy for the conditions of this experiment. In both gases, the measured temperatures and densities are in disagreement with the values expected from the Rankine-Hugoniot relations, unless it is assumed that the conditions in the ambient gas are drastically affected by the initial discharge. Consistency between experiment and shock theory is achieved by considering magnetic pressure and dissociation and excitation

of the ambient gas by uv radiation from the discharge.

*Now at the National Bureau of Standards, Washington, D. C.

ELECTRON PARAMAGNETIC RESONANCE OF EUROPIUM (II) IN SINGLE CRYSTALS OF CADMIUM SULFIDE. Paul B. Dorain, Brandeis University, Waltham, Massachusetts (Received July 5, 1960).

Paramagnetic resonance absorption measurements have been made with single crystals of cadmium sulfide containing europium (II). The results can be fitted to the usual spin-Hamiltonian for ^8S state. The zero-field splitting is about 0.4 cm^{-1}. A comparison of the results with present theories for the crystal field splittings of ^8S is made.

UNRESTRICTED HARTREE-FOCK METHOD: ELECTRON DENSITIES AND MAGNETIC FORM FACTORS FOR SPIN-POLARIZED Ni^{++}. R. E. Watson,* Solid State and Molecular Theory Group, Massachusetts Institute of Technology, Cambridge, Massachusetts, and A. J. Freeman, Materials Research Laboratory, Ordnance Materials Research Office, Watertown, Massachusetts, and Solid State and Molecular Theory Group, Massachusetts Institute of Technology, Cambridge, Massachusetts (Received July 13, 1960).

The effect of relaxing the restrictions associated with the Hartree-Fock method are discussed with particular emphasis on that constraint which requires common radial behavior for wave functions with all quantum numbers except m_S (spin direction) in common. Results of such a "spin polarized" Hartree-Fock self-consistent field calculation are reported for the Ni^{+2} ion and related to earlier calculations of Wood and Pratt, and Heine. Emphasis is placed on a consideration of the effects on the electron density and on x-ray and magnetic form factors. As is discussed, spin polarization of the 3*d* shell and the core results in an interesting effect on the magnetic form factor for this case. The calculation suggests that one would obtain a magnetic form factor which is measurably expanded (hence a contracted charge distribution) in comparison with that appropriate for any single 3*d* electron. Also presented are results of calculations of several hyperfine parameters which are in rough agreement with experiment.

*Now at Avco, RAD, Wilmington, Massachusetts.

CRYSTALLINE FIELD AND SPIN POLARIZATION EFFECTS ON ELECTRON DENSITIES AND MAGNETIC FORM FACTORS. R. E. Watson,* Solid State and Molecular Theory Group, Massachusetts Institute of Technology, Cambridge, Massachusetts, and A. J. Freeman, Materials Research Laboratory, Ordnance Materials Research Office, Watertown, Massachusetts, and Solid State and Molecular Theory Group, Massachusetts Institute of Technology, Cambridge, Massachusetts (Received July 13, 1960).

The combined effects of spin (or exchange) polarization and an external crystalline field on charge densities, x-ray and magnetic form factors, and hyperfine parameters are investigated following the analytic Hartree-Fock self-consistent field approach. The crystalline field was represented by a crude cubic field arising from an octahedral array of point charges surrounding the central ion—in this case Ni^{+2}. In the strong-field approximation the atomic 3*d* electrons are "split" by the crystalline field and the spin polarization effect, resulting in a description of these electrons by a set of three distinct orbitals (each having different radial distributions and called $t_{2g}\uparrow$, $t_{2g}\downarrow$, and $e_g\uparrow$). The ion's spin density leads to a Fermi contact hyperfine term in better agreement with experiment than the value reported in an earlier spin-polarized calculation for the free Ni^{+2} ion and a magnetic form factor whose Fourier transform resembles none of the individual 3*d* charge distributions.

*Now at Avco, RAD, Wilmington, Massachusetts.

DYNAMICS OF RADIATION DAMAGE. J. B. Gibson, A. N. Goland, M. Milgram, and G. H. Vineyard, Brookhaven National Laboratory, Upton, New York (Received July 14, 1960).

Radiation damage events at low moderate energies (up to 400 ev) are studied by machine calculations in a model representing copper. Orbits of knock-on atoms are found and the resulting damaged configurations are observed to consist of interstitials and vacancies. Thresholds for producing permanently displaced atoms (i.e.,

interstitials) are about 25 ev in the ⟨100⟩ direction, 25 to 30 ev in the ⟨110⟩ direction, and around 85 ev in the ⟨111⟩ direction. Collision chains in the directions ⟨100⟩ and ⟨110⟩ are prominent; at low energies the chains focus, at higher energies they defocus. Above threshold, the chains transport matter, as well as energy, and produce an interstitial at a distance. The range of ⟨110⟩ chains has been studied in detail. Localized vibrational modes associated with interstitials, agitations qualitatively like thermal spikes, ring annealing processes, and a higher energy process somewhat like a displacement spike have been observed. Replacements have been found to be very numerous.

The configurations of various static defects have also been studied in this model. The interstitial is found to reside in a "split" configuration, sharing a lattice site with another atom. The crowdion is found not to be stable, and Frenkel pairs are stable only beyond minimum separations, which are found to be very much dependent on orientation.

SPIN-WAVE SPECTRUM OF YTTRIUM IRON GARNET. R. L. Douglass, Department of Physics, University of California, Berkeley, California (Received July 5, 1960).

The spin-wave spectrum of yttrium iron garnet is treated using a Hamiltonian involving nearest-neighbor a-a, d-d, and a-d isotropic exchange interactions. Values of the exchange constants are estimated from the molecular field constants of Pauthenet. Anisotropy and magnetic dipole-dipole interactions are neglected. Twenty spin-wave modes are found, and their energies calculated at points of cubic symmetry in $\vec{k}$ space. The dispersion relation of the single "acoustical" spin-wave mode is found to agree with the value previously reported by Meyer and Harris.

HALL EFFECT AND RESISTIVITY OF Ni-Pd ALLOYS. James A. Dreesen and Emerson M. Pugh, Carnegie Institute of Technology, Pittsburgh, Pennsylvania (Received June 10, 1960).

The two Hall coefficients and the resistivity of Ni-Pd alloys have been measured from 4°K to room temperature using fields up to 3.1 webers/m^2. The ordinary Hall coefficient is found to decrease in magnitude for small additions of Pd in Ni, but to increase as more Pd is added. It is also found that the ordinary Hall coefficient varies more slowly with composition for these alloys than it does for the Ni-Cu alloys. It is shown that a simple treatment successfully correlates the ordinary Hall coefficient, the resistivity, and the saturation magnetization of these alloys. The results indicate that the parallel half of the d band in pure Ni is not quite full at the absolute zero of temperature, and that the relaxation time is not a function only of the energy for the thermal scattering in these alloys. The extraordinary Hall coefficient is found to obey none of the variously proposed theoretical relations.

DETERMINATION OF THE FERMI VELOCITY BY THE HIGH-FIELD TILT EFFECT. Harold N. Spector, Institute for the Study of Metals, University of Chicago, Chicago, Illinois (Received July 14, 1960).

The attenuation of a sound wave in a semimetal in the presence of a magnetic field is examined when the magnetic field is tilted from the direction perpendicular to the direction of propagation of the sound wave. It is found that in the limit of high magnetic fields ($\omega_c\tau \geq 10ql$) the behavior of the attenuation with the angle of tilt gives a point by point determination of the velocity on the Fermi surface. A detailed treatment of a two-spherical-band model is given and the case of a general Fermi surface is examined qualitatively.

COLORATION OF PURE AND DOPED CALCIUM FLUORIDE CRYSTALS AT 20°C AND -190°C. W. J. Scouler* and A. Smakula, Laboratory for Insulation Research, Massachusetts Institute of Technology, Cambridge, Massachusetts (Received July 14, 1960).

Coloration of pure CaF_2 crystals with 2.5-Mev electrons at room temperature results in bands at 580, 400, 335, and 225 mμ. In YF_3-doped crystals the bands are in the same spectral positions as in pure crystals. They are, however, enhanced and their intensity ratios are significantly changed, the 400-mμ band being predominant. NaF-doped crystals show an even more drastic change: Coloration at room temperature produces bands at 605, 385, and 330 mμ and is deeper than in either pure or YF_3-doped

crystals. Since the 400-mμ band is strongly enhanced by YF_3 addition which forms F^- interstitials, it is correlated to neutral fluorine atoms in interstitial positions. Similarly, the 605-mμ band in crystals doped with NaF, which creates F^- vacancies, is correlated to electrons trapped in F^- ion vacancies (*F* centers). The enhancement of the 385-mμ band by NaF is explained by the reduction of the activation energy required for formation of interstitials and vacancies. Of several possible correlations the 330-mμ band is probably connected with a hole trapped in a Ca^{2+} vacancy and that at 225 mμ with an electron trapped by a Ca^{2+} interstitial. The bands at 440 and 200 mμ which appear in NaF-doped crystals only must be connected with Na ions. Coloration at -190°C produces strong changes in the absorption spectrum. In pure and YF_3-doped crystals bands appear at 550, 320, and 270 mμ, while in NaF-doped crystals bands are formed at 440, 390, 315, and 200 mμ in addition to the 550-mμ band. The primary process of coloration at low temperature cannot differ from that at room temperature but the secondary processes are strongly influenced by temperature.

*Present address: Lincoln Laboratory, Massachusetts Institute of Technology, Lexington, Massachusetts.

COLOR CENTERS IN ALKALINE EARTH FLUORIDES. D. Messner* and A. Smakula, Laboratory for Insulation Research, Massachusetts Institute of Technology, Cambridge, Massachusetts (Received July 14, 1960).

Single crystals of CaF_2, SrF_2, and BaF_2 have been colored by x rays (150 kv) and high-energy electrons (2.5 Mev). Five color-center bands in CaF_2 and SrF_2 and nine in BaF_2 have been observed in the spectral region between 0.175 and 0.8 μ. At room temperature the bands in CaF_2 are well resolved, while those in SrF_2 and BaF_2 overlap. At -190° and -255°C the bands sharpen but generally do not shift, except the 580-mμ band in CaF_2 which shifts toward longer wavelengths. Photochemical bleaching of the strongest band shows a certain influence on the others. Three bands could be correlated to the Mollwo relation with the exponent 3.85. A possible correlation of the absorption bands to certain models is discussed.

*Present address: Fa. Kalle A. G., Wiesbaden-Biebrich, Germany.

DISTRIBUTION OF ELECTRONS IN CADMIUM SULFIDE CRYSTALS. Ganesh P. Mohanty and Leonid V. Azároff, Metallurgical Engineering Department, Illinois Institute of Technology, Chicago, Illinois (Received July 14, 1960).

Very accurate x-ray diffraction intensities from a "pure" CdS crystal and one doped with chlorine were used to calculate electron density maps of their crystal structures projected along the *c* axis. To eliminate series termination errors, a difference map obtained by subtracting the electron density of the "pure" crystal from that of the doped crystal was also prepared. According to this map, the electron distribution in the doped crystal is smeared out in the vicinity of the atom centers and an excess of electrons occurs in interstitial sites. This is contrary to the recently reported findings of Shuvalov who observed the formation of "electron bridges" along lines joining adjacent atoms. It is concluded that our observations are consistent with a partial disorder introduced in the doped crystal by the substitution of chlorine into sites normally occupied by sulfur atoms. Observed variations between corresponding x-ray intensities of the doped and undoped crystal can be similarly explained by changes in the extinction effect due to this disorder.

SUBLATTICE MAGNETIZATION AND RESONANCE FREQUENCY OF ANTIFERROMAGNETS WITH LARGE UNIAXIAL ANISOTROPY. Bernard R. Cooper, Department of Physics, University of California, Berkeley, California (Received July 5, 1960).

The effect of large anisotropy on the thermal behavior of the sublattice magnetization and antiferromagnetic resonance frequency is discussed. It is shown that the curves for $M(T)/M(0)$ and $\omega(T)/\omega(0)$ vs T/T_c are shifted upward from those predicted by a Brillouin function magnetization curve. The shifts are due to a combination of the effect of the large anisotropy energy with that of electron exchange correlation. Corrections to the molecular field approximation arising from pair correlations are taken into account by an extension of the Oguchi method. These corrections are expected to be roughly $1/Z$ as large as the more accurate corrections which would arise from correlation with all Z neighbors. This expectation is supported by a comparison

of the values of kT_c/J and $\bar{S}(0)$ for the Oguchi method with those obtained by the Bethe-Peierls-Weiss and spin-wave methods, respectively. The results are related to the experiments on FeF_2 where the anisotropy is comparable to the exchange energy.

RADIOACTIVE PREPARATION OF DEFECTS IN SOLIDS. John Lambe, Scientific Laboratory, Ford Motor Company, Dearborn, Michigan (Received July 5, 1960).

An experimental study has been made of the use of radioactive materials in preparing defects in solids. Paramagnetic resonance was used to study such defects. The systems studied utilized tritium and krypton-85. Solid tritium was studied at 4.2°K. It was found that atomic tritium was formed and showed a characteristic hyperfine splitting of 543 gauss. The krypton-85 was also studied at 4.2°K. This should yield atomic rubidium but no paramagnetic resonance characteristic of this atom was found.

DIFFUSION OF F CENTERS INTO POTASSIUM CHLORIDE SINGLE CRYSTALS. Hiroyuki Mizuno and Morio Inoue, Matsushita Electronics Corporation, Takatsuki, Osaka, Japan (Received June 13, 1960).

Diffusion of F centers into potassium chloride crystals during an additive coloring process has been measured at various temperatures. A diffusion process which can be explained by a simple theory of volume diffusion seems to be predominant at higher temperatures. At lower temperatures, however, the occurrence of a disordered interface diffusion with an F-center concentration decreasing exponentially with the first power of penetration depth, is confirmed.

ELECTRON LEVELS IN A ONE-DIMENSIONAL RANDOM LATTICE. H. L. Frisch and S. P. Lloyd, Bell Telephone Laboratories, Murray Hill, New Jersey (Received July 7, 1960).

Let the potential of a one-dimensional scalar particle be $V(x) = V_0 \sum_{-\infty}^{\infty} \delta(x - x_j)$, $-\infty < x < \infty$, where $V_0 < 0$, and where the sequence (x_j) is random, with a Poisson distribution. The quantity of interest is a certain limiting level distribution, equal numerically to the node density of real solutions $\psi(x)$ of the Schrödinger equation. The random variables $z_j = \psi'(x_j - 0)/\psi(x_j)$, $-\infty < j < \infty$, constitute an ergodic stationary Markov process. The stationary density $T(z)$ of the (z_j) satisfies a first-order linear differential difference equation, and the node density is given (with probability 1) by $\lim_{z\to-\infty} z^2 T(z)$ (Rice's formula). Numerical results are obtained by integrating the second-order linear differential equation satisfied by the Fourier transform of $T(z)$.

THERMAL CONDUCTIVITY OF PURE INDIUM. R. E. Jones and A. M. Toxen, Research Center, International Business Machines Corporation, Poughkeepsie, New York (Received April 19, 1960).

The thermal conductivity of a pure indium specimen was measured in the normal and superconducting states in the range of temperatures 1.3 - 4.2°K. In the normal state the specimen showed sizable magnetothermal resistivity effects which were not in agreement with Kohler's rule for thermal conductivity. Near the transition temperature the ratio of conductivities K_S/K_n exhibited the finite slope with temperature characteristic of electronic conduction limited by phonon scattering. The results were compared with a simple model proposed by Kadanoff and Martin and the agreement was found to be good.

DEMBER EFFECT IN SILVER CHLORIDE. Alvin M. Goodman* and George Warfield, Department of Electrical Engineering, Princeton University, Princeton, New Jersey (Received June 20, 1960; revised manuscript received August 11, 1960).

The Dember effect has been investigated in silver chloride using a chopped light-ac amplification system of measurement. The effect has been resolved into a self-sustaining component which reaches a steady state (for particular wavelength and intensity of incident light) and a non-self-sustaining component which decays with time. The steady-state self-sustaining effect has been found to be of only one polarity (normal polarity) when the illuminated face of the sample is coated with silver, but of both polarities when

the illuminated face is not coated. The normal or positive polarity self-sustaining effect shows up at a shorter wavelength and the inverse self-sustaining effect at longer wavelengths, both in the vicinity of the optical absorption edge. A possible explanation for this behavior based on the existence of surface states is suggested. In the coated sample, the normal polarity effect was found to exhibit a peak at a wavelength of about 0.383 μ at $T = 88°K$.

*Present address: RCA Laboratories, Inc., Princeton, New Jersey.

OPTICAL MEASUREMENT OF THE PLASMA FREQUENCY AND $M_{2,3}$ BAND OF CHROMIUM. Norman N. Axelrod* and M. Parker Givens, Institute of Optics, University of Rochester, Rochester, New York (Received July 7, 1960).

The transmission of thin chromium films has been measured in the extreme vacuum ultraviolet. The onset of transmission at 500 angstroms or 24.8 electron volts agrees well with the theoretical prediction by Pines of 25 electron volts; it also agrees well with the experimental electron eigenlosses measured by Watanabe, and Marton and Leder, of 26 electron volts and 22 electron volts, respectively. The $M_{2,3}$ band was also measured.

*Now at National Aeronautics and Space Administration, Goddard Space Flight Center, Washington, D. C.

CALCULATION OF THE CRYSTALLINE FIELD STRENGTH: CHROME ALUM. A. J. Freeman, Materials Research Laboratory, Ordnance Materials Research Office, Watertown, Massachusetts, and Solid State and Molecular Theory Group, Massachusetts Institute of Technology, Cambridge, Massachusetts, and R. E. Watson,* Solid State and Molecular Theory Group, Massachusetts Institute of Technology, Cambridge, Massachusetts (Received July 1, 1960).

A calculation of the crystalline field strength, Dq, is reported for the case of chrome alum, using the same model and crystal field potential employed by Kleiner and recently determined Hartree-Fock wave functions for the Cr^{+3} ion. On this basis, earlier theoretical attempts at determining, within the framework of crystal field theory, accurate Dq values are reviewed and analyzed. Particular emphasis is placed on a consideration of reported point-charge calculations and Phillips' method of including the effects of orthogonalization of ligand to metal-ion wave functions. Our results indicate that the point-charge model estimates for Dq gave good results mostly because they were based on the use of improper $3d$ wave functions for the transition metal cation. Kleiner's result is significantly improved—his wrong sign for Dq is reversed and a small positive Dq is obtained—but in such a way as to contradict Phillips' conclusions. A discussion is given of the various evidence for the inadequacy of the electrostatic potential theory and some of the necessary modifications are indicated.

*Now at Avco, RAD, Wilmington, Massachusetts.

EXPERIMENTS ON CHARGE-CHANGING COLLISIONS OF LITHIUM IONIC AND ATOMIC BEAMS. S. K. Allison, J. Cuevas, and M. Garcia-Munoz, Enrico Fermi Institute for Nuclear Studies, University of Chicago, Chicago, Illinois (Received July 5, 1960).

Beams of Li^+ ions accelerated to kinetic energies in the range 10 - 475 kev were brought into charge equilibrium in the gases H_2, He, and N_2 and the fractional amounts of Li^-, Li^0, Li^+, Li^{++}, Li^{+++} measured. Because of the relatively large amount of Li^- in an equilibrated beam below 40 kev in energy in propane and nitrous oxide, limited investigations were carried out in these gases. The anomalously large Li^{++} yield in helium at Li^7 energies below 100 kev was noted.

By holding each separated charged constituent successively in an orbit in a magnetic field, admitting gas, and observing the beam attenuation, the total cross section for all charge-changing collisions was observed. Through application of the differential equations for growth or decay of a charged component, certain individual charge-changing cross sections can be deduced from these observed sums. Values are given for $(\sigma_{\bar{1}0} + \sigma_{\bar{1}1})$, σ_{01}, σ_{10}, σ_{12}, σ_{21}, and $(\sigma_{32} + \sigma_{31})$ in H_2, He, and N_2 target gases throughout the energy range. Upper limits can be assigned to $\sigma_{0\bar{1}}$, $\sigma_{1\bar{1}}$, σ_{13}, and σ_{23}. Use of data on $\sigma_{1\bar{1}}$ in H_2 from other sources provides values of $\sigma_{0\bar{1}}$ in that gas. Values for σ_{21} for Li^{++} in helium gas, compared, at common velocities, with σ_{10} for He^+ in helium, and $\sigma_{0\bar{1}}$ for H^0 in helium, shows the exchange nature of the He^+He interaction compared to that of the other isoelectronic structures.

DISINTEGRATION OF Te^{119}. C. W. Kocher, Allan C. G. Mitchell, C. B. Creager, and T. D. Nainan, Physics Department, Indiana University, Bloomington, Indiana (Received July 5, 1960).

The disintegration of Te^{119} has been studied with the help of magnetic spectrometers and scintillation counters. Two half-lives are observed -one of 4.7 ± 0.3 days and one of ~16 hours. These represent the decay from two isomeric states. The isomeric transition is not observed because of the strong competition from the decay to states of Sb^{119}. The 4.7-day disintegration occurs by electron capture and exhibits gamma rays of the following energies: 0.153, 0.270, 0.930, 1.10, 1.22, and 2.12 Mev. The following coincidences are observed: (2.12, 0.270), (1.22, 0.930, 0.153), (1.10, 0.270). The $K/(L+M)$ ratio for the line at 0.153 Mev is 7.85 and for the line at 0.270 Mev is 5.77. The 16-hour isomer exhibits positrons of end-point energy 0.627 Mev; and two gamma rays of energy 1.76 and 0.645 Mev. A disintegration scheme is given.

DECAY OF Si^{26}. E. L. Robinson and O. E. Johnson, Physics Department, Purdue University, Lafayette, Indiana (Received April 8, 1960).

A (2.1 ± 0.3)-sec activity was observed when vacuum-distilled magnesium was bombarded with 8-Mev He^3 ions. Half-life studies using NaI(Tl) scintillation counters yielded evidence that this activity was due to the decay of a positron-emitting isotope with a maximum kinetic energy greater than 3.5 Mev. The features of the gamma-ray spectrum with the exception of a weak line at 824 ± 15 kev could be understood in terms of the decay characteristics of known radioisotopes. An internally consistent argument based on the known decay characteristics of reaction products that may be expected from energy considerations, the results of half-life studies, experimental gamma spectra, and nuclear systematics can be made to support the conclusion that the (2.1 ± 0.3)-sec half-life is that of Si^{26} produced in the reaction $Mg^{24}(He^3, n)Si^{26}$, and a consistent decay scheme can be proposed. The ground state of Si^{26} (0+) decays by the emission of two positron groups to excited states of Al^{26}. The most intense transition, $E_0 = 3.76$ Mev, is to the 0.228-Mev state (0+) of Al^{26}. The second transition, $E_0 = 2.94$ Mev, is to the 1.05-Mev state (1+) of Al^{26}. The 1.05-Mev and 0.228-Mev states are then connected by an (824 ± 15)-kev gamma transition. The energies of the positron transitions are derived from the known levels of Al^{26} and the Si^{26}-Al^{26} mass difference.

ANGULAR DISTRIBUTIONS OF THE $Be^9(d,n)B^{10}$ NEUTRONS. Richard Bardes and George E. Owen, The Johns Hopkins University, Baltimore, Maryland (Received July 7, 1960).

The angular distributions of neutrons to the ground state and to the first excited state of B^{10} in the reaction $Be^9(d,n)B^{10}$ have been studied at incident deuteron energies of 1.41 Mev, 1.88 Mev, and 2.35 Mev. A proton recoil spectrometer utilizing a xenon gas scintillation trigger was developed to study this problem. This spectrometer operated with a resolution of the order of 7% at the neutron energies involved in this reaction.

The analysis of the data in terms of a direct-interaction mechanism indicates that the results are consistent with an interpretation which indicates that the majority of the neutrons emitted at bombarding energies below the Coulomb barrier originate in the Be^9 target nucleus.

MOTT-SCATTERING ANALYSIS OF LONGITUDINAL POLARIZATION OF ELECTRONS FROM Co^{60}. J. S. Greenberg, D. P. Malone,* R. L. Gluckstern, and V. W. Hughes, Yale University, New Haven, Connecticut (Received July 15, 1960).

Mott scattering has been used to analyze the degree of longitudinal polarization of beta particles emitted from radioactive nuclei. The reliability of this method and the influences of the various systematic errors associated with this method on the accuracy of the measurement have been investigated in detail and are discussed. On the basis of a linear extrapolation of the inverse of the Mott asymmetry to zero scatterer thickness, the polarization of 194-kev electrons from Co^{60} was found to be $-(0.994 \pm 0.057)v/c$ with all known corrections applied. The effects of atomic screening and finite nuclear size have not been included. Using the quoted value for the polarization measured in the pure Gamow-Teller transition in Co^{60} yields $C_A' = (0.7 \text{ to } 1.45) \times C_A$.

*Cornell Aeronautical Laboratory, Buffalo, New York.

PHOTONEUTRON CROSS SECTIONS OF COBALT AND MANGANESE. P. A. Flournoy, R. S. Tickle, and W. D. Whitehead, University of Virginia, Charlottesville, Virginia (Received June 15, 1960).

The total photoneutron yields of Mn^{55} and Co^{59} have been carefully measured from threshold to approximately 30 Mev. Analysis of these data using the Leiss-Penfold matrix indicates that the cross sections for both elements show a splitting in the giant resonance region in accord with the predictions of the classical hydrodynamic model. The Mn^{55} peaks occur at energies of 16.8 ± 0.25 Mev and 19.75 ± 0.25 Mev corresponding to cross sections of 90 mb and 77 mb, respectively. Co^{59} maxima occur at 16.75 ± 0.25 Mev and 18.75 ± 0.25 Mev with cross sections of 109 mb and 92 mb. The cross sections $\sigma(\gamma,n)+\sigma(\gamma,2n)+\sigma(\gamma,np)+\ldots$ integrated to 25 Mev are 627 Mev-mb for Mn^{55} and 709 Mev-mb for Co^{59}. Breit-Wigner resonance lines were fitted to both cross sections and the intrinsic quadrupole moments determined from these fits are +0.78 ± 0.10 barn for manganese and +0.76 ± 0.11 barn for cobalt.

CREATION OF THE HEAVY ELEMENTS BY NEUTRON CAPTURE ON A FAST TIME SCALE. Peter Fong, Department of Physics, Utica College of Syracuse University, Utica, New York, and Laboratory for Nuclear Science, Massachusetts Institute of Technology, Cambridge, Massachusetts (Received February 10, 1960).

The mathematical problem concerning the creation of the heavy elements by neutron capture on a fast time scale involves the solution of more than a thousand simultaneous differential equations. This set of equations is solved by replacing them with a mathematical equivalent—a single partial differential equation which turns out to assume the form of the equation of continuity. The stream lines of the analogous hydrodynamical problem are determined, from which the problem of nucleogenesis may be solved once the initial condition is given. By assuming a neutron capture mean lifetime of about 0.1 sec for all nonmagic-number nuclides and by making use of the fact that the neutron magic-number nuclides have smaller neutron capture cross sections, the position, width, and height of the abundance peaks at Br, Xe, and Pt may be determined; these agree reasonably well with the experimental results.

INELASTIC DIFFRACTION SCATTERING. E. Rost and N. Austern, University of Pittsburgh, Pittsburgh, Pennsylvania (Received July 12, 1960).

The method of distorted-wave Born approximation is shown to be equivalent to the first-order adiabatic method for the calculation of inelastic scattering. The flexibility of the distorted-wave method is indicated and tested by numerical calculation for a simplified model. The calculations treat the inelastic scattering of alpha particles from strongly absorbing nuclei, and are directly comparable to the adiabatic calculations considered by Blair in Fraunhofer approximation. Good agreement is found at forward angles. Coulomb wave functions are used, and the energy difference between initial and final states is taken into account. Comparison is made to a few representative experiments and good agreement is found.

GAMMA TRANSITIONS FOLLOWING THE DECAY OF NICKEL-65. R. Jambunathan, M. R. Gunye, and Babulal Saraf, Atomic Energy Establishment, Trombay, Bombay, India (Received April 25, 1960; revised manuscript received August 8, 1960).

The gamma transitions following the decay of 2.6-hour Ni^{65}, have been studied by coincidence scintillation spectrometry. Gamma rays of energies 0.37, 0.51, 0.61, 0.77, 0.85, 0.95, 1.11, 1.48, 1.62, and 1.72 Mev having intensities of 55, 1.5, 0.6, ~1, ~0.6, ~0.3, 140, 290, 10, and 6 per thousand disintegrations, respectively, are emitted in this decay. The gamma-gamma coincidence study is consistent with energy levels of Cu^{65} at 0.77, 1.11, 1.48, 1.62, and 1.72 Mev. The angular correlation of 0.37- and 1.11-Mev gamma rays suggests the spin assignment of 5/2 for the 1.11-Mev level and 7/2 or 3/2 for the 1.48-Mev level. Both the gamma transitions are mixtures of $E2$ and $M1$.

DECAY SCHEME OF Dy^{159}. R. C. Greenwood and E. Brannen, University of Western Ontario, London, Ontario, Canada (Received July 5, 1960).

The electron capture decay of Dy^{159} has been shown to occur appreciably only to the 58-kev state and ground state of Tb^{159}, with branching ratios of 37% and 63%, respectively. The K in-

ternal conversion coefficient of the 58-kev transition has been measured to be $\alpha_K = 8.5^{+0.7}_{-1.2}$, which is consistent with a predominantly $M1$ transition, with the possibility of some $E2$ mixing. The orbital electron capture ratio to the 58-kev state of Tb^{159} was obtained as $P_{LM...}/P_K = 0.17 \pm 0.15$. From this value, a minimum decay energy to the ground state of Tb^{159} was assigned as 230 kev. The upper limit on transitions to the 138-kev and 364-kev states of Tb^{159} was placed at 0.1%. A spin and parity of 3/2- was assigned to the ground state of Dy^{159} from a consideration of logft values. An upper limit of 450 kev was placed on the decay energy to the ground state of Tb^{159}.

NUCLEAR SPINS OF SIX NEUTRON-DEFICIENT GOLD ISOTOPES. W. Bruce Ewbank, Lawrence L. Marino,* William A. Nierenberg, Howard A. Shugart, and Henry B. Silsbee,† Lawrence Radiation Laboratory and Department of Physics, University of California, Berkeley, California (Received July 5, 1960).

The nuclear spins of six neutron-deficient isotopes of gold have been measured by atomic-beam magnetic-resonance methods. The results of these measurements are as follows: Au^{191} (3.0 hr), 3/2; Au^{192} (4.8 hr), 1; Au^{193} (17.5 hr), 3/2; Au^{194} (39 hr), 1; Au^{195} (190 day), 3/2; Au^{198} (5.6 day), 2.

*Present address: Convair, San Diego, California.
†Present address: University of Washington, Seattle, Washington.

FINE STRUCTURE IN THE ENERGY SPECTRA OF PHOTOPROTONS FROM He^4. Carmelo Milone, Istituto di Fisica dell'Università, Centro Siciliano di Fisica Nucleare, Catania, Italy (Received June 27, 1960).

The energy spectra of the photoprotons from He^4 irradiated with 31- and 32-Mev bremsstrahlung were studied by means of nuclear photoemulsions in ΔE_γ steps of 0.4/3 Mev. In the region of the giant resonance several peaks have been distinguished. The more evident of these have widths less than 0.5 Mev and are located at He^4 excitation energies of 24.7 ± 0.2 and 26.1 ± 0.1 Mev. Previous experiments on the photoproton spectra from He^4 could not give evidence of these narrow resonances because the spectra were examined in energy steps much larger than the width of these resonances.

Other types of experiments which have been performed in order to obtain information on the existence of excited states in He^4 are discussed. The fact that narrow resonances are distinguished only in the present experiment is attributable to the selective nature of the (γ, p) process, the most important contribution in the $He^4(\gamma, p)$ reaction coming only from the states of He^4 having $J = 1^-$ and $T = 1$.

INTERPRETATION OF ISOMERIC CROSS-SECTION RATIOS FOR (n, γ) AND (γ, n) REACTIONS. J. R. Huizenga and R. Vandenbosch, Argonne National Laboratory, Argonne, Illinois (Received July 11, 1960).

The relative probability of forming each member of a pair of nuclear isomeric states has been compared with theoretical predictions in order to learn which nuclear parameters can be determined from these data. For thermal neutron capture reactions, the observed ratios do not give much information about the dependence of the nuclear level density on spin, but they are consistent with a spin cutoff factor, $\exp[-(J+\frac{1}{2})^2/2\sigma^2]$, where $\sigma \leq 5$. The calculations are sufficiently consistent with experiment to make their predictions usable as a guide for assigning spins to the compound states formed in thermal or resonant energy neutron capture. For (γ, n) reactions, the calculations reproduce the energy dependence of the experimentally observed isomeric cross-section ratios. In order to obtain quantitative information about the spin dependence of the nuclear level density, it is necessary to consider reactions where particles are emitted which can carry off enough angular momentum to reach many spin states of the residual nucleus.

ISOMERIC CROSS-SECTION RATIOS FOR REACTIONS PRODUCING THE ISOMERIC PAIR $Hg^{197,197m}$. R. Vandenbosch and J. R. Huizenga, Argonne National Laboratory, Argonne, Illinois (Received July 11, 1960).

Excitation functions and isomeric cross-section ratios were determined for the $Au^{197}(p, n)$ and $Au^{197}(d, 2n)$ reactions. Isomeric cross-section ratios were also determined for the $Hg^{196}(n, \gamma)$, $Hg^{196}(d, p)$, $Hg^{198}(n, 2n)$, $Hg^{198}(\alpha, \alpha n)$, and $Pt(\alpha, xn)$ reactions. Those reactions for which

compound nucleus formation predominates are treated by a statistical model. In this treatment the compound state is characterized by angular momentum and excitation energy. The analysis yields a value of 4 ± 1 for the parameter σ which characterizes the dependence of the nuclear level density on angular momentum. Relatively small amounts of angular momentum are transferred in reactions which proceed predominantly by a direct-interaction mechanism. Such reactions, therefore, give a larger yield of the isomer with spin closer to that of the target nucleus.

$Ni^{58}(n,p)Co^{58}$ CROSS SECTION FOR NEUTRONS OF ENERGIES BETWEEN 2.2 AND 3.6 Mev. L. González, J. Rapaport, and J. J. van Loef, Instituto de Física y Matemáticas, Universidad de Chile, Santiago, Chile (Received July 1, 1960).

The relative cross section for $Ni^{58}(n,p)Co^{58}$ has been measured by an activation method for neutron energies of 2.2 to 3.6 Mev. The absolute cross section at 3.55-Mev neutron energy is found to be 167 ± 27 mb by comparing the intensity of the 810-kev gamma ray of Co^{58} with the amount of Si^{31} formed in the $P^{31}(n,p)Si^{31}$ reaction, which has a previously known cross section of 96.2 ± 9.0 mb. The cross section rises from 120 mb at 2.2 Mev to a maximum value of 185 mb at 3.0 Mev. Observed cross sections are compared with the predictions of the statistical theory of nuclear reactions by using a square well potential and a diffuse edge potential. In neither case could a satisfactory agreement with experimental data be obtained.

FISSION OF GOLD BY CARBON IONS. Glen E. Gordon,* Almon E. Larsh, Torbjørn Sikkeland, and Glenn T. Seaborg, Lawrence Radiation Laboratory and Department of Chemistry, University of California, Berkeley, California (Received July 14, 1960).

Angular distribution and kinetic-energy spectra of fragments, and cross sections for fission of gold with 68- to 124-Mev C^{12} ions have been obtained by observation of the fragments in two types of detectors, gas scintillation chambers and silicon p-n junctions. From the parameters used to fit the angular distributions to the theoretical curves of Halpern and Strutinski, we have obtained the average excitation energy of the fissioning nucleus at the time of fission. This quantity is approximately 25 Mev, which is nearly independent of bombarding energy, suggesting that fission is preceded by the emission of several particles from the compound nucleus. The fission cross section increases from a value of 100 mb at 68 Mev to 1.28 b at 124 Mev. Over this range of bombarding energies, the total fragment kinetic-energy release rises from 142 ± 6 to 146 ± 6 Mev. At all bombarding energies, the variation of laboratory-system kinetic energy of the fragments with laboratory-system angle indicates full momentum transfer by the bombarding particle to the fissioning system.

*Present address: Department of Chemistry, Massachusetts Institute of Technology, Cambridge, Massachusetts.

SINGLE AND MULTIPLE STRIPPING OF α PARTICLES. M. el Nadi,* Sloane Physics Laboratory, Yale University, New Haven, Connecticut (Received June 9, 1960).

Assuming the stripping process to take place mainly at the nuclear surface, expressions are derived for the differential cross sections for the processes in which one, two, or three nucleons are stripped from an incident α particle by the target nucleus. Comparison between the derived formulas and experimental data was carried out for the (He^3,p) and (α,p) reactions and shows fairly good agreement.

*Present address: Faculty of Science, Cairo University, Cairo, Egypt.

HYPERFINE STRUCTURE OF AMERICIUM-241. Richard Marrus, William A. Nierenberg, and Joseph Winocur, Lawrence Radiation Laboratory, University of California, Berkeley, California (Received July 8, 1960).

Atomic-beam measurements on Am^{241} have confirmed that the nuclear spin is $I = 5/2$, and have established that the electronic ground state is characterized by an angular momentum $J = 7/2$ and a Landé splitting factor $g_J = -1.9371(10)$. In addition, the magnetic-dipole and electric-quadrupole hyperfine-structure coupling constants have been found to be, respectively, $A = \pm 17.144(8)$ Mc/sec and $B = \mp 123.82(10)$ Mc/sec. It is hypothesized that these values arise from a state that is primarily formed from the Hund's

rule term ^8S of the configuration $(5f)^7(7s)^2$. However, important contributions to the measured g_J, A, and B values are shown to come from the admixture of other terms in the ground state by means of the spin-orbit interaction, and also from the excitation of s electrons in the core to higher s states.

RADIOACTIVE DECAY OF Yb^{167}. R. G. Wilson and M. L. Pool, Department of Physics and Astronomy, Ohio State University, Columbus, Ohio (Received May 27, 1960).

Erbium oxide enriched to 35.1% in the mass number 164 was irradiated with 17- and 24-Mev alpha particles. An activity decaying by electron capture with a half-life of (17.7 ± 0.2) minutes was produced and its assignment to Yb^{167} confirmed by the identification of the thulium K x ray and the well-known daughter activity of Tm^{167}. Gamma rays with energies of 106, 113, and 176 kev were observed in the spectrum of Yb^{167}. Gamma-gamma coincidence measurements were performed on the observed radiations. Transition probabilities, multipole order admixtures, and electron capture branching ratios have been calculated. Approximately 89% of the electron capture transitions occur to the 292.7-kev (7/2-) level of Tm^{167}.

LIFETIMES OF ROTATIONAL LEVELS IN SOME ODD-A NUCLEI MEASURED BY A MICROWAVE METHOD. A. E. Blaugrund, Y. Dar, and G. Goldring, Department of Physics, The Weizmann Institute of Science, Rehovoth, Israel (Received June 1, 1960; revised manuscript received August 15, 1960).

Measurements of mean lives of the first excited states of a number of odd-A nuclei have been carried out with the intention of obtaining more accurate information on magnetic transition probabilities than is at present available. Most of these mean lives are in the range of $2\text{-}20 \times 10^{-11}$ sec, and for this measurement a special timing apparatus has been devised which consists of a microwave beam pulsing system and a beta-ray spectrometer and cavity combination which acts as a microwave shutter. In four cases the exponential decay could be determined directly; these were the first excited states of Lu^{175}, Hf^{179}, and Ta^{181} and the 118-kev level of Tm^{169}. The results for these levels are: $\tau(Tm^{169}) = (9.0 \pm 0.4) \times 10^{-11}$ sec, $\tau(Lu^{175}) = (14.6 \pm 1) \times 10^{-11}$ sec, $\tau(Hf^{179}) = (5.4 \pm 0.4) \times 10^{-11}$ sec, $\tau(Ta^{181}) = (6.0 \pm 0.5) \times 10^{-11}$ sec. Lifetime measurements were also carried out for the first excited states of Hf^{177}, Re^{185}, and Re^{187}. The limitations and scope of this method of measuring lifetimes are discussed.

SURVEY OF TRITIUM-PRODUCING NUCLEAR REACTIONS. Jose Gonzalez-Vidal and William H. Wade,* Lawrence Radiation Laboratory, University of California, Berkeley, California (Received July 8, 1960).

(p, t), (d, t) and (α, t) reactions have been investigated throughout the periodic table by bombarding stacked metal foils and determining directly the tritium produced in the reaction. In the (α, t) reactions, there is conclusive evidence that most of the tritons are produced with high energies, thus indicating the presence of direct-interaction processes. The curve representing the integrated cross section vs Z of the target rises with decreasing Z. This, and the appearance of low-energy peaks in the individual excitation functions of low-Z targets indicate that at low and intermediate values of Z the relative number of low-energy tritons increases. These tritons are probably the product of a compound-nucleus mechanism. For the (p, t) and (d, t) reactions the same compound-nucleus and direct-interaction effects are noticed.

*Chemistry Department, University of Texas, Austin, Texas.

ENERGY LEVELS OF Ne^{21} AND Ne^{23}. Joan M. Freeman,* Laboratory for Nuclear Science, Massachusetts Institute of Technology, Cambridge, Massachusetts (Received June 28, 1960).

The energies of twenty-seven excited states of Ne^{21} and seventeen of Ne^{23} have been established by a study of the (d, p) reactions in Ne^{20} and in Ne^{22}. Seven deuteron bombarding energies between 4.75 and 7.5 Mev were used, and the target was a cell with thin windows, containing either natural or Ne^{22}-enriched neon gas. The proton groups emitted at 90 degrees were analyzed with a broad-range magnetic spectrograph. The established calibration of the spectrograph, in terms of alpha particles from polonium, together with some well-known reactions, provided the

data necessary for precise energy determinations. The Q values obtained for the ground-state reactions $Ne^{20}(d,p)Ne^{21}$ and $Ne^{22}(d,p)Ne^{23}$ were 4.534 ± 0.009 Mev and 2.791 ± 0.009 Mev, respectively. Deuteron groups inelastically scattered from Ne^{20} and Ne^{22} were also observed. The higher energy groups were used in the calibration procedure; the lower energy groups gave the results 4.250 ± 0.008 Mev and 3.356 ± 0.008 Mev for the second excited states of Ne^{20} and Ne^{22}, respectively. The interpretation of the level schemes of Ne^{21} and Ne^{23} in terms of the collective model has been considered and is discussed here briefly.

*Now returned to Atomic Energy Research Establishment, Harwell, Berkshire, England.

DECAY OF 16-MINUTE Ta^{182m}. A. W. Sunyar, Brookhaven National Laboratory, Upton, New York, and P. Axel, Physics Department, University of Illinois, Urbana, Illinois (Received July 5, 1960).

A revised decay scheme of the 16-minute isomer Ta^{182m} involves three states of Ta^{182} at excitation energies of 147 kev, 319 kev, and 503 kev. Transition multipolarities were classified by measuring both gamma-ray coincidences and internal conversion electrons. The 503-kev isomeric state decays mainly (98%) by a 184-kev $E3$ transition to the 319-kev state. This 319-kev state decays mainly (94%) to the 147-kev state by means of a 172-kev transition that is predominantly $M1$. The 147-kev transition to the ground state is also predominantly $M1$. Two of the three possible crossover transitions were observed; a 356-kev $M4$ transition originates at the isomeric level and a 319-kev $E2$ transition connects the second excited state with the ground state.

The 147-kev and the 319-kev states are probably the first and second excited rotational states of the ground-state configuration. The relevant rotational parameters are of particular interest because very little is known about moments of inertia for odd-odd nuclei.

The relative probabilities were determined for pile neutron activation of the 16-minute isomer, Ta^{182m}, and the 112-day ground state, Ta^{182}. If the ground-state formation cross section is taken as 21 barns, the corresponding value for the isomer is only 9 mb.

LEVEL STRUCTURE OF Eu^{153}. R. E. Sund and M. L. Wiedenbeck, Harrison M. Randall Laboratory of Physics, The University of Michigan, Ann Arbor, Michigan (Received July 1, 1960).

Gamma rays in Eu^{153} following the decay of Sm^{153} and Gd^{153} have been studied using coincidence and angular correlation methods. Results for the strong transitions are in agreement with the decay scheme given by McCutchen. Measurements were made of spectra of gamma rays in coincidence with the x-ray, 70-kev, and the 97-kev and 103-kev transitions in the decay of Gd^{153}, and with eight energy regions in the decay of Sm^{153}. A number of new, weak transitions were observed in the decay of Sm^{153}, and a consistent decay scheme is proposed. Directional correlation measurements were made on the 70-kev–103-kev cascade from the decay of Sm^{153} and from the decay of Gd^{153}. Possible spin assignments are discussed.

PSEUDOSCALAR INTERACTION IN NUCLEAR BETA DECAY. C. P. Bhalla,* University of Tennessee, Knoxville, Tennessee, and M. E. Rose, Oak Ridge National Laboratory, Oak Ridge, Tennessee (Received July 5, 1960).

The experiments on the allowed beta transitions, which lead almost uniquely to the $V - 1.2A$ interaction, do not have any bearing on a possible contribution from the pseudoscalar interaction. To determine whether or not any contribution from the pseudoscalar interaction is really needed, an examination has been made of the β longitudinal polarization and the β shape factor in the $0 \rightarrow 0$ (yes) beta transitions. The theoretical polarization for the mixture of the pseudoscalar and the axial vector interactions has been developed. In this work, the formulation of the pseudoscalar interaction as given by Rose and Osborn has been used. The numerical results on the β longitudinal polarization and the shape factor depend on two parameters, namely, the coupling constant ratio, C_P/MC_A, and λ, the ratio of the two relevant nuclear matrix elements. M is the nucleon mass in units of the electron mass. The electronic functions occuring in the theoretical formulas for these effects are tabulated for Pr^{144} $(0^- \rightarrow 0^+)$ and Ho^{166} $(0^- \rightarrow 0^+)$. All the electronic radial functions were computed considering the nucleus as a sphere of a uniform charge distribution with a nuclear radius of $1.2A^{1/3} \times 10^{-13}$ cm, and taking into account the finite deBroglie wavelength effect.

The results of extensive numerical analysis are presented. We conclude that the absence of the pseudoscalar interaction is consistent with the existing experimental data. The value of C_P/MC_A, which also gives a satisfactory fit to the experimental data, depends on λ. The upper limit of the value of $|C_P/MC_A|$ is found to be 0.05 for $|\lambda| = 200$. In this work, time-reversal invariance is assumed valid for the weak as well as the strong interactions, and the two-component theory of the neutrino has been used.

*Present address: Westinghouse Electric Corporation, Atomic Power Department, Pittsburgh, Pennsylvania.

DEPOLARIZATION DUE TO TARGET MOTION. Albert E. Werbrouck,* Palmer Physical Laboratory, Princeton University, Princeton, New Jersey (Received July 14, 1960).

The projection upon both of the lab scattering planes of a spin component along the center-of-mass angular momentum direction is computed for arbitrary target motion. The resulting depolarization of Λ hyperons produced by 1080-Mev/c pions on nuclear matter and on deuterons is presented as a function of production angle. At this energy, the polarization, if constant for all production angles, would be reduced to 85% and 95% of the original value in heavy nuclei with respect to the $\pi \times \Lambda$ and $K \times \Lambda$ planes, respectively. In deuterium, the reductions would be to 98.4% and 99.5% of the initial polarization.

*Present address: Istituto di Fisica, Turin, Italy.

SLOW-NEUTRON INTENSITY AT HIGH BALLOON ALTITUDES. R. C. Haymes and S. A. Korff, New York University, University Heights, New York, New York (Received June 22, 1960).

In order to extend measurements of cosmic-ray neutrons to top balloon altitudes, a flight was conducted on August 24, 1959, in which our system of identical counters filled with enriched and natural $B^{10}F_3$ was used. An altitude of 122 000 feet at a geomagnetic latitude of 55°N was attained, corresponding to 4-millibar pressure, which is considerably higher than previous measurements. The counting rate dropped to about 1% of the maximum rate, which occurs at 60 000 feet. If one extrapolates this curve to the top of the atmosphere, one obtains an upper bound for the slow-neutron albedo of 0.03 neutron per cm^2-sec. The background due to highly ionizing events in the counters increased exponentially to about 63 000 feet, with a derived mean free path of 152 g/cm^2. The background continued an exponential increase up to 122 000 feet, but with a mean free path of 15 g/cm^2.

METHOD FOR DETERMINING THE K^0 SPIN. Philippe Eberhard, Laboratoire de Physique Atomique et Moleculaire, College de France, Paris, and M. L. Good, University of Wisconsin, Madison, Wisconsin (Received July 11, 1960).

A method is presented for determining the K^0 spin, using only angular momentum conservation and the rules of quantum mechanics. The method is based on a proof that, in the reaction $\pi^- + p \rightarrow \Lambda + K^0$, the K_1^0 decay intensity associated with a given direction of the Λ spin cannot be isotropic at any production angle, if the K^0 spin is equal to or greater than two.

Account is taken of the particle-mixture aspect of the K_1^0 and of possible magnetic moment precession.

DECAY OF BOUND MUONS. Victor Gilinsky and Jon Mathews, California Institute of Technology, Pasadena, California (Received July 11, 1960).

The decay rate of bound muons from the K shell is calculated for elements up to lead. The muon is represented by a relativistic wave function for a point nucleus with parameters adjusted for finite-nuclear-size effects. The outcoming electron is represented by a Sommerfeld-Maue wave function. The decay rate is found to be a monotonically decreasing function of the atomic number. An estimate of the error is obtained by comparing with an exact calculation for the lowest electron angular state. The spectrum and angular distribution of the electrons are also presented.

LOW-ENERGY NEUTRAL PION PHOTOPRODUCTION IN H_2 AND He. A. Odian,* G. Stoppini,† and T. Yamagata,‡ University of Illinois, Urbana, Illinois (Received July 11, 1960).

The results of an experiment on the photoproduction of neutral pions from H_2 and He in the very low energy region are compared with the

dispersion relation calculations of Chew, Goldberger, Low, and Nambu (C.G.L.N.). For H_2, agreement was found for incident γ-ray energies above 155 Mev for $N^+ \simeq +0.065$ and disagreement below for all constant values of N^+. The He results give support to the C.G.L.N. effective-range formulas for the small p-wave phase shifts.

*Now at the Istituto Superiore di Sanità, Rome, Italy.
†Now at the Istituto di Fisica dell'Università, Rome, Italy.
‡Now at CERN, Geneva, Switzerland.

LEPTON DECAYS OF HYPERONS. D. R. Harrington, Carnegie Institute of Technology, Pittsburgh, Pennsylvania (Received July 5, 1960).

An expression is given for the lepton energy spectrum and asymmetry for the lepton decay modes of hyperons in terms of six form factors. A weak interaction having the form of the usual lepton current coupled to an unspecified strong current is assumed, and the momentum transfer dependence of the form factors is neglected. Some applications to the decays $\Lambda \to p + e + \bar{\nu}$ and $\Lambda \to p + \mu + \bar{\nu}$ are given.

COMPLEX SINGULARITIES OF PARTIAL-WAVE AMPLITUDES IN PERTURBATION THEORY. J. G. Taylor and A. E. A. Warburton, Department of Applied Mathematics and Theoretical Physics, Cambridge University, Cambridge, England (Received July 11, 1960).

We show that the complex singularities which invalidate Mandelstam's representation do not cause complex singularities of partial wave amplitudes for two-particle scattering processes, except for the expected "kinematic" complex branch points.

OSCILLATORY CHARACTER OF REISSNER-NORDSTRÖM METRIC FOR AN IDEAL CHARGED WORMHOLE. John C. Graves and Dieter R. Brill, Palmer Physical Laboratory, Princeton, New Jersey (Received July 15, 1960).

A transformation is presented to remove coordinate ("pseudo") singularities from metrics of a certain class, a special case of which is the transformation of Kruskal, extending the Schwarzschild metric beyond its pseudosingularity. The transformation is applied to the Reissner-Nordström metric, which describes a concentration of charge and mass in general relativity. On an initial surface this metric shows the same general behavior as the Schwarzschild metric, describing a "wormhole," or bridge, between two asymptotically flat spaces, but with electric flux flowing through the wormhole. It is found that the region of minimum radius, the so-called "throat" of the wormhole, begins to contract, but reaches a minimum and re-expands after a finite proper time, rather than pinching off as in the Schwarzschild-Kruskal case: the radius of the throat pulsates periodically in time, "cushioned" by Maxwell pressure of the electric field through the throat. The motion of charged particles in this metric is investigated, and it is shown that no particle can hit the geometric singularity at $r = 0$, (1) quite in general, provided only that the mass of the test particle exceeds the value associated in general relativity with its charge, and (2) in particular when the test particle has no charge at all; but (3) such collisions are not avoided when the throat itself is not endowed with an electric flux.